Targeting Breast Cancer Stem Cells with

the Curcumin Nanomedicine

BY

ECE GULCUR
B.S., Istanbul Technical University, 2007

THESIS

Submitted as partial fulfillment of the requirements
for the degree of Master of Science in Biopharmaceutical Sciences
in the Graduate College of the
University of Illinois at Chicago, 2012

Chicago, Illinois

Defense Committee:

Dr. Hayat Onyuksel, Chair and Advisor
Dr. Seungpyo Hong
Dr. Michael Cho, Bioengineering

This thesis is dedicated to my family and my dear Francisco for their endless support and encouragement.

ACKNOWLEDGEMENTS

This thesis would not have been possible without the guidance and the help of several individuals for whom I would like to extend my gratitude.

First and foremost, I owe my deepest gratitude to my advisor, Dr. Hayat Onyuksel for offering me the great opportunity to learn about cutting edge scientific research as well as her invaluable assistance, support and guidance throughout my thesis. Above all, her willingness to explore new areas made this research possible. I also gratefully acknowledge my professors and committee members, Dr. Seungpyo Hong and Dr. Michael Cho for the inspiring classes that they taught and also for graciously giving their time to serve on my thesis committee.

I am also thankful to Dr. Richard Gemeinhart and the members of his lab for allowing me to use the microscope for long hours.

I am most grateful to my fellow labmates for their invaluable assistance in the laboratory as well as their friendship: Sok Bee Lim, Stephanie Drake, Mentor Thaqi, Dr. Antonina Kuzmis, Amrita Banerjee and Fatima Khatib. In particular, I would like to thank Mentor Thaqi for his previous work in the lab, which served as a basis for this research, and also for all his help and support. I am thankful to Dr. Antonina Kuzmis, especially for her help with peptide conjugation. My sincere thanks go to Amrita Banerjee and Fatima Khatib, whose support and kind friendship made this a pleasant experience for me. I would also like to thank Ahmet Dirim Arslan for all his help and friendship.

Last, but by no means least, I would like to express my gratitude to my college professor, Dr. Nezih Hekim, who has inspired me to work on stem cells.

EG

TABLE OF CONTENTS

TABLE OF CONTENTS

TABLE OF CONTENTS

LIST OF TABLES

LIST OF FIGURES

LIST OF FIGURES

FIGURE PAGE

LIST OF ABBREVIATIONS

ABC	Adenosine-triphosphate-binding cassette
APC	Allophycocyanin
ALDH	Aldehyde dehydrogenase isoform 1
ATP	Adenosine-triphosphate
BSA	Bovine serum albumin
CD	Cluster of differentiation endothelial cell marker
C-DMSO	Curcumin solution in DMEM containing DMSO
CMC	Critical micelle concentration
CSC(s)	Cancer stem cell(s)
C-SSM	Curcumin-loaded sterically stabilized micelles
C-SSM-VIP	Curcumin-loaded sterically stabilized micelles surface grafted with vasoactive intestinal peptide
DAPI	4',6-Diamidino-2-phenylindole
DLS	Dynamic light scattering
DMEM	Dulbecco's modified eagle's medium
DMSO	Dimethylsulfoxide
DNA	Deoxyribonucleic acid
DSPE-PEG_{2000}	1,2-Distearoyl-*sn*-glycero-3-phosphoethanolamine-*N*-methoxy-[poly(ethylene glycol); molecular weight 2,000]
DSPE-PEG_{3400}-NHS	[1,2-Dioleoyl-*sn*-glycero-3-phosphoethanolamine-*n*-[poly(ethylene glycol)]-*N*-hydroxy succinamide; PEG molecular weight 3,400]

LIST OF ABBREVIATIONS

EDTA	Ethylenediaminetetraacetic acid
EGFR	Epidermal growth factor receptor
EPR	Enhanced permeability and retention
ESA	Epithelial specific antigen
FAM	5-carboxyfluorescein
FBS	Fetal bovine serum
FDA	U.S. Food and Drug Administration
FOLFOX	5-Fluorouracil and oxaliplatin
HBSS	Hank's balanced salt solution
HEPES	(N- [2-Hydreoxyethyl] piperazine-*N'*-[2-ethanesulfonic acid])
HER2	Human epidermal growth factor 2
HPLC	High performance liquid chromatography
IC_{50}	Half maximal inhibitory concentration
Lin	Lineage marker
MFI(s)	Mean fluorescence intensity (intensities)
M_w	Molecular weight
NF-κB	Nuclear factor kappa-light-chain-enhancer of activated B cells
NOD/SCID mice	Nonobese diabetic/severely combined immunodeficient mice
PBS	Phosphate buffered saline
PE	R-Phycoerythrin
PEG	Polyethylene glycol

LIST OF ABBREVIATIONS

Pgp	Multidrug transporter P-glycoprotein
PLGA	Poly(lactic-co-glycolic acid)
RP-HPLC	Reverse-phase high performance liquid chromatography
SD	Standard deviation
SFE	Sphere forming efficiency
SSM	Sterically stabilized micelles
SSM-VIP	Vasoactive intestinal peptide-surface grafted sterically stabilized micelles
SP	Side population
VIP	Vasoactive intestinal peptide

SUMMARY

Breast cancer is the most commonly occurring cancer and the leading cause of cancer death in women worldwide. Despite decreasing breast cancer death rates in North America and Europe over the past two decades, partially as a result of significant advances in systemic chemotherapy, treatment of breast cancer still remains challenging. Conventional chemotherapy has major limitations such as the non-specificity of systemically administered chemotherapy drugs to cancerous cells leading to adverse side effects, formulation issues due mostly to poor solubility of the drug, and also the multidrug resistance of cancer cells to chemotherapeutic agents due to the abundant expression of P-glycoprotein efflux pumps.

Targeted drug delivery approaches aim to overcome the limitations of conventional systemic chemotherapy by accumulating the anticancer drug in the disease site(s) while minimizing drug exposure at the off-target organs and tissues. Nano-sized carriers have been developed to take advantage of the 'enhanced permeability and retention' (EPR) effect of the leaky tumor vasculature to accumulate the drug in the tumor site, and hence enhance its anticancer efficacy. In addition to passive targeting strategies, active targeting strategies are also being developed, which involve attaching a ligand on nanocarriers that will specifically recognize and bind to receptors expressed on target cells, in order to further enhance selectivity and cellular uptake of anti-cancer agents.

Our laboratory has been investigating biocompatible and biodegradable, sterically stabilized phospholipid micelles (SSM) as nano-sized drug delivery vehicles of water-insoluble anticancer agents for more than a decade. These self-assembled structures made of amphiphilic molecules efficiently solubilize poorly water-soluble anticancer agents inside their

hydrophobic core and provide protection with their hydrophilic polyethylene glycol (PEG) palisade. The latter reduces opsonization and uptake by the reticuloendothelial system, and thereby renders these micelles sterically stabilized. SSM can be targeted to the cancer tissue by passive and active targeting mechanisms. SSM can be actively targeted to the vasoactive intestinal peptide (VIP) receptors - previously shown to be overexpressed on breast cancer cells - by surface grafting SSM with VIP (SSM-VIP). Previous work from our laboratory has demonstrated that SSM-VIP promoted selective accumulation of cytotoxic drugs in breast cancer cells, and thereby improved their biodistribution and therapeutic index.

Curcumin, a hydrophobic polyphenol derived from the tumeric spice, has been the focus of an extensive amount of research in recent years due to its vast array of pharmacological activities including cancer chemopreventive and chemotherapeutic activities. It has been shown to exert these anticancer activities by modulating a variety of molecular targets such as transcriptional factors, inflammatory cytokines, growth factors, receptors, kinases, other enzymes, and genes regulating cell proliferation and apoptosis in a variety of different cancers including breast cancer. Despite curcumin's vast potential in cancer treatment, studies addressing pharmacokinetics of curcumin have revealed that the usefulness of curcumin was curtailed as a result of its poor bioavailability. In order to address this issue, a lipid-based nanomedicine of curcumin in SSM (C-SSM) was recently developed in our laboratory. The characterization studies demonstrated that curcumin's solubility as well as stability in aqueous media in the form of the C-SSM nanomedicine was remarkably improved compared to free drug. In addition, this formulation was also shown to significantly amplify the cytotoxicity of

SUMMARY

curcumin against MCF-7 human breast cancer cells, suggesting its potential for enhancing curcumin's *in vivo* anticancer efficacy by circumventing its bioavailability problems.

A new paradigm has emerged in recent years, revealing that cancers contain a small, therapy-resistant sub-population of cells – the cancer stem cells (CSCs) – displaying tissue-specific stem cell properties, responsible for tumor initiation, propagation and regeneration. According to this cancer stem cell concept, only CSCs within the tumor possess the capacity to self-renew and to differentiate into the heterogeneous lineages of cancer cells that comprise the tumor. Moreover, these cells are intrinsically more resistant to therapy than other cancer cells, and hence survive and regenerate the tumor after treatment. Conventional therapies, on the other hand, have been designed to target the bulk of a tumor with the assumption that all cells within a cancer are equally tumorigenic. The cancer stem cell paradigm suggests that the relative failure of conventional breast cancer therapies, as revealed by the high percentage of patients experiencing relapses, is strongly related to the enrichment of CSCs after therapy. Therefore, it is of high importance to develop novel strategies to target the resistant CSCs for a relapse-free cure of the patient's disease.

Curcumin's activity against the CSCs has been investigated in recent years. These studies have revealed the therapeutic potential of curcumin to target CSCs from a number of cancers including breast cancer, as a regulator of multiple self-renewal and differentiation pathways. However, the highly resistant disposition of CSCs necessitates novel targeted-delivery strategies promoting higher drug exposure to these cells. In this respect, nanomedicines that can be tailored to actively target these cells can overcome the challenge of drug delivery to CSCs.

SUMMARY

The overall goal of this thesis project was to develop a safe and efficacious nanomedicine for the treatment of breast cancer that will target and eliminate the cancer stem cell population. For this purpose, we first evaluated the *in vitro* inhibitory effect of the C-SSM nanomedicine on the cancer stem cell population from MCF-7 human breast cancer cells. We hypothesized that delivering curcumin as the C-SSM nanomedicine would significantly improve its efficacy against breast CSCs compared to free curcumin. Next, to improve the anti-CSC activity of C-SSM even further, we aimed to integrate an active targeting strategy to this formulation. For this purpose, we first determined the level of VIP receptors on the cancer stem cell population of MCF-7 cells compared to the normal cancer cells in order to reveal a novel cellular target overexpressed on the surface of breast CSCs. We hypothesized that breast CSCs would express high levels of VIP receptors and therefore could be employed for active targeting of these cells. Lastly, we developed a novel formulation of curcumin in VIP-surface grafted SSM (C-SSM-VIP), and tested its ability to amplify the *in vitro* anti-CSC activity of C-SSM and free curcumin on MCF-7 breast cancer cells. We hypothesized that actively targeted delivery of curcumin as the C-SSM-VIP nanomedicine would further improve its efficacy to eliminate the resistant CSC population in breast cancer cells.

The putative breast CSCs were first identified as cells isolated based on a $CD44^{+}/CD24^{-/low}$ immunophenotypical profile. Shortly after, cancer stem/progenitor cells were also found to be enriched in tumorspheres derived from breast cancer cells, owing to the unique ability of stem cells to grow and form spherical clusters in non-adherent culturing conditions. In order to evaluate the *in vitro* inhibitory effect of C-SSM to breast CSCs, we tested

its effect on the primary and secondary tumorsphere-forming ability, as well as on the $CD44^{+}/CD24^{-/low}$ CSC population of the MCF-7 human breast cancer cell line.

Samples of C-SSM and empty SSM were prepared by the film rehydration method and characterized for curcumin's self-association with SSM through dynamic light scattering (DLS) and HPLC studies. The DLS data showed one single peak at around 15 nm for both formulations. Thereafter, MCF-7 cells were treated for 72 hours with 10 µM and 20 µM concentrations of C-SSM or free curcumin, and empty SSM, DMSO or PBS control samples in adherent conditions. Treated cells were then detached and plated in ultra-low attachment plates. At the end of 7 days of tumorsphere culture, sphere forming efficiencies and average sphere sizes were evaluated from the first passage (primary spheres) and after the second passage (secondary spheres) of tumorspheres. C-SSM was found to significantly suppress the primary tumorsphere formation in a dose-dependent manner, indicating its ability to eliminate the tumorsphere-initiating breast CSCs. Moreover, 20 µM C-SSM inhibited the tumorsphere formation by 64% ($P < 0.001$), which was more than 2 times higher in comparison with free curcumin ($P = 0.01$). Furthermore, C-SSM was also found to impair the self-renewal and proliferative capacities of CSCs, as demonstrated by its efficacy to inhibit secondary tumorsphere formation ($P < 0.05$) and to reduce the size of both primary and secondary spheres ($P < 0.05$), respectively.

For determining C-SSM's effect on the $CD44^{+}/CD24^{-/low}$ breast CSC population, MCF-7 cells were treated for 72 hours with the treatment groups and treated cells were incubated with antibodies against human CD44 and CD24. The effect of the treatment groups on the percentage of surviving $CD44^{+}/CD24^{-/low}$ cells, as well as on the internalization of curcumin by

SUMMARY

the CSC and normal cancer cell populations were analyzed using flow cytometry. The C-SSM nanomedicine, at 10 μM and 20 μM concentrations, were found to result in a marked increase in the cellular uptake of curcumin compared to free drug in both normal cancer cell and cancer stem cell populations of the MCF-7 cell line (1.8-fold – 6.4-fold). In addition, 20 μM C-SSM reduced the percentage of the $CD44^{+}/CD24^{-/low}$ CSCs by 56% ($P < 0.05$), while no significant change was observed with free curcumin.

Next, a fluorescence-based ligand binding assay was conducted on MCF-7 cells to determine the level of VIP receptor expression on breast CSCs compared to the expression on normal breast cancer cells. MCF-7 cells were sorted using flow cytometry into $CD44^{+}/CD24^{-/low}$ cancer stem cell and $CD44^{+}/CD24^{high}$ normal cancer cell populations. The VIP receptors on the sorted cells were stained with fluorescence-labeled VIP and fluorescence from the slides was visualized under a confocal microscope. We demonstrated that the VIP receptors were overexpressed by approximately 3-fold in the $CD44^{+}/CD24^{-/low}$ cancer stem cell population compared to the normal cancer cells of the MCF-7 cell line ($P < 0.05$).

In order to develop a novel nanomicellar curcumin formulation actively targeted to breast CSCs, C-SSM was surface-grafted with VIP and characterized for particle size distribution and curcumin concentration. The DLS data showed a homogeneous species with a slight increase in the mean particle size (~ 17 nm). Thereafter, a tumorsphere formation assay was employed to determine whether active targeting of VIP receptors with C-SSM-VIP further improved the inhibitory effect of curcumin on breast CSCs from MCF-7 cells. 5 μM C-SSM-VIP was found to enhance inhibition of tumorsphere formation by approximately 20% compared to

both C-SSM and free curcumin ($P < 0.05$). These data suggest the augmentation of the overall cellular uptake of curcumin, and hence its anti-CSC activity, by the receptor-mediated particle internalization.

In this thesis, we were able to develop a novel strategy for targeting and eliminating breast cancer stem cells in a safe and efficacious way. We were able to demonstrate the benefits of the SSM nanomedicine as a delivery system for curcumin in improving its anti-cancer stem cell activity. In addition, we were able to identify VIP receptors as a potential cellular target overexpressed on breast CSCs. Furthermore, we integrated an active targeting strategy to the C-SSM formulation and were able to demonstrate that the *in vitro* efficacy of curcumin to eliminate breast cancer stem cells as the C-SSM-VIP nanomedicine was significantly enhanced compared to both C-SSM nanomedicine and free curcumin.

The successful completion of this project provides a first step to employ nanotechnology applications to actively target CSCs. This may eventually lead to safe and more effective therapies for breast cancer, as well as other types of cancers possessing a CSC population, with a potential to eliminate recurrence, and thereby increasing tumor remission and survival of patients.

I. INTRODUCTION

A. BREAST CANCER

Breast cancer is a malignant, uncontrolled growth of epithelial cells lining the ducts or lobules of breast tissue arising through a series of molecular mutations at the cellular level (Lippman, 2005). It is the most commonly occurring cancer and the leading cause of cancer death in females worldwide. In 2008 alone, 1.38 million new cases of breast cancer were diagnosed and 458,400 women died of breast cancer (Jemal et al., 2011).

The causes of most breast cancer cases remain to be unknown. However, recent years have shown numerous advances in the identification of various risk factors including gender, environment, hormones, genetic factors, and lifestyle (Michaud et al., 2008). The incidence of breast cancer among women may increase with advancing age, late age at first birth (>= 30), the use of postmenopausal hormone replacement therapy, prior family history, higher dietary fat intake, obesity, and alcohol intake (Michaud et al., 2008).

The current treatment of breast cancer often comprises treatment with surgery, radiotherapy, or both for local diseases, and treatment with cytotoxic chemotherapy, endocrine therapy, biologic therapy, or combinations of these for systemic diseases (Carlson et al., 2009). Identification of the disease stage and biologic features such as axillary node status and tumor hormone receptor content is required for selecting the optimum treatment among a variety of local and systemic therapies.

1. Current Cytotoxic Chemotherapies for Breast Cancer

A series of laboratory and clinical studies during the 1960s and 1970s have tested the notion that breast cancer is a metastatic disease that cannot be cured with locoregional therapy alone. Findings from these investigations illustrated that high response rates and rapid onset of action could be achieved with systemic chemotherapy (Michaud et al., 2008; Kardinal et al., 2008). Numerous cytotoxic drugs have since been introduced as single agent-regimens or as combinations for the chemotherapeutic treatment of breast cancer. In general, these drugs target deregulated cell division cycle, a common attribute of cancer cells, and can be categorized as deoxyribonucleic acid (DNA)-damaging agents, antimitotics, and antimetabolites (Prendergast et al., 2007).

DNA-damaging agents include platinum compounds and antitumor antibiotics. Platinum compounds such as cisplatin and carboplatin cross-link DNA strands leading to inhibition of DNA synthesis and transcription (Kardinal et al., 2008; Marsh et al., 2009). Antitumor antibiotics such as doxorubicin and epirubicin act by blocking topoisomerase II leading to disruption of DNA replication and transcription (Kardinal et al., 2008; Marsh et al., 2009). Antimitotic agents act on microtubules to inhibit cell division and include taxanes and vinorelbine. The taxanes [specifically paclitaxel (Taxol®, Bristol-Myers Squibb) and docetaxel (Taxotere®, Sanofi Aventis)] are the most active and constitute a relatively new class of chemotherapy agents with remarkable clinical activity (Kardinal et al., 2008; Michaud et al., 2008; Marsh et al., 2009). Vinorelbine is a semi-synthetic vinca alkaloid approved for use in patients with advanced breast cancer. Lastly, antimetabolites serve as substrates for major cellular enzymes due to their structural similarity to naturally occurring compounds required for cellular mechanisms. These

agents generally inhibit DNA synthesis by blocking purine and pyrimidine nucleoside synthesis pathways and include the 5-Fluorouracil analog, one of the most widely used chemotherapeutics, and gemcitabine, a prodrug of the cytotoxic triphosphate nucleotide metabolite.

2. Limitations of Conventional Chemotherapy Approaches

Despite decreasing breast cancer death rates in North America and Europe over the past two decades (largely as a result of early detection through mammography and improved treatment strategies) a significant proportion of patients with early stage breast cancer and almost all patients with metastatic disease experience relapse (Nicholson et al., 2005; Normanno et al., 2005). These treatment failures reveal the major limitations in systemic chemotherapy, mainly attributable to drug non-specificity, formulation limitations, and multidrug resistance.

2.1. Lack of Drug Specificity

The specificity and activity of current chemotherapy agents towards target disease sites are typically evaluated based on their ability to alter pathological cellular mechanisms. However, the selective accumulation of the drug in the target site (intracellular compartment, cell, organ or tissue) is usually overlooked when assessing the specificity of these drugs. Majority of cytotoxic anticancer drugs are systemically or orally administered small molecules. Upon administration, these drugs get rapidly distributed throughout the body including off-

target healthy organs and tissues. In addition, as a result of this rather even distribution of the drug, large doses of drug have to be administered in order to reach a required therapeutic concentration at the target site, leading to narrow therapeutic index and severe side effects (Torchilin, 2010; Onyuksel et al., 2011).

2.2. Formulation Limitations

One of the major challenges of the pharmaceutical industry today is formulation problems, which was reported to be responsible for 12 percent of clinical failures in the year 2000 for 10 large pharmaceutical companies (Kola et al., 2004). In fact, it is estimated that more than 40 percent of all newly discovered drugs are poorly soluble or insoluble in water and thus require special formulation techniques (Connors et al., 2004). One of the techniques to solubilize the hydrophobic anticancer drugs for their clinical administration is the use of adjuvants, which may itself cause severe hypersensitivity reactions and/or toxicity. One example for this is Taxol®, a paclitaxel formulation in Cremophor EL (polyoxyethylated castor oil) and alcohol. In addition to solubility issues, *in vivo* instability and rapid metabolism are other formulation-related limitations in cancer drug development.

2.3. Multidrug Resistance

A broad class of lipophilic chemotherapeutic agents such as vinorelbine, paclitaxel and doxorubicin are actively exported from cells by an adenosine-triphosphate (ATP-)-dependent efflux pump, known as multidrug transporter P-glycoprotein (Pgp) (Dean et al., 2005). Cancer

cells express high levels of these plasma membrane transporters serving to protect them from cytotoxic agents. As a result of this multidrug resistance, at least a portion of the cancer cells can survive chemotherapy and initiate as well as sustain tumor relapse. In breast cancer clinical trials, approximately 41 percent of breast tumors were reported to express Pgp and this expression was shown to increase after therapy (Gottesman et al., 2002). Moreover, a three-fold reduction in response to chemotherapy was reported among tumors expressing Pgp after treatment (Szakacs et al., 2006).

The limitations of conventional chemotherapeutic approaches listed above provide a clear indication for the need to develop new drug delivery and/or treatment approaches.

3. Targeted Delivery in Cancer Therapy

The development of new strategies that guide systemically administered anticancer drugs selectively to the target tumor site is necessary to minimize toxicity caused by these cytotoxic agents. In this respect, targeted drug delivery approaches aim to increase the therapeutic index by accumulating the drug in the disease site(s) while minimizing drug exposure at the other off-target organs and tissues, and thereby may overcome the limitations of systemic delivery of anticancer drugs. Targeted delivery systems generally comprise an anticancer agent, a pharmaceutical carrier (polymeric particles, liposomes, micelles, nanoemulsions, and many others) used to transport the drug cargo, and optionally a targeting moiety that will recognize the target site (Torchilin, 2010). Currently, numerous passive targeting and active targeting approaches are being investigated for drug delivery into a variety of tumors.

3.1. Passive Targeting

It is now well established that all solid tumors share two features: 1) highly irregular tumor blood vessels and 2) a dysfunctional lymphatic drainage (Peer et al., 2007; Matsumura et al., 1986). The endothelial cells lining the blood vessels are loosely interconnected, resulting in a high permeability of the tumor vessels to large molecules and particles (10 – ~500 nm in size) (Serpe, 2006; Torchilin, 2010). Hence, 'passive' drug delivery approaches for cancer therapy take advantage of this so-called 'enhanced permeability and retention' (EPR) effect of the leaky tumor vasculature to accumulate the nano-sized carriers (nanocarriers) inside the interstitial space. Moreover, the compromised lymphatic clearance in tumors also extends the retention of the nanocarriers inside the tumoral interstitium, where release of the encapsulated drug or its internalization by the cancer cells via endocytosis/phagocytosis takes place. As a result of this increased accumulation of the drug at the target disease site, passive delivery of chemotherapeutical agents can successfully enhance their anticancer efficacy. However, for most tumors outside the mononuclear phagocytes system, the usefulness of this type of targeting is limited to the circulation half-life of the nanocarrier in the blood due to its elimination by the macrophages (Koo et al., 2005b). Therefore, long-circulating, sterically stabilized carriers have been developed by coating the surface of the carriers with hydrophilic polymers such as poly(ethylene glycol) (PEG), poloxamines, poloxamers and polysaccharides in order to reduce the binding of plasma proteins as well as the recognition by phagocytes. For example Doxil®, a U.S. Food and Drug Administration (FDA)-approved PEG-coated liposomal formulation of doxorubicin, was shown to have a longer half-life (~275 times), as well as

several-fold enhancement of the drug accumulation in the tumor compared to free doxorubicin (Gabizon, 2001).

3.2. Active Targeting

While passive targeting approaches are widely used in clinical therapy, active targeting strategies are currently being developed to achieve enhanced selectivity and drug uptake, as well as to prevent expelling of drugs from the cells in the case of multidrug resistance. These strategies involve the targeting of a ligand that can bind to a receptor overexpressed on the surface of tumor cells or tumor vasculature (Allen, 2002). The "ligand-targeted therapeutics" are classified according to their drug delivery approach. Antibodies (monoclonal antibodies or fragments) bind to, and thereby alter the activity of, receptors that indirectly regulate cancer cell proliferation such as trastuzumab (Herceptin®, Genentech) targeting the human epidermal growth factor receptor (EGFR) 2 (HER2) used for the therapy of certain breast cancers (Danhier et al., 2010). Another class of ligand-targeted therapeutics is immunoconjugates, which consist of a therapeutic molecule coupled to an antibody that localizes in tumors. ^{90}Yttrium–ibritumomab tiuxetan (Zevallin®, Spectrum Phamaceuticals) is a clinically approved radiotherapy antibody targeted to CD (a cluster of differentiation endothelial cell marker)-20 (Danhier et al., 2010). Lastly, targeted nanocarriers feature a targeting ligand on the surface of a nano-sized drug delivery system carrying a cytotoxic drug (Koo et al., 2005b; Lammers et al., 2008; Peer et al., 2007).

Antibodies in their native states or fragments, peptides, aptamers (short single-stranded DNA or ribonucleic acid oligonucleotides), vitamins, and carbohydrates have been explored as

targeting moieties for nanocarriers (Serpe, 2006; Lammers et al., 2008). Although current clinical evidence for the benefits of active targeting strategy is insufficient, preclinical data from animal studies over the past decade have shown promise. However, in these studies, significant enhancement in the anticancer efficacy was achieved only with carriers targeting internalizing receptors (Marcucci et al., 2004; Lammers et al., 2008; Kirpotin et al., 2006). This implies that the enhancement in efficacy is due to receptor-mediated endocytosis of the carrier, but not to its higher accumulation inside the tumoral interstitium. These findings have led to the development of drug delivery systems targeted to internalizing surface receptors, such as the folate receptor (Lee et al., 1994; Leamon et al., 2003), HER2 (Park et al., 2002), and vasoactive intestinal petide (VIP) receptors (Krishnadas, 2004; Koo et al., 2011; Onyuksel et al., 2009b). In addition to the targeting strategies based on receptor-mediated endocytosis, surface-modification of the carriers with cell penetrating peptides and protein transduction domains such as TAT could also be utilized to achieve internalization into the cytosol without interacting with surface receptors (Peer et al., 2007; Marcucci et al., 2004; Torchilin et al., 2001). However, these peptides are not cell specific, and therefore may have limited application.

3.3. Sterically Stabilized Phospholipid Micelles for Targeted Delivery

Nanoparticulate pharmaceutical carriers are nanostructures typically made of one or several different materials, including natural or synthetic polymers and lipids. Rational design approaches over the years have led to the development of numerous nanocarriers such as polymeric nanosphere, nanoemulsions, dendrimers, nanocapsules, liposomes, and micelles (Torchilin, 2010). In order to achieve a clinical success, nanovectors for anti-cancer therapy

should meet several goals: (1) simple and relatively inexpensive preparation, (2) a particle size preferably less than 200 nm (to take advantage of the EPR effect), (3) sufficiently high drug-loading capacity, (4) biodegradability and biocompatibility, (5) longevity in circulation, and (6) selective accumulation at the target site (Torchilin, 2010).

Sterically stabilized phospholipid micelles (SSM), nano-sized self-assembled complexes composed of the PEGylated phospholipid, distearoyl phosphatidylethanolamine-polyethylene glycol 2000 (DSPE-PEG_{2000}; Figure 1), stand out as a highly promising nanovector as it was shown to meet the goals stated above. Phospholipids are amphiphilic molecules made up of a nonpolar hydrocarbon region and a polar phosphate headgroup. When added to aqueous media, the lipid molecules self-aggregate in a variety of structures depending on the specific characteristics of the molecule, in such a way that the unfavorable hydrophobic interactions are minimized. DSPE-PEG_{2000} molecules are conical in shape due to the Gaussian random coils of PEG anchored to the polar head group of the phospholipid, and therefore favor the formation of micelles in aqueous media above a certain lipid concentration known as the critical micelle concentration (CMC). Figure 2 depicts the formation of micelles from the aggregation of DSPE-PEG_{2000} molecules in aqueous medium above the CMC. The relatively low CMC value of SSM in the range of 0.5 to 1.0 μM provides a high thermodynamic stability and negligible disruption of micelles upon dilution when administered into the body (Ashok et al., 2004). In addition, the hydrophilic PEG palisade on the micelle surface forms a protective layer by suppressing the adsorption of serum proteins such as opsonins and hence the recognition by the cells of the reticuloendothelial system, leading to steric stabilization and prolonged *in vivo* circulation of SSM (Torchilin et al., 1995). Moreover, DSPE-PEG_{2000} is a component of the FDA-approved

product, Doxil® (stealth liposomal doxorubicin, Janssen), and was demonstrated to be a biodegradable and biocompatible material safe for human use (Working et al., 1996).

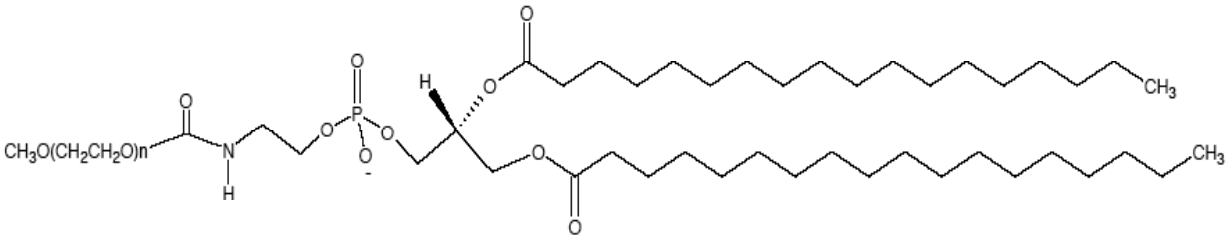

Figure 1. The molecular structure of distearoylphosphatidylethanolamine conjugated to polyethylene glycol of molecular weight of 2000 Daltons.

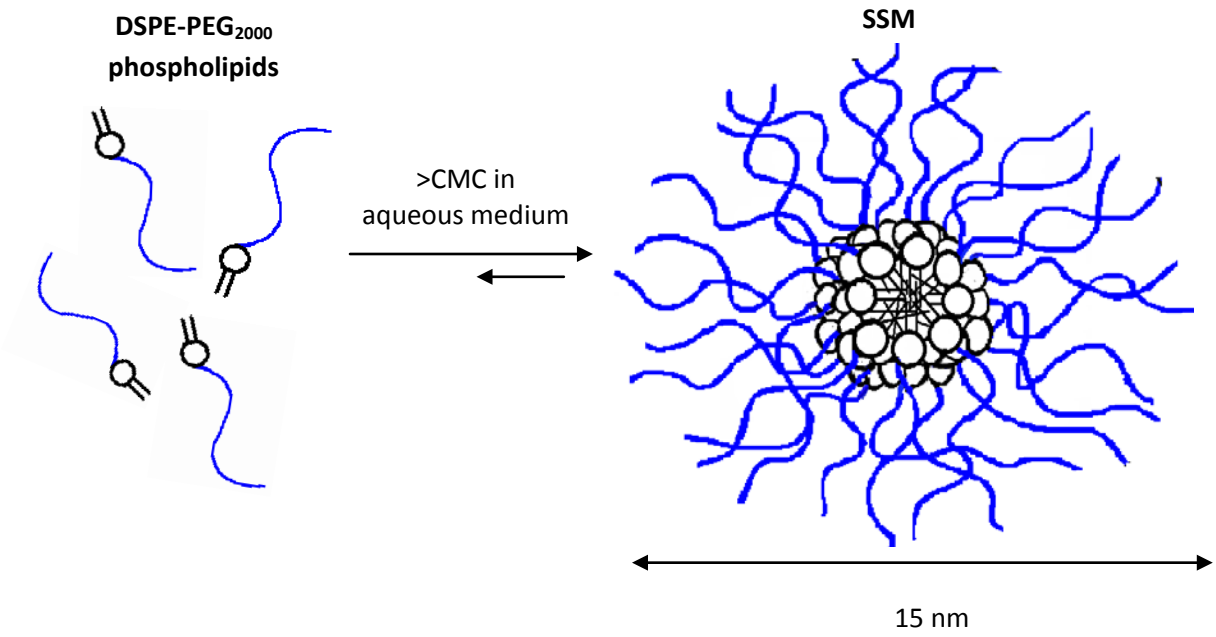

Figure 2. Illustration showing the formation of SSM from DSPE-PEG_{2000} phospholipids. Figure depicts the dynamic equilibrium between the phospholipids in monomeric state and the formation of SSM above the critical micelle concentration (CMC). Adopted from (Thaqi, 2011).

To date, numerous hydrophobic small molecules including the anticancer drugs such as paclitaxel, camptothecin and amphipathic peptides have been solubilized in SSM (Sezgin et al., 2006; Krishnadas et al., 2003; Koo et al., 2005a; Onyuksel et al., 1999; Lim et al., 2011b). In

water, hydrophobic molecules preferentially migrate to the micelle core where they get solubilized, while hydrophilic molecules adsorb on the micelle surface, and amphiphilic molecules are generally dispersed along phospholipid molecules (Torchilin, 2010).

Phospholipid micelles can be targeted to the cancer tissue by passive and/or active targeting mechanisms. SSM are approximately 15 nm in size, and hence suitable for passive targeting via the EPR effect. Moreover, the remarkably smaller size of micelles renders them superior over other nanocarriers such as liposomes, since the extent of penetration into the tumor interstitium has been shown to be strongly dependent on the vesicle size (Jain et al., 2010). SSM can also be actively targeted to the tumor site by attaching specific ligands such as peptides to the distal end of their PEG chains (Onyuksel et al., 2009b; Krishnadas, 2004).

3.4. Vasoactive Intestinal Peptide Receptors as Targets for Breast Cancer Chemotherapy

Vasoactive intestinal peptide is an endogenous 28-amino acid mammalian neuropeptide that elicits a broad spectrum of biological functions related to reproduction, development, growth, immune responses, circadian rhythms, the modulation of neuronal and endocrine cells, tumors and diseases as well as the functions of digestive, respiratory, reproductive and cardiovascular systems (Laburthe et al., 2002; Laburthe et al., 2007). The amino acid sequence of VIP is given in Figure 3. VIP selectively binds to surface membrane receptors known as $VPAC_1$ and $VPAC_2$ and PAC_1, belonging to the large family of G-protein coupled receptors that have common central domains of seven transmembrane helices and a large N-terminal extracellular domain (Dickson et al., 2009). VIP was found to show a high affinity for $VPAC_1$ and $VPAC_2$

receptors and an affinity 1000 times lower for PAC_1 receptor (half maximal inhibitory concentration, IC_{50} = 1000 nM) (Harmar et al., 1998). These receptors have been identified in a variety of human tissues including mammary gland, heart, lung, brain, kidney, pancreas, muscles, gastrointestinal tract, testis, and also immunocompetent cells (Usdin et al., 1994; Dickson et al., 2009).

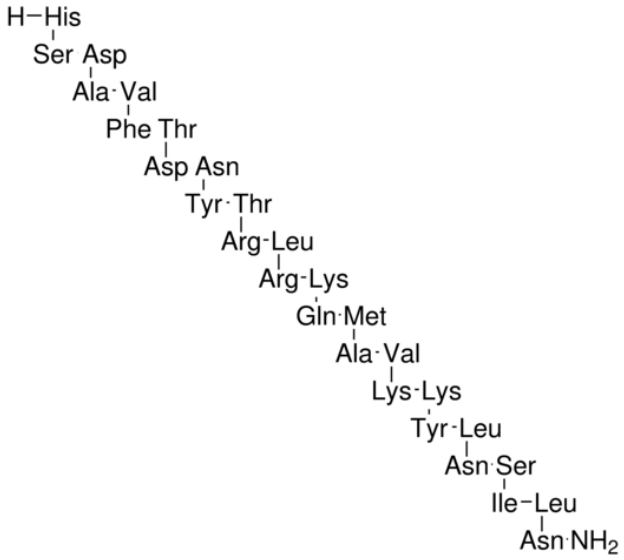

Figure 3. The amino acid sequence of vasoactive intestinal peptide.

It has been demonstrated that VIP receptors are expressed at high densities in a variety of human tumors including breast, prostate, pancreas, colorectal, gastric, and liver carcinomas, and lymphomas (Reubi et al., 2000). In breast cancer, the overexpression of these receptors at the messenger ribonucleic acid (RNA) and/or protein levels and their coupling to cyclic adenosine monophosphate (cAMP) production have been reported in a number of human cell lines including MCF-7, MDA-MB-231, ZR-75-1, and T-47D as well as in tissues from human breast carcinomas (Gespach et al., 1988; Schulz et al., 2004; Garcia-Fernandez et al., 2005).

Moreover, Reubi *et al.* have reported that VIP receptors were present in 100% of the 68 different human breast cancer tissue sections tested, with $VPAC_1$ being the predominant subtype among the three receptors (Reubi et al., 2000). Previous studies in our laboratory also showed that the level of VIP receptor expression in human and rat breast cancer tissues were approximately 5 times higher than the level in normal breast tissues (Dagar et al., 2001b). Given these issues, VIP receptors stand out as attractive targets for diagnosis, prevention and treatment of breast cancer, specifically by receptor-targeted delivery of chemotherapeutic agents.

Previously in our laboratory, human VIP was successfully grafted on the surfaces of SSM and sterically stabilized mixed micelles (composed of a 9:1 mixture of DSPE-PEG_{2000} and phosphatidylcholine) to develop novel drug delivery systems. We have tested these VIP-grafted phospolipid micelles (SSM-VIP) as nanocarriers for water-insoluble chemotherapeutic agents such as paclitaxel, 17-allylamino-17-demethoxy geldanamycin and camptothecin (Krishnadas, 2004; Onyuksel et al., 2009b; Koo et al., 2011). *In vivo* biodistribution studies of paclitaxel-loaded SSM-VIP formulation on MNU-induced breast cancer-bearing rats showed reduced drug accumulation in healthy tissues associated with toxicity, e.g. bone marrow, spleen and kidney, accompanied with a significantly increased accumulation of the drug at the tumor site after 30 days of treatment with a 1mg/kg dose (Krishnadas, 2004). Moreover, tumor size was reduced by approximately 80% with paclitaxel-loaded SSM-VIP, compared to the 40% reduction observed with non-targeted micellar formulation of paclitaxel and to the 25% reduction with the commercial paclitaxel formulation Taxol® (Krishnadas, 2004). These findings indicate that drug-loaded SSM-VIP promotes selective accumulation of these nanocarriers in breast cancer

cells, first, through the EPR effect, followed by binding of VIP to its receptors on these cells. As a result, the biodistribution and therapeutic index of the anticancer drug is further improved through active targeting of SSM to VIP receptors.

An advantage of VIP-surface grafted micelles over other ligand-targeted therapeutics is that VIP receptors are not expressed in the vascular endothelium (Reubi, 2003). Therefore, when VIP is associated with micelles, it only extravasates at the tumor site and cannot interact with healthy tissues, leading to reduced side effects. We have previously demonstrated in our laboratory that association of VIP (a potent vasodilator) with SSM eliminates the VIP-mediated decrease in the systemic arterial blood pressure of healthy mice (Onyuksel et al., 2011).

B. CURCUMIN

Numerous epidemiological studies in the last few decades have shown the chemopreventive effect of naturally-occurring dietary compounds, which have been partly attributed to the high content of bioactive, non-nutrient phytochemicals commonly found in fruits, vegetables, grains, spices, and beverages (Block et al., 1992; Rafter, 2002). Phytochemicals were found to possess anti-oxidant, anti-proliferative, and pro-apoptotic effects against many cancers, such as leukemia, prostate, breast, colon, brain, melanoma, and pancreatic cancer (Chan et al., 2009). Among these compounds, curcumin, owing to its numerous therapeutic effects, has been the focus of an extensive amount of research.

Curcumin is a hydrophobic polyphenol derived from the ancient Indian spice tumeric, the powdered rhizome of the herb *Curcuma longa* belonging to the ginger family (Aggarwal et al., 2007b). It has been used for generations in traditional Asian Indian medicine for the treatment of many disorders such as various respiratory conditions, wound-healing, inflammation, hepatic diseases, cough, sinusitis, and certain tumors (Goel et al., 2010; Lopez-Lazaro, 2008). Numerous studies over the past fifty years have suggested that curcumin is effective for lowering blood cholesterol levels; inhibiting platelet aggregation and thrombosis; suppressing type II diabetes-related symptoms, rheumatoid arthritis, colitis, inflammatory bowel disease, multiple sclerosis, and Alzheimer's disease; enhancing wound healing; inhibiting HIV replication, as well as preventing and treating certain types of cancer (Aggarwal et al., 2007b).

1. Chemistry and Pharmacology

Curcumin (diferuloylmethane; see Figure 4) is an orange-yellow colored crystalline powder, hydrophobic in nature and soluble in dimethylsulfoxide (DMSO), ethanol, acetone, and oils (Aggarwal et al., 2007b). Its structure has been identified as 1,6-heptadiene-3,5- dione-1,7-bis(4-hydroxy-3-methoxyphenyl)-(1E,6E) (Aggarwal et al., 2007b; Ravindran et al., 2009). This bis-α,β-unsaturated β-diketone structure exhibits keto-enol tautomerism. It has a pre-dominant keto form in acidic and neutral pH values and takes on an enol form at pH values above 7.0 which is unstable and degraded to ferulic acid and feruloylmethane (Anand et al., 2008; Kunnumakkara et al., 2008). Curcumin has a molecular formula of $C_{21}H_{20}O_6$, molecular weight of 368.37 and a melting point of 183°C (Aggarwal et al., 2003).

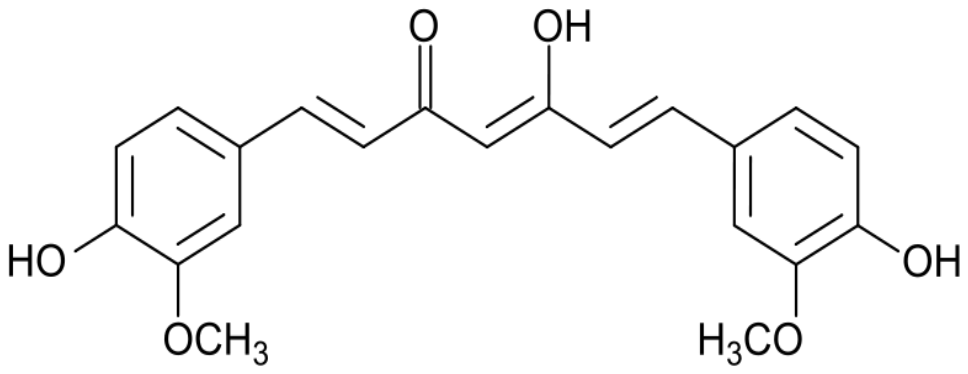

Figure 4. Chemical structure of curcumin.

Natural and synthesized analogs of curcumin have been described previously (Anand et al., 2008). These analogs reveal that the hydroxyl groups of curcumin are essential for its antioxidant activity, whereas the methoxy groups are indispensable for its antiinflammatory and antiproliferative activities (Ravindran et al., 2009). Commercially available preparations of

curcumin typically contain approximately 77% diferuloylmethane, 18% demethoxycurcumin, and 5% bisdemethoxycurcumin (Aggarwal et al., 2007b; Anand et al., 2008). Phase I studies with these preparations have demonstrated that curcumin is innocuous when administered at oral doses of up to 8 g per day (Cheng et al., 2001; Sharma et al., 2004). However, animal studies over the past three decades addressing pharmacokinetics of curcumin have revealed its extremely poor systemic bioavailability. Limitations such as poor aqueous solubility, poor absorption from intestine, low tissue distribution, degradation in gastrointestinal tract at neutral and alkaline pH, rapid metabolism leading to a short half-life, and rapid systemic elimination have been reported as the reasons for its poor bioavailability (Anand et al., 2007; Bansal et al., 2011).

Although the pharmacokinetic data in humans are inconclusive, a number of pilot and phase I clinical studies performed with curcumin have supported the findings in the preclinical models. In a study on healthy subjects, 2 g pure curcumin powder showed less than 10 ng/mL plasma curcumin 1 h postdose (Shoba et al., 1998). In a phase I clinical trial, oral doses of 4, 6, and 8 g curcumin daily for three months were administered to 25 patients with various precancerous lesions. The serum curcumin concentrations were detected as only 0.51, 0.63, and 1.77 μM, respectively (Cheng et al., 2001). Altogether, these studies have pointed out that the usefulness of curcumin may be curtailed as a result of its poor bioavailability.

Curcumin has been shown to possess a broad array of pharmacological activities including enhancement of wound healing; neuroprotection; analgesic, anti-viral, anti-fungal and anti-bacterial effects; as well as anti-inflammatory, anti-oxidant, anti-mutagenic, anti-metastatic, and anti-angiogenic activities (Aggarwal et al., 2007b). Numerous studies have

revealed that curcumin exerts these pharmacological activities by modulating a variety of molecular targets such as transcriptional factors, inflammatory cytokines, growth factors, receptors, kinases, other enzymes, and genes regulating cell proliferation and apoptosis, many of which are highly related to its cancer chemopreventive and chemotherapeutic activities (Aggarwal et al., 2007b). Up to now, as many as 33 proteins have been identified as direct targets of curcumin (Kunnumakkara et al., 2008). Given that multiple signaling pathways are involved in tumor formation and progression, curcumin, with its multi-targeting ability, has been suggested to possess a high therapeutic potential against cancer.

To date, numerous *in vitro* and *in vivo* studies have demonstrated the chemopreventive and chemotherapeutic potential of curcumin in a variety of different cancers including breast, lung, ovarian, prostate and pancreatic cancers, gastrointestinal cancers, leukemia, lymphoma, and many more (Anand et al., 2008; Lopez-Lazaro, 2008). Moreover, curcumin's biological activity against pancreatic cancer was recently confirmed in a phase II clinical trial (Dhillon et al., 2008). In this study, 25 patients with pancreatic cancer were given oral curcuminoids 8 g daily for up to 18 months, which was tolerated without toxicity. Despite its poor bioavailability (circulating curcumin levels peaked at 22 to 41 ng/mL), curcumin was shown to elicit biological activity in two patients, accompanied by increases in serum cytokine levels and down-regulated expression of nuclear factor kappa-light-chain-enhancer of activated B cells (NF-κB) and cyclooxygenase-2 (Dhillon et al., 2008).

2. Chemotherapeutic Potential of Curcumin in Breast Cancer

The anti-carcinogenic activity of curcumin in breast cancer has been reported in several studies (Kim et al., 2008; Ramachandran et al., 1999; Bachmeier et al., 2007; Aggarwal et al., 2005). A wide variety of mechanisms have been implicated for the anticancer activity of curcumin, including inhibition of mutagenicity, inhibition of proliferation, induction of apoptosis, generation of reactive oxygen species, and inhibition or suppression of different survival pathways, transcription factors such as NF-κB and activator protein-1, cell-cycle related proteins, and certain oncogenes. In addition, curcumin has also been shown to suppress inflammation, chromosomal damage, Pgp activity, angiogenesis, telomerase activity, and metastasis (Aggarwal et al., 2003; Kunnumakkara et al., 2008; Anand et al., 2008).

In a preclinical study on human breast cancer cells including hormone-dependent, hormone-independent, and multidrug-resistant cell lines, the antiproliferative effect of curcumin was shown to be time- as well as dose-dependent and correlated to the ability of curcumin to inhibit ornithine decarboxylase, an enzyme involved in polyamine synthesis which plays important roles in cell growth (Aggarwal et al., 2007a). Bachmeier *et al.* also evaluated the effect of curcumin *in vitro* on the human breast cancer cell line MDA-MB-231, as well as *in vivo* in a mouse metastasis model (Bachmeier et al., 2007). The *in vitro* study demonstrated that the apoptosis induced by curcumin was correlated with suppression of the survival pathway NF-κB. In addition, downregulation of major MMPs as a result of reduced activation of NF-κB by curcumin led to diminished invasion of MDA-MB-231 cells (Bachmeier et al., 2007). The *in vivo* study was performed on nude mice fed with a diet containing 1% curcumin after intercardiac inoculation of MDA-MB-231 cells. Thirty-five days after tumor implantation the animals were

sacrificed and the lung metastases were enumerated. Only 17% of the animals in the untreated group were found to have no or very few lung metastasis, while 68% of animals in the treated group were shown to be metastasis-free (Bachmeier et al., 2007). Aggarwal *et al.* also investigated the anti-metastatic effect of curcumin in mice (Aggarwal et al., 2005). In this study, primary human breast cancers were xenografted on nude mice and surgically removed after 58-60 days of inoculation. Dietary curcumin (2%) was given to animals beginning from the fifth day to the end of fifth week after the removal of the primary tumor. As a result of the curcumin treatment, the incidence of breast cancer metastasis to the lung was shown to decrease significantly. Moreover, this decrease was found to correlate with the suppression of NF-κB and matrix metalloproteinase-9 expression.

Overall, available experimental evidence suggest that curcumin has a vast potential for the chemotherapy of breast cancer. However, development of advanced drug delivery strategies that will overcome curcumin's bioavailability issues is essential for the future clinical development of this promising natural agent.

3. Nanoparticulate Formulations of Curcumin

In the last two decades, various formulation approaches including oral, injectable and topical formulations have been investigated to enhance the chemical stability, systemic bioavailability, and antitumoral activities of curcumin. These formulations have employed numerous novel drug delivery systems including polymeric nanoparticles, nanoemulsions, liposomes, and micelles (Bansal et al., 2011). Partitioning or encapsulation of lipophilic curcumin into the hydrophobic core of amphiphilic polymers or phospholipids of nanocarriers

not only increases the accumulation at the disease site, but also provides protection against degradation. For instance, in an *in vivo* rat model, encapsulation of curcumin in poly(lactic-co-glycolic acid) (PLGA) nanoparticles was shown to increase the bioavailability 26-fold as compared to oral curcumin suspension (Shaikh et al., 2009). In another study, encapsulation into PLGA polymeric nanospheres was found to improve the *in vitro* cytotoxic effects of curcumin on metastatic prostate cancer cell lines compared to free curcumin (Mukerjee et al., 2009). Moreover, an active targeting strategy via conjugation of curcumin-loaded PLGA nanoparticles with an ovarian cancer-specific antibody was demonstrated to be feasible as a means of increasing specificity for and internalization into the cancer cells (Yallapu et al., 2010). Similarly, active targeting of curcumin to folic acid overexpressing cancer cells was evaluated in a folic acid-conjugated polymeric carrier, in which folic acid was attached to a cyclodextrin ring through a PEG spacer (Salmaso et al., 2007). Encapsulation of curcumin in these targeted carriers was shown to efficiently increase its solubility (~3200 times) and stability (~12 times), while improving its cytotoxicity on folic acid overexpressing human nasopharyngeal tumor cells. Furthermore, a liposomal system prepared from dimyristoyl-sn-glycero-3-phosphocholine was also investigated for the delivery of curcumin (Li et al., 2005). In a xenograft murine model, this formulation was shown to inhibit the growth of tumors from BXPC3 and MiaPaCa2 cells when administered at 40 mg/kg for three times a week. The liposomal curcumin treatment on tumor-bearing animals was also found to reduce the expression of angiogenic markers such as CD31 and vascular endothelial growth factor, indicating the anti-angiogenic effect of curcumin (Li et al., 2005).

Novel nanotechnology-based formulations of curcumin are also found to be implicated in increasing the anticancer activity of a variety of chemotherapeutic agents. In an orthotopic pancreatic xenograft model in nude mice, the combination of gemcitabine plus polymeric micelle-encapsulated curcumin was found to improve the tumor growth inhibitory and antimetastatic effects compared to either single agent (Bisht et al., 2010).

Taken together, these data reveal that the development of nanotechnology-based formulations for the delivery of curcumin is critical to circumvent its bioavailability problems and hence realize its full potential in the clinical arena.

4. Curcumin-Loaded Sterically Stabilized Micelles

Recently, a novel lipid-based nanomedicine of curcumin in sterically stabilized micelles prepared from DSPE-PEG_{2000} was developed in our laboratory (Thaqi, 2011). Curcumin was efficiently solubilized in 1 mM SSM at concentrations as high as 180 µg/mL, giving a unimodal size distribution with a mean particle size of ~15 nm as determined by Dynamic Light Scattering (DLS). In addition, when the lipid concentration was scaled-up to 10 mM, solubility of curcumin was increased $1.6x10^5$ times compared to its solubility in aqueous media (~11 ng/ml) (Thaqi, 2011; Barry et al., 2009). As illustrated in Figure 5, curcumin was proposed to reside in the hydrophobic core of the micelles. Stability studies indicated that curcumin in 1 mM SSM (C-SSM) formulation remained stable in suspension for more than 10 days at room temperature. No degradation was detected for C-SSM for at least 8 hours, whereas 50% of free curcumin in phosphate buffer saline was found to decompose in the first 10 minutes, thus indicating the protective action of SSM against the influence of outside environment. Furthermore, an *in vitro*

cytotoxicity study on MCF-7 human breast cancer cell line showed that the anticancer activity of C-SSM formulation was significantly higher compared to free curcumin (IC_{50} 14 µM vs. 26 µM) which may be attributable to the protection of the drug in SSM, as well as efficient internalization of the drug-loaded micelles into cells (Thaqi, 2011). The latter was confirmed by the fluorescence microscopy images of MCF-7 cells, showing an approximately 3-fold increase in the uptake of curcumin after 48 hours of C-SSM treatment compared to free curcumin (Gulcur et al., 2011).

These preliminary data suggest that C-SSM hold a vast potential for enhancing curcumin's *in vivo* anticancer efficacy by overcoming its bioavailability issues through increased solubility and protection from degradation, leading to an increased circulation half life, and through increased accumulation of the drug at the target site. Moreover, C-SSM also possess all the advantages of sterically stabilized micelles over other delivery systems such as its (i) remarkably small size, (ii) ease of preparation, and (iii) FDA-approved biodegradable and biocompatible components.

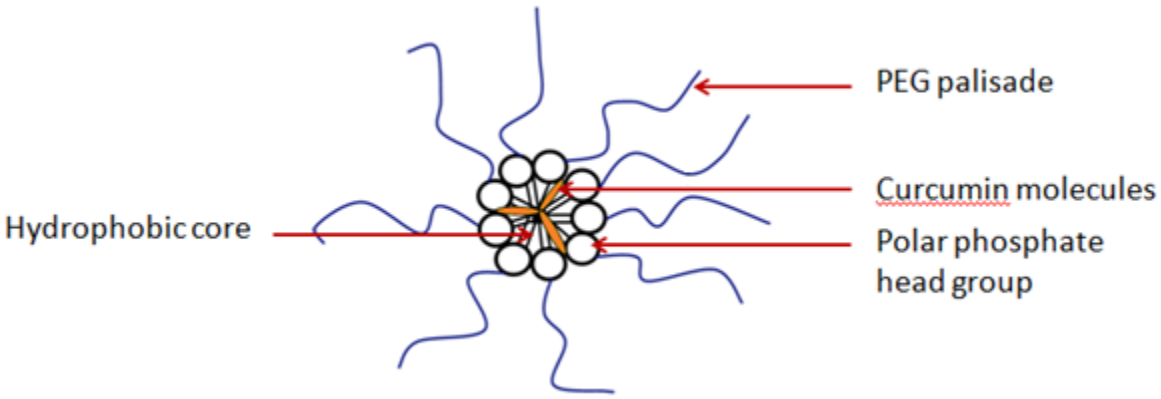

Figure 5. A cross-sectional representation of the proposed interaction of curcumin within the sterically stabilized micelles [adopted from (Thaqi, 2011)]. It is suggested that while one end of curcumin molecules interacts with the polar head groups through hydrogen bonding, the other end gets inserted deeper into the hydrophobic core due to the hydrophobic interactions between curcumin and the acyl chains of the phospholipid.

C. CANCER STEM CELLS AND CLINICAL IMPLICATIONS

Despite recent advances in breast cancer therapy and diagnosis, patients experience relapses in approximately 40% of all cases, accounting for more than 60% of breast cancer deaths, which underscores the relative failure of conventional chemotherapy and/or radiotherapy to provide a complete cure (Gerber et al., 2010; Widakowich et al., 2007). Conventional therapies have been designed to target the bulk of a tumor with the assumption that all cells within a cancer are equally tumorigenic. However, evidence is accumulating that each tumor contains a small, therapy-resistant sub-population of cells – the cancer stem cells (CSCs) – displaying tissue-specific stem cell properties, responsible for tumor initiation, propagation and regeneration.

The cancer stem cell (CSC) model of tumor propagation postulates that many cancers are hierarchically arranged, with CSCs, also referred to as the tumor-initiating cells, lying at the apex of the hierarchy (Velasco-Velazquez et al., 2011a). According to this model, only CSCs within the tumor possess the capacity to self-renew and to differentiate into the heterogeneous lineages of cancer cells that comprise the tumor (Figure 6A). Moreover, these cells are intrinsically more resistant to therapy than other cancer cells, and hence survive and repopulate the tumor after treatment (Figure 6B). Therefore, according to this model, it is of high importance to develop novel strategies to target the resistant CSC population for a relapse-free cure of the patient's disease.

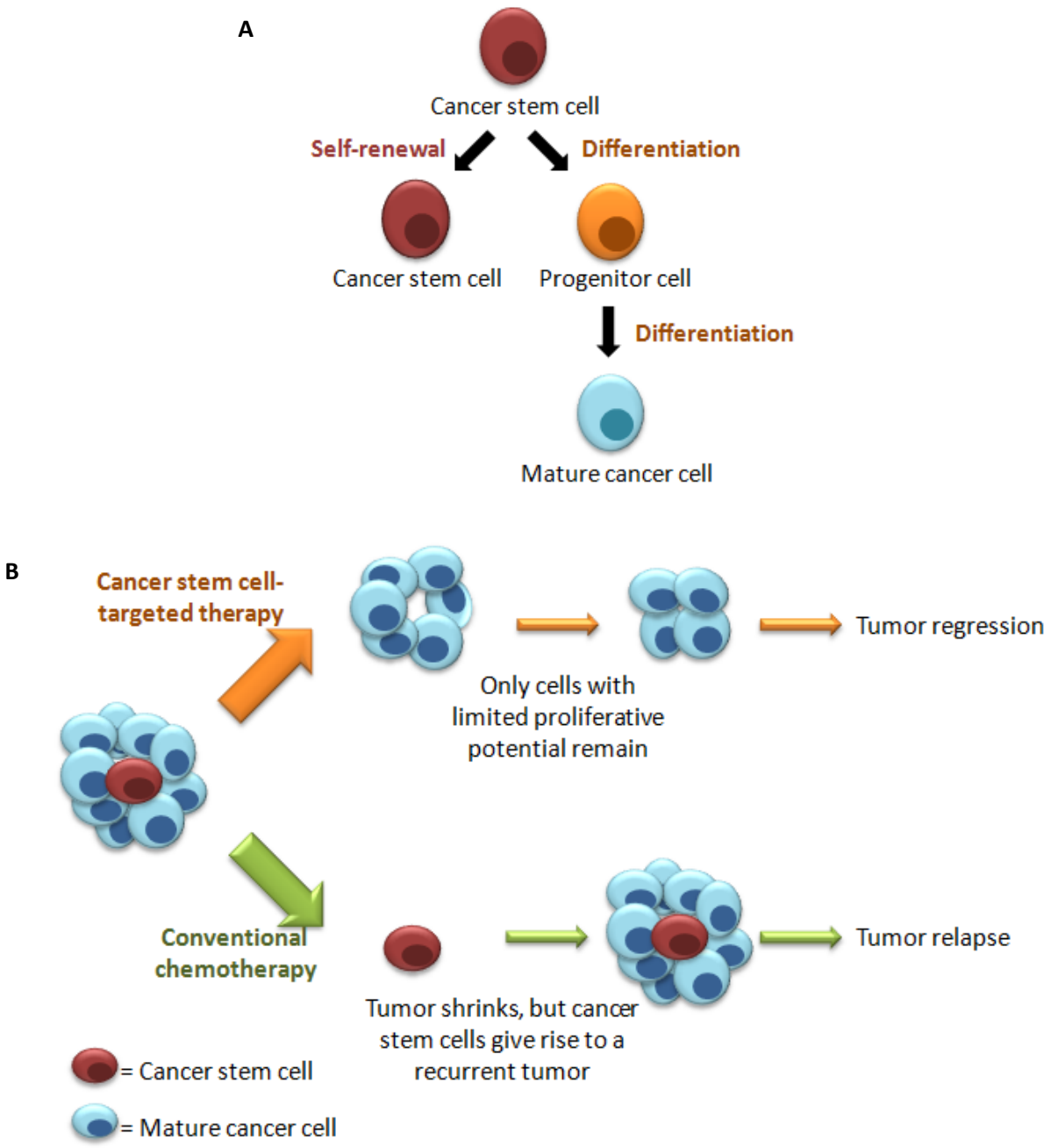

Figure 6. The cancer stem cell theory. (A) The hierarchy of cells as suggested by the cancer stem cell theory. According to this theory, cancer stem cells possess the ability to self-renew extensively, and also to differentiate into more mature cells called progenitor cells. After a certain number of divisions, the progenitor cells can further differentiate to give rise to mature cancer cells. (B) Cancer stem cell-targeted versus conventional chemotherapy. Conventional chemotherapies kill the bulk of the tumor, but leave behind cancer stem cells, which may cause tumor relapse. By contrast, the cancer stem cell-targeted therapies render tumors unable to generate new cells, and hence lead to tumor regression [adopted from (Reya et al., 2001)].

1. Identification and Isolation of Breast Cancer Stem Cells

Ever since the emergence of the CSC theory with the discovery of CSCs in leukaemia, CSCs have been identified in several solid tumors including breast, colon, prostate, pancreas, brain, lung, and head and neck tumors (Bonnet et al., 1997; Al-Hajj et al., 2003; Velasco-Velazquez et al., 2011b). The identification of putative CSCs in a solid tumor was first reported in the work of Al-Hajj *et al.* using cell surface $CD44^+/CD24^{-/low}/ESA^+$ (epithelial specific antigen-positive) markers and lineage$^-$ (Lin^-; lack of expression of CD2, CD3, CD10, CD16, CD18, CD31, CD64, and CD140b) to isolate cells from plural effusion or primary tumors of breast cancer patients (Al-Hajj et al., 2003). As few as 100 cells with this immunophenotype were able to form tumors when injected into the mammary fat pads of nonobese diabetic/severely combined immunodeficient (NOD/SCID) mice, while 5×10^4 unsorted cells were nontumorigenic. Moreover, tumors generated by $CD44^+/CD24^{-/low}Lin^-/ESA^+$ cells resembled the parent tumor with respect to the phenotypic heterogeneity of CD44, CD24 and ESA surface marker expressions, confirming the stem-like disposition of these cells.

Similarly, high aldehyde dehydrogenase isoform 1 (ALDH) activity has also been identified as a functional marker to isolate breast CSCs, as well as normal mammary stem cells (Ginestier et al., 2007; Charafe-Jauffret et al., 2009). ALDH, a detoxifying enzyme responsible for the oxidation of intracellular aldehydes into their corresponding carboxylic acids, has been shown to play important roles in the self-protection and differentiation mechanisms of normal stem cells (Sladek, 2003). Using the fluorometic Aldefluor® assay (StemCell Technologies, Vancouver, BC, Canada), Ginestier *et al.* demonstrated that high ALDH expression correlated with a poor clinical outcome (Ginestier et al., 2007). Moreover, a small overlap of $ALDH^+$ and

$CD44^{+}/CD24^{-/low}Lin^{-}$ cells was identified to possess the highest capacity to initiate tumor formation with as few as 20 cells injected. Ever since their identification, these CSC markers have been successfully utilized in numerous experimental protocols *in vitro* and *in vivo* to evaluate the potential efficacy of drugs to eliminate the CSC population (Gupta et al., 2009; Hirsch et al., 2009; Ginestier et al., 2010; Li et al., 2010).

It has been well established that CSCs show elevated expression of multidrug resistance efflux pumps compared to normal cancer cells, which may protect these cells from the intracellular accumulation of cytotoxic agents including chemotherapeutic agents, and thereby sustain tumor growth (Hirschmann-Jax et al., 2004; Dean et al., 2005). This property of CSCs has been used as a marker in the isolation and identification of a side population (SP) fraction displaying stem cell-like properties from a variety of cancer cells including breast cancer cells (Hirschmann-Jax et al., 2004; Christgen et al., 2007). SP fraction is detected by the exclusion of the fluorescent DNA-binding dye Hoechst 33342 as a result of its elevated expression levels of Pgp multidrug resistance efflux pumps compared to the non-SP cell fraction (Wu et al., 2008). However, this approach has several limitations as the SP fraction contains both stem cells and non-stem cells and as some stem cells are not contained in this fraction (Dean et al., 2005).

Breast CSCs have also been isolated from primary breast cancer cells and from breast cancer cell lines after *in vitro* propagation in suspension culture (Ponti et al., 2005; Fillmore et al., 2008). These studies demonstrated that breast cancer stem/progenitor cells, similar to human breast stem/progenitor cells, could be enriched in floating mammospheres based on their unique ability to survive in non-adherent suspension as spherical clusters. In this system, cells are seeded as single cells in low-attachment plates in serum-free media containing basic

fibroblast growth factor, epidermal growth factor, and insulin. Under these conditions, the normal cancer cells, lacking the ability to survive in an anchorage-independent manner, die, while a small number of cancer stem/progenitor cells survive to generate *tumorspheres*. These tumorspheres can be serially passaged at clonal density in an undifferentiated state, which is considered as an indirect marker of stem cell self-renewal. Hence, the tumorsphere forming efficiency of breast cancer cells upon serial passaging is commonly used to evaluate the functionality of the breast CSC population (Deng et al., 2009; Ginestier et al., 2010; Li et al., 2010).

2. Breast Cancer Stem Cells and Therapy Resistance

Although conventional chemotherapies and radiotherapies are initially effective in controlling tumor growth or even reducing tumor volume, many patients experience relapse over time (Gerber et al., 2010). Accumulating data from breast cancer cell lines and human breast cancer specimens provide supportive evidence that intrinsic resistance of tumorigenic CSCs could be the underlying reason for the recurrence of tumor after therapy (Phillips et al., 2006; Li et al., 2008; Gupta et al., 2009). These studies revealed that chemotherapy/radiotherapy enriched for the $CD44^{+/}CD24^{-/low}$ breast CSCs and increased the tumorsphere formation efficiency. Several mechanisms have been suggested to explain the observed therapy resistance of CSCs including their (i) relative quiescence as cytotoxic agents often target actively replicating cells, (ii) active DNA-repair machinery, (iii) resistance to drugs and toxins caused by the elevated expression of ATP-binding cassette (ABC) multidrug efflux pumps, (iv) elevated ALDH activity allowing to metabolize cytotoxics, and (v) evasion of

apoptosis (Dean et al., 2005; Al-Ejeh et al., 2011). As a result, a small sub-population of inherently resistant CSCs in tumors can survive following conventional chemotherapy/radiotherapy and mutate as a reaction to the effect of the therapy. Subsequently, the surviving and mutated CSCs can repopulate the tumor and generate recurrent tumors with a drug resistant phenotype.

3. Self-renewal and Differentiation Pathways in Breast Cancer Stem Cells

Normal adult stem cells possess the ability to produce the cells that constitute the organ and to propagate themselves through tightly regulated self-renewal and differentiation mechanisms unique to these cells. Self-renewal is defined as the ability of a cell to undergo division and form at least one daughter cell with a developmental potential identical to the mother cell, whereas differentiation is described as the ability of a cell to give rise to one or more types of mature cells with distinct developmental potentials (Rothenberg et al., 2009). A number of studies provide evidence that CSCs share these mechanisms for self-renewal and differentiation with the adult stem cells. However, most stem cell signaling pathways, including Notch, Hedgehog, B lymphoma Mo-MLV insertion region-1 (Bmi-1), and Wnt/β-catenin, appear to be aberrantly expressed in CSCs (Harrison et al., 2010; Liu et al., 2006; Li et al., 2003; Korkaya et al., 2009). Recently, Korkaya *et al.* showed that genetic knockdown of the protein phosphatase and tension homolog (PTEN) in normal human mammary epithelial cells enriches for the $ALDH^+$ breast CSCs and increases tumorigenicity in a xenograft model as a result of an Akt pathway-mediated increase in Wnt/β-catenin signaling (Korkaya et al., 2009). This work

reveals that Wnt pathway is implicated in the initiation and maintenance of breast CSCs, and that agents inhibiting this pathway may potentially be effective in targeting CSCs.

4. Targeting Breast Cancer Stem Cells with Curcumin

A growing body of experimental evidence has revealed curcumin's therapeutic potential to target cancer stem cells as a downregulator of a vast array of signaling pathways such as Wnt, Notch-1 and NFκ-B playing crucial roles in stem cell survival, as well as of many P-glycoproteins overexpressed on resistant cancer stem-like cells (Park et al., 2005; Wang et al., 2006; Choi et al., 2008). Recently, curcumin's inhibitory effect on this resistant population of cancer cells has been examined by several groups (Yu et al., 2009; Fong et al., 2010; Kakarala et al., 2010; Lim et al., 2011a). These reports have shown that curcumin inhibits the growth of tumorigenic and sphere-forming stem-like cells and improves the cytotoxicity of a variety of chemotherapeutic agents on these highly resistant cancer cells.

Yu *et al.* reported that the treatment of colon cancer cells with 5-fluorouracil and oxaliplatin (FOLFOX), led to the enrichment of cancer stem-like cells expressing high levels of CD133, CD44, CD166 and/or EGFR (Yu et al., 2009). On the contrary, treatment of FOLFOX-surviving colon cancer cells with curcumin, alone or in combination with FOLFOX, resulted in a marked inhibition of cancer stem-like cells, as evidenced by the reduction in CD44 and CD166 levels, as wells as by the impairment in colonosphere formation.

Fong *et al.* have examined curcumin's effect on the SP cell fraction of rat C6 glioma cells (Fong et al., 2010). In this study, curcumin treatment for 3-10 days or during the dye exclusion assay led to a marked depletion of the SP cell fraction suggesting curcumin's inhibitory effect on

the ABC transporter ABCG2 in stem cell-like glioma cells (Fong et al., 2010). These findings indicate that curcumin can reverse the chemoresistance of cancer stem-like cells caused by the overexpression of Pgp multidrug resistance efflux pumps, and improve the cytotoxic effects of other chemotherapeutic agents on these cells.

In their recent study, Kakarala *et al.* demonstrated curcumin's chemopreventive activity through its ability to modulate self-renewal of normal and malignant mammary stem cells (Kakarala et al., 2010). Curcumin, alone or in combination with piperine, suppressed mammosphere formation of cells from breast cancer cell lines or normal breast tissue and reduced the percentage of ALDH-positive cells. By contrast, it did not have toxicity to differentiated cells. The effect of curcumin on mammary stem cells was suggested to be mediated through its ability to inhibit Wnt signaling cascade as demonstrated by utilizing a TCF-Lef reporter assay system in MCF-7 cells (Kakarala et al., 2010).

Very recently, Lim *et al.* tested the effect of a polymeric nanoparticle formulation of curcumin on tumor-derived neurospheres from glioblastoma and medullablastoma cultures and showed that curcumin treatment resulted in a marked depletion of $CD133^+$ stem-like brain tumor cells (Lim et al., 2011a). These results suggested that suppression of insulin like growth factor, Akt 3 and hedgehog signaling pathways by curcumin could play a role in its effects on brain tumor stem-like cells. Additional studies are, however, required to test whether curcumin might also have an effect on non-neoplastic stem cells in the brain, which would lead to severe side effects.

Taken together, these studies indicate that curcumin, as a regulator of multiple signaling pathways involved in stem cell self-renewal and differentiation and multidrug resistance

transporters, holds great promise for developing treatment strategies targeting CSCs. However, development of a delivery system that will circumvent curcumin's bioavailability problems while sustaining the accumulation of the drug in these cancer cells will be necessary for achieving success in the clinical environment.

5. VIP Receptors as Targets for Breast Cancer Stem Cells

Although targeting the self-renewal pathways of CSCs with curcumin has yielded promising results in preclinical settings, efficient delivery of the drug into these cells remains an unresolved limitation. The highly resistant disposition of CSCs forces us to consider novel targeting strategies promoting higher drug exposure to these cells. In this respect, nanomedicines that can be tailored to actively target CSCs hold a great potential for the delivery of anti-CSC therapies with enhanced cell selectivity and maximum drug exposure. However, identification of targetable CSC-specific surface markers is still in its infancy due to limitations such as the low levels of CSCs in a cancer population and overlapping of certain markers with normal stem cells (Schatzlein, 2006; Deonarain et al., 2009). Despite these challenges, development of CSC-targeted nanomedicines may have a significant impact on reversing the occurrence of resistance and relapse in cancer therapy.

VIP receptors, as growth factor receptors highly overexpressed on the surface membrane of human breast cancer cells, stand out as a promising molecular target of CSCs for multiple reasons. First, breast CSCs have previously been shown to overexpress other peptide growth factor receptors such as EGFR and human epidermal growth factor receptor 2 (Winquist

et al., 2009; Mill et al., 2009; Korkaya et al., 2008; Magnifico et al., 2009). Second, there is a large body of evidence showing that VIP receptors are involved in stem cell-like properties such as regulating the expression of pluripotency transcription factors and cell differentiation (Callihan et al., 2011). Moreover, recent data from our laboratory demonstrated that paclitaxel loaded in SSM-VIP significantly increased cytotoxicity of the drug in multidrug resistant MCF-7 breast cancer cells transfected to overexpress multidrug resistance protein 1 [(Onyuksel et al., 2009a). This effect was proposed to be mediated by (i) receptor-mediated internalization of VIP-grafted micelles, rendering the drug inaccessible to membrane efflux transporters, and (ii) subsequent release of large concentrations of paclitaxel, overwhelming efflux pumps and eventually leading to cell death. The findings of this study indicated that VIP receptor targeting of SSM could by-pass the multidrug resistance of breast cancer cells expressing high levels of membrane efflux transporters similar to the breast CSC population.

D. SIGNIFICANCE OF THE PROJECT

Breast cancer is the most commonly occurring cancer and the leading cause of cancer death in females worldwide. In 2008 alone, 1.38 million new cases of breast cancer were diagnosed and 458,400 women died of breast cancer (Jemal et al., 2011). Despite decreasing breast cancer death rates in North America and Europe over the past two decades, largely as a result of early detection through mammography and improved treatment strategies, a significant proportion of patients with early stage breast cancer and almost all patients with metastatic disease experience a relapse. One possible explanation for the occurrence of relapse is the existence of a rare subpopulation of treatment resistant CSCs with high tumorigenic and invasive capacity that may drive tumor initiation, propagation and relapse. According to the CSC model, conventional chemo/radiation therapies can deplete the bulk of the tumor, but selectively enrich resistant CSCs, which remain quiescent in the G-null phase until stimulated to proliferate and eventually to give rise to a recurrent tumor. Therefore, the CSC paradigm has important implications for the urgent need to re-examine current cancer therapies and to develop novel strategies to target CSCs. However, targeting CSCs has significant technical challenges due mostly to their resistance mechanisms and lack of identified molecular and cellular targets.

In this thesis project, we aimed to address the important issue of developing a cancer therapy that can target CSCs in a safe and effective way. To begin to address this issue, we first demonstrated the enhanced anti-CSC activity of C-SSM (a novel, sterically stabilized nanomicellar formulation of curcumin previously developed in our lab) on a breast cancer cell line. Next, we identified a novel cellular target overexpressed on CSCs and developed an

actively targeted nanomicellar formulation of curcumin based on the use of this marker. Lastly, we demonstrated the benefit of using an active targeting strategy to further improve curcumin's ability to eliminate breast CSCs.

The successful completion of this project bridges an important gap between the implications of the cancer stem cell hypothesis to develop new cancer treatment strategies and the nanotechnology applications to target CSCs. This should eventually lead to safe and more effective therapies for breast cancer, as well as other types of cancers possessing a CSC population, with a potential to eliminate recurrence, thereby increasing tumor remission and survival of patients.

E. HYPOTHESIS AND SPECIFIC AIMS

The overall goal of this thesis project was to develop a safe and efficacious nanomedicine for the treatment of breast cancer that will target and eliminate the cancer stem cell population. We hypothesized that significant *in vitro* elimination of breast cancer stem cells could be achieved with curcumin-loaded nanomicelles and that the efficacy of this formulation could be further improved by incorporating an active targeting strategy.

Accordingly, the specific aims of this project were as follows:

Aim 1. *Evaluate the <u>in vitro</u> inhibitory effect of C-SSM on the breast CSC population.*

It is hypothesized that using SSM as a drug delivery vehicle for curcumin significantly improves its anti-CSC activity compared to free curcumin.

1.1. Evaluate the inhibitory effects of C-SSM or free curcumin on primary and secondary tumorsphere forming efficiency of MCF-7 human breast cancer cells

1.2. Determine the cytotoxic effects of C-SSM or free curcumin on the $CD44^{+}/CD24^{-/low}$ breast CSC population of MCF-7 cells

Aim 2. *Reveal a novel cellular target overexpressed on the surface of breast CSCs.*

Determine the level of VIP receptor expression on $CD44^{+}/CD24^{-/low}$ CSCs from MCF-7 cells. It is hypothesized that breast CSCs express high levels of VIP receptors and therefore are good candidates for active targeting of these cells.

Aim 3. *Develop and characterize a novel formulation of curcumin in VIP-surface grafted SSM (C-SSM-VIP), and test its ability to improve the anti-CSC activity of C-SSM and free curcumin <u>in vitro</u> on breast cancer cells.*

It is hypothesized that curcumin can successfully be encapsulated in VIP-grafted SSM, and that actively targeted delivery of this natural compound will further improve its efficacy to eliminate the resistant CSC population in breast cancer cells.

3.1. Prepare and characterize C-SSM-VIP

3.2. Evaluate the inhibitory effects of C-SSM-VIP, C-SSM or free curcumin on the tumorsphere forming efficiency of MCF-7 cells

II. MATERIALS AND METHODS

A. MATERIALS

1. Preparation and Characterization of Nanomicellar Formulations of Curcumin

1,2-Distearoyl-*sn*-glycero-3-phosphoethanolamine-*N*-methoxy-[poly(ethylene glycol); PEG M_W 2,000] (DSPE-PEG_{2000}) was obtained from LIPOID GmbH (Ludwigshafen, Germany). Curcumin (98% pure) was obtained from ChromaDex (Irvine, CA). VIP was synthesized by the Protein Research Laboratory at the Research Resources Center, University of Illinois at Chicago. Sunbright® DSPE-PEG_{3400}-NHS [1,2-dioleoyl-*sn*-glycero-3-phosphoethanolamine-*n*-[poly(ethylene glycol)]-*N*-hydroxy succinamide; PEG M_W 3,400] was purchased from NOF Corporation (Tokyo, Japan). Gibco® phosphate buffered saline (PBS; pH 7.4) was obtained from Mediatech Cellgro® (Herndon, VA). (N- [2-Hydreoxyethyl] piperazine-*N'*-[2-ethanesulfonic acid]) (HEPES) was obtained from Sigma Chemical Company (St. Louis, MO). High performance liquid chromatography (HPLC)-grade methanol was obtained through Fisher Scientific (Pittsburgh, PA).

2. Cell Culture and Treatment

MCF-7 human breast cancer cell line was obtained from American Type Culture Collection (Manassas, VA, US). Dulbecco's Modification of Eagle's Medium (DMEM), penicillin-streptomycin solution, trypsin-ethylenediaminetetraacetic acid (EDTA) solution, and PBS (pH 7.4) were all from Mediatech Cellgro® (Herndon, VA). Fetal bovine serum (FBS) was purchased from Invitrogen (Carlsbad, CA). Sterile-filtered DMSO was from Sigma (St. Louis, MO).

3. Tumorsphere Culture

24-well ultra-low attachment plates were obtained from Corning (Corning, NY). MammoCult® Human Medium Kit with basal medium and proliferation supplements and Heparin were from StemCell Technologies (Vancouver, Canada). Hydrocortisone was from Sigma (St. Louis, MO). Hank's balanced salt solution (HBSS) was from Invitrogen (Carlsbad, CA).

4. Flow Cytometric Analysis of $CD44^{+}/CD24^{-/low}$ Breast CSCs

R-Phycoerythrin (PE)-conjugated $IgG2_{a\kappa}$ antibody against human CD24 (CD24-PE; clone ML5), Allophycocyanin (APC)-conjugated $IgG2_{b\kappa}$ antibody against human CD44 (CD44-APC; clone G44-26) and corresponding mouse isotype-matched antibodies were obtained from BD Pharmingen (San Diego, CA). Bovine serum albumin (BSA) and EDTA were from Sigma (St. Louis, MO).

5. VIP Receptor Ligand-Binding Analysis

Fisherbrand® single cytology funnels and paraformaldehyde were obtained from Fisher Scientific (Pittsburgh, PA). Poly-L-lysine-coated adhesive microscope slides were from Labscientific Inc. (Livingston, NJ). 5-carboxyfluorescein (FAM)-labeled VIP was obtained from Anaspec (Fremont, CA). VIP (unlabeled) was synthesized by the Protein Research Laboratory at the Research Resources Center, University of Illinois at Chicago. Bacitracin was from Research Products International (Mount Prospect, IL). Pefabloc was from Sigma (St. Louis, MO). Vectashield® mounting medium with 4',6-diamidino-2-phenylindole (DAPI) fluorescent stain was from Vector Laboratories (Burlingame, CA).

B. METHODS

1. Evaluation of the *In Vitro* Inhibitory Effect of C-SSM on the Breast Cancer Stem Cell Population

The putative breast CSCs were first identified as cells isolated from primary breast tumors or mammary cell lines based on a $CD44^{+}/CD24^{-/low}$ immunophenotypical profile (Al-Hajj et al., 2003). Shortly after, cancer stem/progenitor cells were also found to be enriched in tumorspheres derived from breast cancer cells, owing to the unique ability of stem cells to grow and form spheres in non-adherent culturing conditions (Dontu et al., 2003; Ponti et al., 2005). Therefore, in order to evaluate the *in vitro* anti-CSC activity of C-SSM, we tested its effect on the primary and secondary tumorsphere-forming ability, as well as on the $CD44^{+}/CD24^{-/low}$ CSC population of the MCF-7 human breast cancer cell line and determined whether the observed effects are similar to or greater than that of free curcumin.

For determining C-SSM's effect on tumorsphere formation, two different concentrations of curcumin, one above and one below the IC_{50} value of C-SSM (10 μM and 20 μM), were tested. Samples of C-SSM and empty SSM were prepared and characterized for particle size by dynamic light scattering (Agilent 7030 NICOMP DLS, Agilent Technologies, Santa Clara, CA). C-SSM samples were also characterized for curcumin content using Prominence series high performance liquid chromatography (Shimadzu; Columbia, MD). Thereafter, MCF-7 cells were treated for 72 hours with 10 μM and 20 μM concentrations of C-SSM or free curcumin, as well as with empty SSM, DMSO or PBS control samples in adherent conditions. Treated cells were then detached and plated in 24-well ultralow attachment plates for tumorsphere culture. At the

end of 7 days of culture, sphere forming efficiencies and average sphere sizes were evaluated from the first passage (primary spheres) and after the second passage (secondary spheres) of tumorspheres.

For determining C-SSM's effect on the $CD44^{+}/CD24^{-/low}$ breast CSC population, MCF-7 cells were treated for 72 hours with the treatment groups as described above. Thereafter, treated cells were collected by dissociation and incubated with antibodies against human CD44 and CD24. The effect of the treatment groups on the percentage of surviving $CD44^{+}/CD24^{-/low}$ cells, as well as on the internalization of curcumin by the CSC and normal cancer cell populations were analyzed using flow cytometry.

1.1. Preparation of the Curcumin Nanomedicine C-SSM

A stock solution of 180 µg/mL curcumin in 1 mM sterically stabilized phospholipid micelles was prepared using the film rehydration method as previously described in our laboratory (Thaqi, 2011). Briefly, weighed amount of DSPE-PEG_{2000} and curcumin were dissolved in methanol in separate vials and vortexed with a Thermolyne type 37600 vortex mixer till complete dissolution. Equal volumes of DSPE-PEG_{2000} and curcumin solutions were then added to round bottom flasks and the mixtures were vortexed. Methanol was subsequently removed using a vacuum rotary evaporator (BUCHI Labortechnik AG; Flawil, Switzerland) under a stream of argon and a vacuum (650 mm Hg pressure) at 55°C and 150 rpm for 30 minutes. The residual solvent from the resulting film was removed under vacuum overnight in dark. Thereafter, the dried film was rehydrated with PBS (pH 7.4). Flasks were vortexed till the film was dissolved and sonicated for 5 minutes in a Fisher B2200R-1 bath sonicator (Pittsburgh, PA). Flasks were then

flushed with Argon, sealed, and allowed to equilibrate in dark for 2 hours at 25°C to produce C-SSM.

1 mM stock dispersions of empty SSM were prepared following the same procedure described above, but with no drug.

1.2. Characterization of C-SSM

1.2.1. Particle size analysis

Hydrodynamic diameters of the C-SSM and empty SSM samples were measured by dynamic (also known as quasi-elastic) light scattering (DLS) using Agilent 7030 NICOMP DLS/ZLS particle sizer (Santa Clara, CA). DLS uses scattered light to measure the hydrodynamic dimeter [*d(H)]* of particles suspended in a solvent, as derived from the Stokes-Einstein relation,

(Eq. 1) $$d(H) = \frac{kT}{3\pi\eta D}$$

where, *k* is the Boltzmann's constant (1.38 X 10^{-16} erg K^{-1}), *T* is the absolute temperature, *η* the shear viscosity of the solvent, and *D* is the diffusion coefficient of the particles (Malvern Instruments).

The hydrodynamic particle diameter distributions of C-SSM in aqueous media were obtained from this equation using the following parameters: *η* = 0.933 cP, *T* = 296 K, refractive index = 1.33, scattering angle = 90˚. Samples were run for a minimum of 5 cycles with 3 minutes run time for each cycle. The collected data were analyzed as NICOMP intensity- and volume-weighted particle size distributions.

1.2.2. High performance liquid chromatography (HPLC) analysis

The curcumin content of 180 µg/mL curcumin in 1 mM C-SSM samples prepared in Section 1.1 above was analyzed by reversed-phase HPLC (RP-HPLC). RP-HPLC utilizes a non-polar stationary phase (a column containing a microparticulate porous packing material grafted with hydrophobic ligands) and an aqueous, moderately polar liquid mobile phase for the separation of a wide variety of solutes (Aguilar, 2004). The separation of a mixture of solutes in RP-HPLC stems from their differential affinity for and hence the adsorption to the stationary phase. This degree of binding affinity determines the retention time of the solute in the stationary phase and depends highly on the structure of the solute and the immobilized ligands. As a result, solutes are generally eluted in order of increasing molecular hydrophobicity.

For the RP-HPLC analysis of curcumin, a protocol previously described in our laboratory was followed (Thaqi, 2011). Briefly, the C-SSM samples were diluted with methanol and vortexed. 100 µL from each sample was added into HPLC vials. Each sample was analyzed in triple run using the HPLC parameters listed in Table 1 and average absorbance values corresponding to average peak areas were calculated.

A curcumin calibration curve was generated by analyzing standard curcumin solutions of a range of known concentrations (12.5 – 100 µg/mL curcumin in methanol) in triple run using HPLC. The average peak areas were plotted to determine a best fit line using the linear regression model, which served as the calibration curve. The linear equation obtained from the calibration curve was used to determine the actual curcumin concentration of the C-SSM samples.

TABLE I. HPLC parameters used in the setup of curcumin concentration detection

Mobile phase	Methanol : water (with 0.1%trifluoro acetic acid) : acetonitrile (39.5 : 350 : 460)
Rate of flow	0.750 mL/min
Sample volume injection	20 µL
Detection wavelength	425 nm
Temperature	25˚C
Column type	Zorbax 300 SB-C18, 5µm pore size (250 x 4.6 mm, Agilent Technologies, Santa Clara, CA)
Sample run time	10 minutes
Retention time	6.1 minutes

1.3. Cell Culture

MCF-7 human breast cancer cells were grown as monolayers until 80 – 90% confluency in DMEM supplemented with 10% FBS and 1% penicillin-streptomycin solution at 37˚C in a humidified 5% CO_2 atmosphere. The medium was changed every other day. For passaging, cells were washed three times with PBS and incubated with trypsin-EDTA for 5-7 minutes at 37˚C and 5% CO_2. Thereafter, cells were suspended in medium and centrifuged at 1000 rpm for 5 minutes. The cell pellet was resuspended in medium and divided at optimal subcultivation ratio to be cultured at 37˚C and 5% CO_2.

1.4. Treatment of MCF-7 Breast Cancer Cells in Adherent Conditions

C-SSM samples prepared in section 1.1 above were diluted with 1 mM DSPE-PEG_{2000} lipid solution (for keeping the lipid concentration above the CMC to prevent breaking of micelles) to

obtain the final concentrations of 10 µM curcumin in approximately 20 µM SSM (10 µM C-SSM) and 20 µM curcumin in approximately 40 µM SSM (20 µM C-SSM) when added to the wells for treatment. Likewise, empty SSM control samples were also diluted with 1 mM lipid solution to give a 40 µM lipid concentration in the wells. In addition, curcumin solutions with 0.5% sterile-filtered DMSO in DMEM were prepared by dissolving a weighted amount of curcumin in warm (~37°C) 100% DMSO, vortexing until dissolution and diluting this solution with DMEM to obtain 10 µM and 20 µM final curcumin concentrations in the wells. Necessary cautions were taken to minimize light exposure in the handling of curcumin-containing solutions in order to prevent degradation by light.

For growing MCF-7 human breast cancer cells, a cell suspension was prepared as described above in Section 1.3 and cell density was adjusted to 1.1 x 10^5 cells/ml. Suspended cells were then seeded in adherent 6-well plates and allowed to attach overnight. On the following day, cells were treated with 600 µl of the treatment samples listed in Table 2. Four wells were treated per treatment group. Thereafter, plates were incubated for 72 hours at 37˚C and 5% CO_2.

TABLE II. LIST OF THE TREATMENT GROUPS USED IN THE STUDY PRESENTED IN SECTION II.B.1.4

Treatment Type	**Treatment Name**
Treatment Groups	10 µM C-SSM
	20 µM C-SSM
	10 µM C-DMSO
	20 µM C-DMSO
Vehicle Controls	40 µM empty SSM
	0.5% DMSO
Negative Control	PBS

1.5. Tumorsphere Formation Assay

The procedures for the tumorsphere culture were adopted from manufacturer's (StemCell Technologies, Vancouver, Canada) instructions and the previously described procedures of Dontu *et al.* and Ponti *et al.* (Dontu et al., 2003; Ponti et al., 2005). Mammocult® Human Medium Kit (StemCell Technologies), a commercially available serum-free culture medium optimized for the culture of tumorspheres from human breast cancer cell lines, was used for the tumorsphere culture. Complete Mammocult® medium was prepared according to company instructions by supplementing the medium with heparin and hydrocortisone.

The work flow for the tumorsphere formation assay is illustrated in Figure 7. After incubating the treated MCF-7 cells from Section 1.4 for 72 hours, cells were rinsed twice with HBSS to remove excess culture medium, dissociated enzymatically with trypsinization as described in Section 1.3 as well as mechanically with a 22-gauge needle, and resuspended in the complete Mammocult® medium. Cells from two wells of each treatment group were collected together to obtain two test groups per treatment group. Thereafter, cells were strained through a 40 µm cell strainer to obtain a single cell suspension and enumerated using Z^{TM} Series Coulter Counter® (Beckman Coulter, Inc.; Schaumburg, IL). Subsequently, the single cell suspension was plated in 24-well ultra-low attachment plates at a density of 15,000 cells/mL.

After 7 days of culture, average sphere-forming efficiency (SFE) of each treatment group was evaluated under inverted Olympus IX70 fluorescent microscope equipped with a CCD camera (4x objective lens; UIC Biopharmaceutical Sciences Department, Gemeinhart Lab) by scanning wells and enumerating spheres that are larger than 60 µm in diameter manually using

ImageJ Software. In addition, primary tumorspheres from 3 wells of each test group were harvested together by centrifugation and dissociated enzymatically with trypsin as well as mechanically by triturating the tumorsphere pellet with a pipette for 2 minutes. Thereafter, average tumorsphere size was measured by manually performing a viable cell count using trypan blue and recording the number of live cells per well (N_c). The tumorsphere size was calculated in terms of the average number of live cells per sphere as shown below:

$$\text{Tumorsphere size} = N_c / N_s \quad \text{[cells/tumorsphere]} \qquad \text{(Eq.2)}$$

where N_s is the number of cells plated in one well of the ultra-low attachment plates (6,000 cells/well).

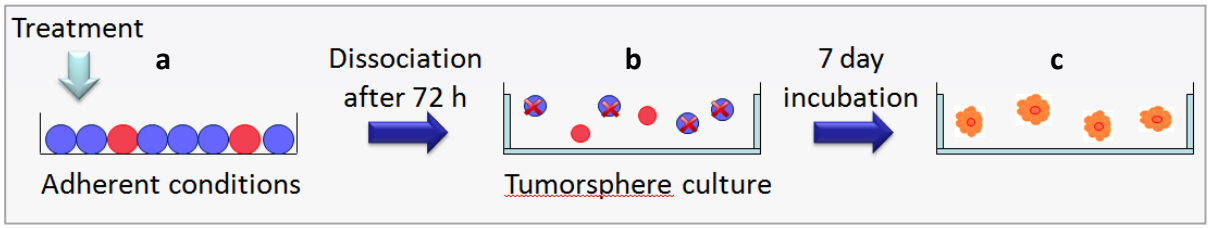

Figure 7. Schematic work flow for the tumorsphere formation assay. (a) MCF-7 cells consisting of cancer stem cells (CSCs; showin in red) and mature cells (shown in blue) are treated in adherent conditions for 72 h. (b) Treated cells are seeded in the tumorsphere culture as a single cell suspension. Only CSCs can survive and form tumorspheres. (c) At the end of 7 days of culture, tumorspheres, consisting of CSCs and their progenitors (shown in orange), are evaluated.

The single cell suspension obtained from the primary tumorspheres was re-seeded in ultra-low attachment plates at a low density of 2,000 cells/mL and incubated for 7 days to generate the second generation of tumorspheres (secondary tumorspheres). Sphere-forming efficiency and average tumorsphere size of the secondary spheres were evaluated as described above.

1.6. Flow Cytometric Analysis of the $CD44^{+}/CD24^{-/low}$ Breast Cancer Stem Cell Population

Flow cytometry is a powerful tool for measuring and analyzing the physical and chemical characteristics of fluorescently labeled cells, as well as for sorting them based on their characteristics so as to isolate the population of interest. Figure 8 shows a simplified diagram of a flow cytometer, where cells or particles individually pass through a focused laser beam as they flow in a fluid stream. A flow cytometer has forward and side scatter detectors to detect the amount of scattered light or emission of a fluorescence label, which can be converted to digital data by a computer (Mittag et al., 2011). Flow cytometry offers high precision and sensitivity, in addition to the capacity to rapidly analyze large numbers of cells, and hence provides high levels of statistical validity even with very rare subpopulations (Preffer et al., 2009).

In this experiment, flow cytometric analysis was employed to test the effect of C-SSM treatment on the $CD44^{+}/CD24^{-/low}$ CSC population of MCF-7 breast cancer cells. Briefly, cells were seeded in tissue culture dishes at a cell density of $1.1x10^{5}$ cells/mL and allowed to attach overnight. On the next day, they were treated with the treatment samples (listed in Table 2) prepared as described in Sections 1.1 and 1.4 above. After 72 hours of incubation, MCF-7 cells were rinsed thrice with PBS (pH 7.4), dissociated enzymatically with trypsin and resuspended in 1 mL ice cold PBS. Cells from the suspensions were enumerated using Coulter Counter® and incubated in the antibody solution of CD24-PE and CD44-APC in PBS with 3% BSA for 10 minutes on ice (1:3.2:20 v/v/v, respectively; $5x10^{6}$ cells/mL). Isotype-matched antibodies were used as negative controls and for gating purposes. After incubation, cells were washed twice by

centrifugation at 1200 rpm and 4˚C for 5 minutes in ice-cold PBS with 3% BSA, resuspended in PBS and passed through 35-µm filter just prior to sort. The samples were analyzed for fluorescence from CD44-APC, CD24-PE and curcumin with a Cyan™ ADP Analyzer (Beckman Coulter, Inc.; Schaumburg, IL) by Research Resources Center Flow Cytometry Service at the University of Illinois at Chicago. Dead cells were excluded by gating for cells based on forward versus side scatter.

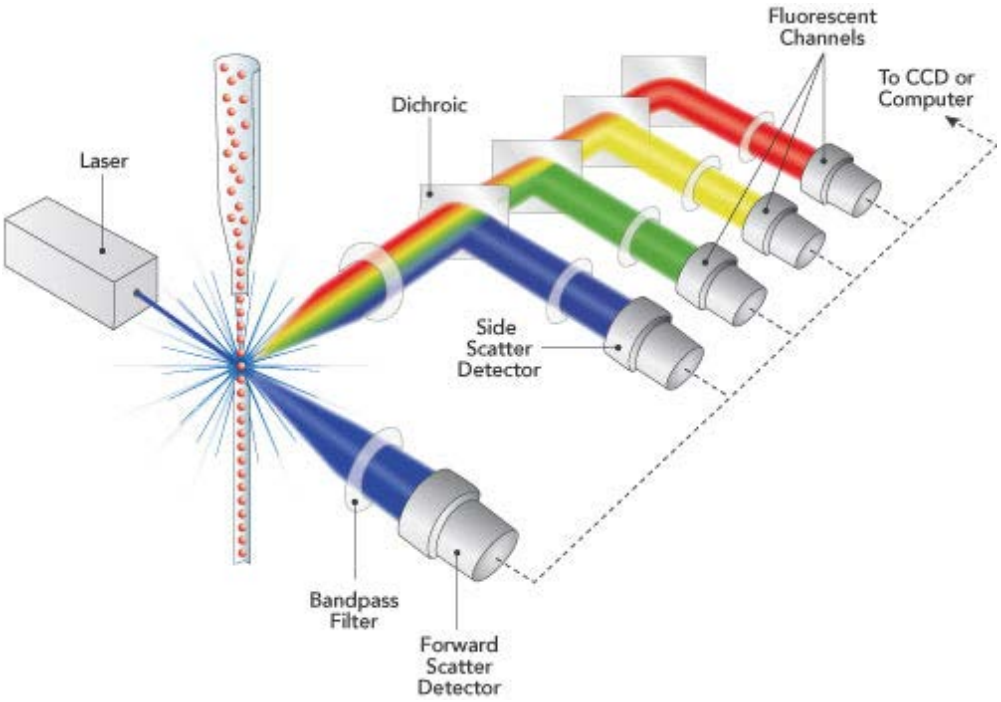

Figure 8. Schematic diagram of a flow cytometer [from (Semrock Inc.)].

2. Determination of the Level of VIP Receptor Expression on $CD44^{+}/CD24^{-/low}$ MCF-7 Cancer Stem Cells

Accumulated evidence, including previous studies in our laboratory, suggests that VIP receptors hold great potential as molecular targets for diagnosis, prevention and treatment of breast cancer, specifically by receptor-targeted delivery of chemotherapeutic agents (Dagar et

al., 2001a). The expression of VIP receptors on human and rat breast cancer tissues has been previously examined in our laboratory using a fluorescence-based ligand binding assay, followed by visualization with a fluorescence microscope (Dagar et al., 2001b).

This experiment was designed to investigate the level of VIP receptor expression on breast CSCs compared to the expression on normal breast cancer cells from the MCF-7 cell line, with the aim of revealing a novel cellular target overexpressed on the surface of breast CSCs. For this purpose, MCF-7 cells were sorted using flow cytometry into $CD44^{+}/CD24^{-/low}$ CSC and $CD44^{+}/CD24^{high}$ normal cancer cell populations. The sorted cells were cytospun to glass slides and a ligand-binding assay was used to stain VIP receptors as described previously in our laboratory with some modifications (Dagar et al., 2001b). Lastly, fluorescence from the slides was visualized under a confocal microscope.

2.1. Confocal Microscopy

Confocal microscopy is a widely used method for imaging either fixed or living tissues that have been labeled with fluorescent probes. The confocal microscope eliminates the drawback of defocused light experienced in conventional light microscopes by exploiting the confocal principle (Erie et al., 2009). As demonstrated in Figure 9, light from a laser source is used to illuminate a pinhole aperture whose image is focused at a single point on the specimen by an objective lens. The emitted light by this point on the specimen is collected and focused onto a second pinhole aperture by another objective lens. Light leaving this conjugate aperture reaches the observer or camera. The light reflected by the specimen is only detected from the

focal point when it is co-focused with the detection aperture. Emitted light from any other (out of focus) point on the specimen is not detected, and therefore does not contribute to the final image. This way, the confocal design improves both axial and lateral resolution compared to conventional light microscopes.

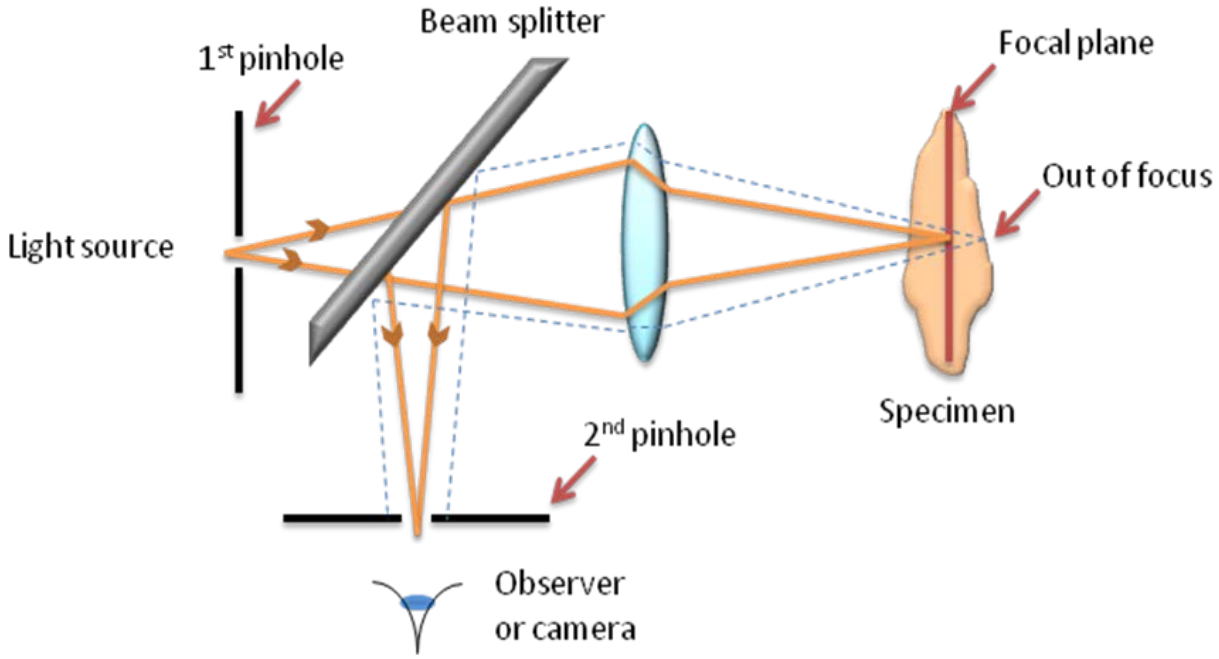

Figure 9. Schematic representation of the optical principles of confocal microscopy [adopted from (Erie et al., 2009)].

2.2. Procedures

Briefly, MCF-7 cells (untreated) were first stained with antibodies against CD44 and CD24, as well as isotype matched antibodies as described above in Section 1.6. After two washes with 3% BSA in PBS (pH 7.4), cells were resuspended in ice-cold sorting buffer (1% BSA and 2mM EDTA in PBS). Thereafter, stained MCF-7 cells were sorted into $CD44^{+}/CD24^{-/low}$ CSC and $CD44^{+}/CD24^{high}$ normal cancer cell populations with a Beckman Coulter MoFlo™ (Beckman

Coulter, Inc.; Schaumburg, IL) by Research Resources Center Flow Cytometry Service at the University of Illinois at Chicago.

Sorted cells were washed twice with PBS by centrifugation and cytospun onto poly-L-lysine coated glass slides ($5x10^4$ cells/mL) at 1000 rpm for 5 minutes using a Shendon CytoSpin Cytocentrifuge (Thermo Fisher Scientific, Waltham, MA; UIC Biopharmaceutical Sciences Department, Beck's Lab) within 1 hour after sorting. The resulting cell smears were allowed to moderately air dry, which was followed by fixing the cells with a 4% paraformaldehyde solution at 37^{o}C for 10 min. Unspecific binding to cells was blocked by 30 minute incubation in PBS with 10% FBS, whereupon cells were stained with 0.5 µM FAM-labeled VIP in binding buffer (DMEM with 0.1% bacitracin and 50µM Pefabloc to prevent enzymatic degradation of VIP *in vitro*) at 37^{o}C for 1 hour. Controls included an autofluorescence control, where cells were incubated in binding buffer without FAM-VIP, and a nonspecific binding control, where cells were treated with unlabeled VIP before incubation with FAM-labeled VIP. After excessive washing with PBS, cells were mounted with Vectashield® mounting medium (containing DAPI nuclear stain) under glass coverslips.

The fluorescence signals from FAM (excitation/emission: 492/518 nm) and DAPI (excitation/emission: 360/460 nm) were detected with a Carl Zeiss LSM 510 Meta confocal microscope (25x magnification; Research Resource Center Confocal Microscopy Facility, University of Illinois at Chicago). The levels of VIP receptor expression on MCF-7 CSCs and normal cancer cells were evaluated by quantifying the mean fluorescence intensities from the micrographs with the Zeiss LSM Image Browser software.

3. Development, Characterization and the *In Vitro* Anti-Cancer Stem Cell Activity of a Novel Formulation of Curcumin in VIP-Surface Grafted SSM

This study was designed to determine whether delivering curcumin through active targeting of VIP receptors can further improve the anti-CSC activity of C-SSM on MCF-7 cells. For this purpose, a curcumin formulation actively targeted to VIP receptors was developed through surface modification of C-SSM with covalently conjugated VIP, which was followed by characterization of this formulation for particle size and drug content. Thereafter, MCF-7 cells were treated with C-SSM-VIP, C-SSM, C-DMSO, or with vehicle controls (empty SSM, DMSO and PBS) in tumorsphere culture and the effect of the treatments on sphere-forming efficiency was evaluated.

3.1. Preparation and Characterization of C-SSM-VIP

A stock dispersion of 225 µg/mL curcumin in 1.25 mM SSM was prepared in PBS by the film-rehydration method as described in Section 1.1 above.

VIP was conjugated to the distal end of DSPE-PEG_{3400} as previously described in our laboratory (Dagar et al., 2003; Krishnadas, 2004). Activated DSPE-PEG_{3400}-NHS was used to conjugate VIP to DSPE-PEG_{3400}. Briefly, VIP and DSPE-PEG_{3400}-NHS were dissolved separately in cold isotonic HEPES buffer (10 mM, pH 6.6). The DSPE- PEG_{3400} solution was then added in small increments to the VIP solution at 4°C with gentle stirring to yield final concentrations of 0.3 mM VIP and 1.5 mM DSPE-PEG_{3400}-NHS (1:5 molar ratio). The reaction was allowed to continue at 4^{o}C for 2h and stopped by adding 5 µl of 1M glycine solution to the reaction mixture to

consume the remaining NHS moieties. The DSPE PEG_{3400}-VIP conjugation was verified by SDS-PAGE electrophoresis. Thereafter, DSPE- PEG_{3400}-VIP reaction mixture was added to the 225 µg/mL curcumin in 1.25 mM C-SSM dispersion in 1:4 (v/v) ratio. This mixture was equilibrated at 25°C for 30 min in dark to obtain the final C-SSM-VIP nanomedicine containing 180 µg/mL curcumin, 1 mM DSPE- PEG_{2000} and 0.06 mM VIP.

The final C-SSM-VIP formulation was characterized for particle size using dynamic light scattering and for curcumin concentration using HPLC analysis as described in Section 1.2.

3.2. Evaluation of the Inhibitory Effects of C-SSM-VIP, C-SSM or Free Curcumin on MCF-7 Cancer Stem Cell Tumorspheres

C-SSM-VIP nanomedicine and the 225 µg/mL curcumin in 1.25 mM SSM C-SSM stock dispersion was prepared as described above. 1.25 mM empty SSM was prepared following the same procedures as C-SSM, but with no drug. Thereafter, C-SSM and empty SSM dispersions were mixed with 1 µM lipid diluent at 4:1 (v/v) ratio and characterized for particle size and curcumin concentration (C-SSM only) as described above in Section 1.2. The prepared formulations were further diluted with the lipid diluent to obtain 5 µM and 10 µM final curcumin concentrations (in wells) for C-SSM-VIP and C-SSM, and 20 µM final lipid concentration for empty SSM. In addition, 5 µM and 10 µM curcumin in 0.5% DMSO samples were prepared as described in Section 1.4 above.

The tumorsphere formation assay was performed as described in Section 1.5 above with some modifications. Briefly, single cells from untreated MCF-7 cell suspension were plated in

24-well ultra-low attachment plates at a cell density of 15,000 cells/mL. On the following day, 80 µL of the 5 µM and 10 µM C-SSM-VIP, C-SSM and C-DMSO samples, as well as the empty SSM, 0.5% DMSO and PBS control samples were added to the wells in tumorsphere culture. After 7 days of culture, sphere forming efficiencies were evaluated under light microscope from two wells per treatment group.

4. Statistical Analysis

The *in vitro* experiments were performed repeatedly to obtain at least 3 independent trials for each experiment. Data of all experiments were expressed as mean ± standard deviation (SD). Any statistical comparison between 2 groups was performed using two-tailed independent Student's t-test. Differences were considered significant when $P < 0.05$. All the statistical analyses were conducted using SPSS version 17.0 and Microsoft Excel 2007.

III. RESULTS AND DISCUSSION

A. *IN VITRO* INHIBITORY EFFECT OF C-SSM ON MCF-7 BREAST CANCER STEM CELLS

Curcumin was previously shown to inhibit stem cells from breast cancer cell lines or normal breast tissue through suppression of the mammosphere formation and elimination of ALDH-positive cells (Kakarala et al., 2010). In order to determine whether curcumin has similar or greater anti-CSC activity when delivered as the C-SSM nanomedicine compared to free curcumin, we evaluated C-SSM's ability to inhibit tumorsphere formation as well as to eliminate the $CD44^{+}/CD24^{-/low}$ cancer stem cell population of MCF-7 cells.

1. Characterization of the C-SSM Formulation

For determining C-SSM's effect on breast cancer stem cells, C-SSM and empty SSM (as vehicle control) samples were prepared to treat MCF-7 cells. Both formulations were characterized for particle size by DLS and curcumin concentration of C-SSM was detected by HPLC.

1.1. Particle Size Analysis

Particle size analysis of 180 μg/mL curcumin in 1mM SSM (C-SSM) and 1 mM empty SSM, depicted in Figures 10 and 11, respectively, showed a unimodal system as observed by one single peak at around the intensity-weighted particle size diameter of 15 nm and a clean time history. In addition, a chi-squared value < 3 also indicated a uniform distribution. The mean particle sizes of C-SSM and empty SSM were found to be 14.5 ± 0.4 nm and 16.2 ± 0.6 nm, respectively (P = 0.01). These results agree with the previous data from our laboratory

showing a mean diameter of ~15 nm for C-SSM (Thaqi, 2011) and ~16 nm for SSM (Ashok et al., 2004), and therefore suggest the complete solubilization of curcumin in SSM.

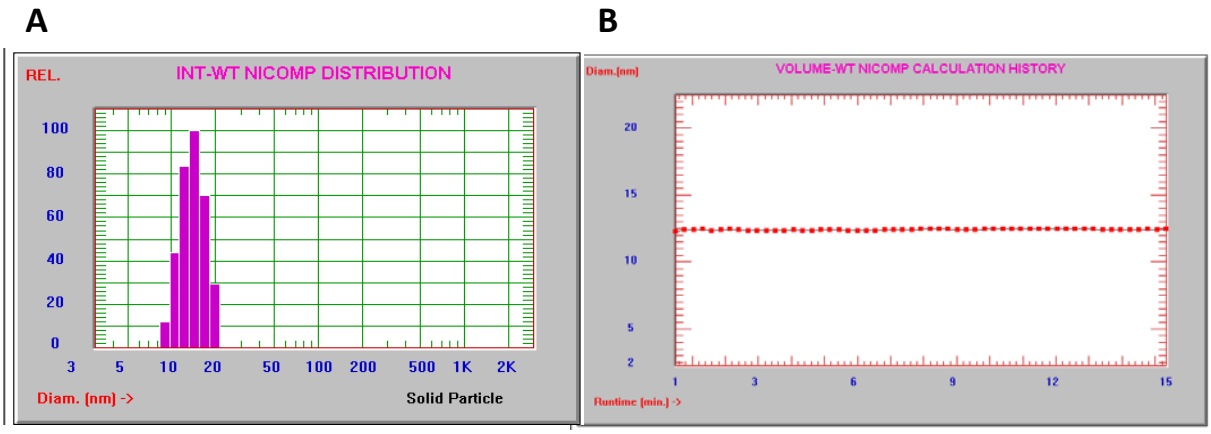

Figure 10. Representative DLS data of C-SSM. (A) Intensity-weighted NICOMP particle size distribution with a single peak at ~15 nm. (B) Time history with a single specie present.

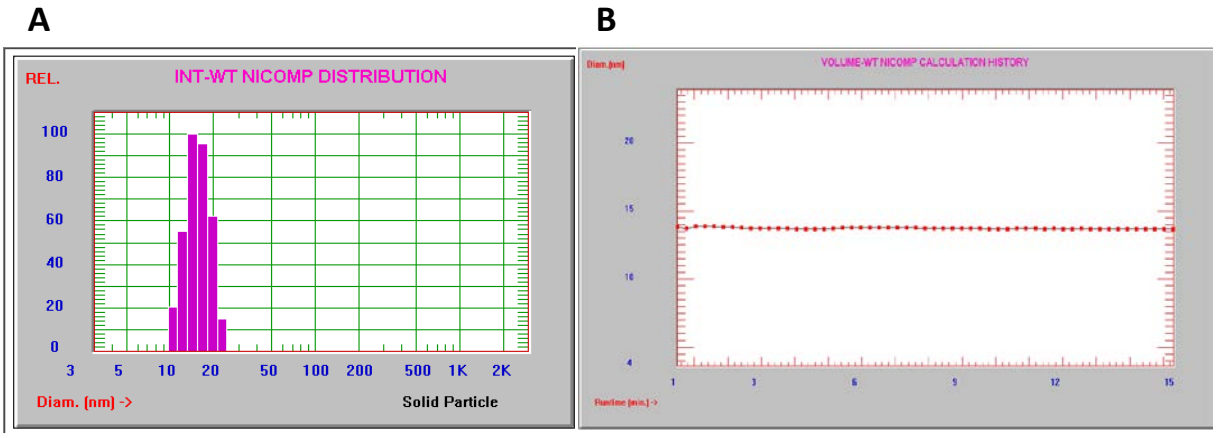

Figure 11. Representative DLS data of 1mM empty SSM. (A) Intensity-weighted NICOMP particle size distribution with a single peak at ~15 nm. (B) Time history with a single specie present.

1.2. HPLC Analysis

The exact concentration of curcumin in C-SSM samples was determined by RP-HPLC. Curcumin calibration curves were generated from curcumin standard solutions of a range of concentrations (25 - 100 µg/mL) for each trial. A representative calibration curve is illustrated in Figure 12. Curcumin from C-SSM and standard solutions gave a peak at 425 nm with an average retention time of 6.1 minutes as shown in Figure 13. Each sample was analyzed in triple run and curcumin concentrations of C-SSM samples were calculated from the average peak areas using the calibration curve.

The exact curcumin concentration was found to be ~180 µg/mL, similar to the previously reported drug concentration of C-SSM (Thaqi, 2011). Following characterization, C-SSM samples were diluted to obtain 10 µM and 20 µM curcumin concentration according to the HPLC data.

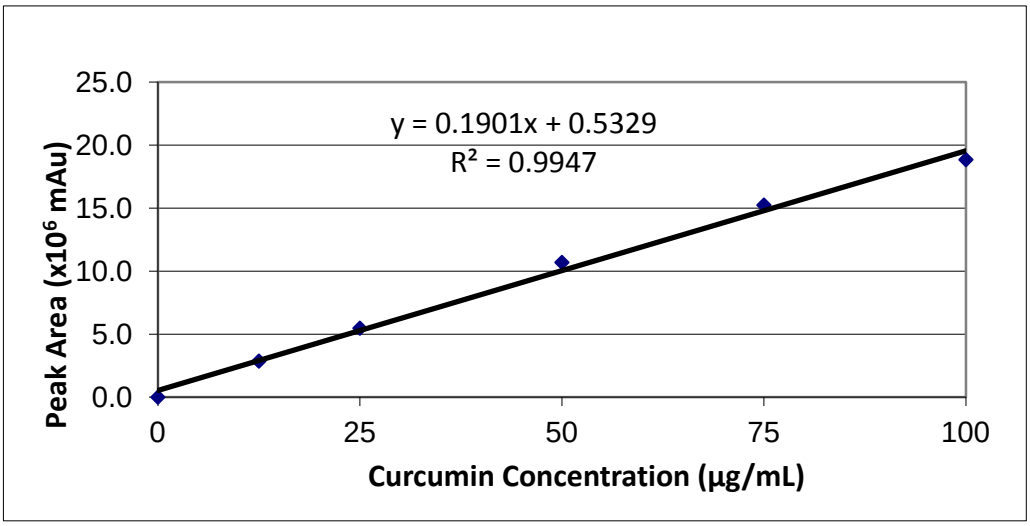

Figure 12. Representative curcumin calibration curve in methanol generated from HPLC analysis (mAu: miliabsorption unit).

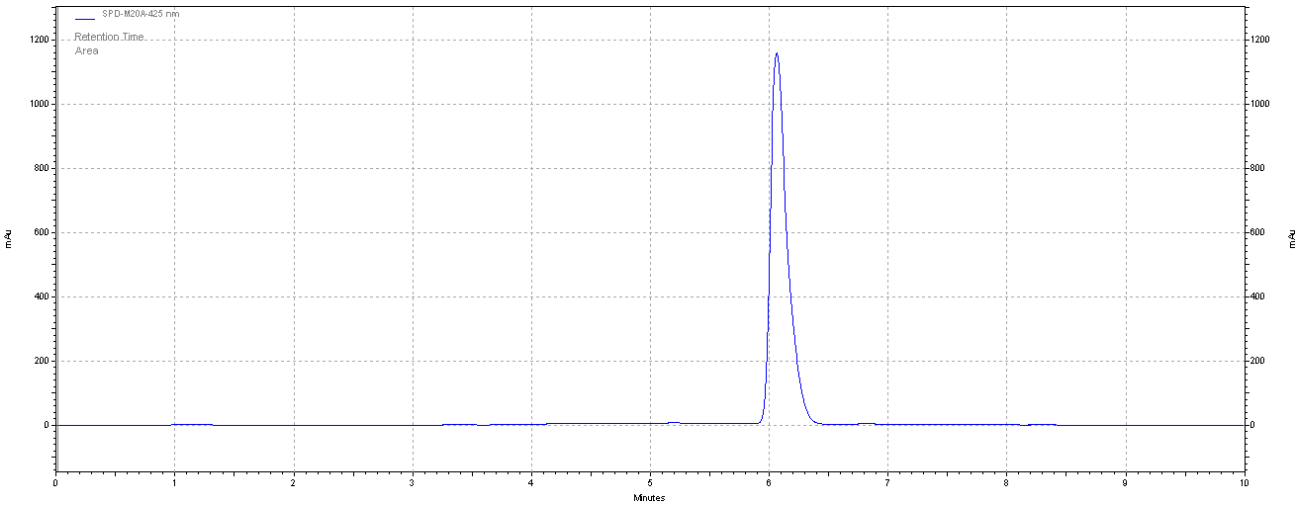

Figure 13. Representative curcumin peak obtained at 425 nm from HPLC analysis of C-SSM.

2. C-SSM Improve Curcumin's Inhibitory Effect on MCF-7 Cancer Stem Cell Tumorspheres

Recent studies have demonstrated that breast cancer stem/progenitor cells, similar to human breast stem/progenitor cells, could be enriched in floating mammospheres (also known as tumorspheres) based on their unique ability to survive in non-adherent suspension as spherical clusters (Dontu et al., 2003; Ponti et al., 2005). These tumorspheres have the capacity to be serially passaged, generating new generations of tumorspheres (self-renewal), and also to differentiate along different mammary epithelial lineages. In order to determine whether delivering curcumin as C-SSM nanomedicine could improve its efficacy to suppress tumorsphere formation *in vitro*, MCF-7 cells were treated with 10 µM and 20 µM concentrations of C-SSM or C-DMSO, or with controls including PBS, DMSO and empty SSM for 72 hours in adherent conditions. Treated cells were detached and plated in ultra-low attachment plates. At the end of 7 days of culture, normal cancer cells died and only a small

population of cancer cells with stem-like properties survived to form floating spherical clusters (tumorspheres). Thereafter, the dissociated tumorspheres were re-plated in ultralow attachment plates and secondary tumorspheres were grown in the absence of treatment.

2.1. Inhibition of Primary Tumorsphere Formation

As shown in Figure 14, while 10 μM C-DMSO did not have a significant effect on tumorsphere formation, 10 μM C-SSM, 20 μM C-DMSO and 20 μM C-SSM treatments resulted in significantly lower sphere forming efficiencies compared to the PBS control (SFE: 63%, 73% and 36% of the PBS control, respectively; $P < 0.05$ for 10 μM C-SSM and 20 μM C-DMSO, and $P < 0.001$ for 20 μM C-SSM). In addition, both 10 μM and 20 μM C-SSM increased the inhibition of tumorsphere formation by more than 6-fold and 2-fold, respectively, compared with free curcumin ($P < 0.03$), indicating its enhancing effect on curcumin's activity against tumorspere-initiating breast CSCs. Furthermore, as shown in Figure 15, 20 μM C-SSM also reduced the sphere size by approximately 2-fold compared to PBS control ($P < 0.05$), while 20 μM C-DMSO did not show a significant effect on this property. However, the empty SSM control was also found to significantly reduce the size of spheres. One possible explanation for this is that SSM, at concentrations as high as 40 μM, could be involved in the inhibition of the proliferative capacity of breast cancer stem cells as reflected on the reduction of the size of tumorspheres from SSM-treated MCF-7 cells. In fact, phosphatidylethanolamine, a constituent of the DSPE-PEG_{2000} molecule in SSM, is a natural component of the mammalian cell membrane also known to be involved in biological processes and cell signaling (Vance, 2008). Therefore, exogenously available phosphatidylethanolamine as a degradation product of SSM may change the tightly

regulated cellular level of this phospholipid, and thereby lead to the impairment of biological processes such as proliferation. On the other hand, this finding may also suggest that DSPE-PEG_{2000} molecules get inserted into the cell membranes and make it thermodynamically less favorable for cells to form spherical clusters, leading to the dissociation of tumorspheres (Lentz, 2007). Either way, the implications of this finding clearly require further investigation.

Figure 16 shows overlapping bright field and fluorescence images of tumorspheres from 20 µM C-SSM and 20 µM C-DMSO pre-treated MCF-7 cells. These images indicate that tumorspheres contain single cells that transmit green fluorescence resulting from curcumin's intrinsic fluorescence. These fluorescent cells most likely represent the tumorsphere-initiating cancer stem-like cells continuing to retain curcumin even on the seventh day of tumorsphere culture.

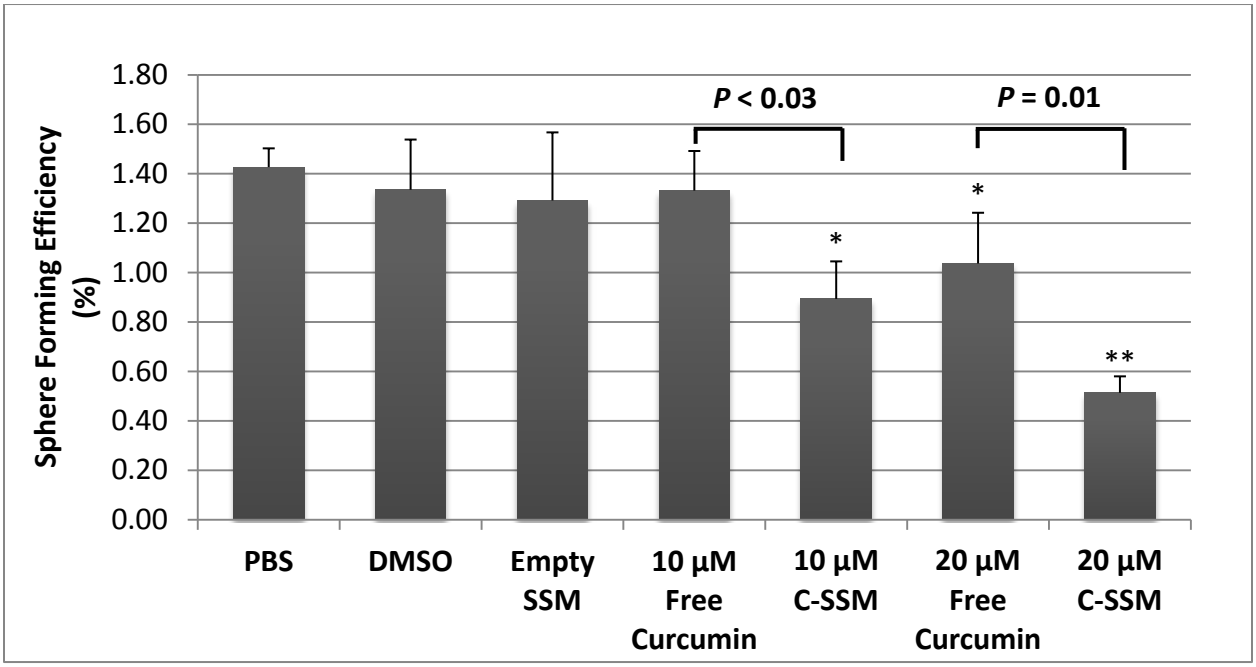

Figure 14. Inhibitory effect of curcumin pre-treatments on primary sphere formation efficiency of MCF-7 cells (n=3), *$P < 0.05$ and ** $P < 0.001$, compared to the PBS control. Data are mean normalized to control ± SD.

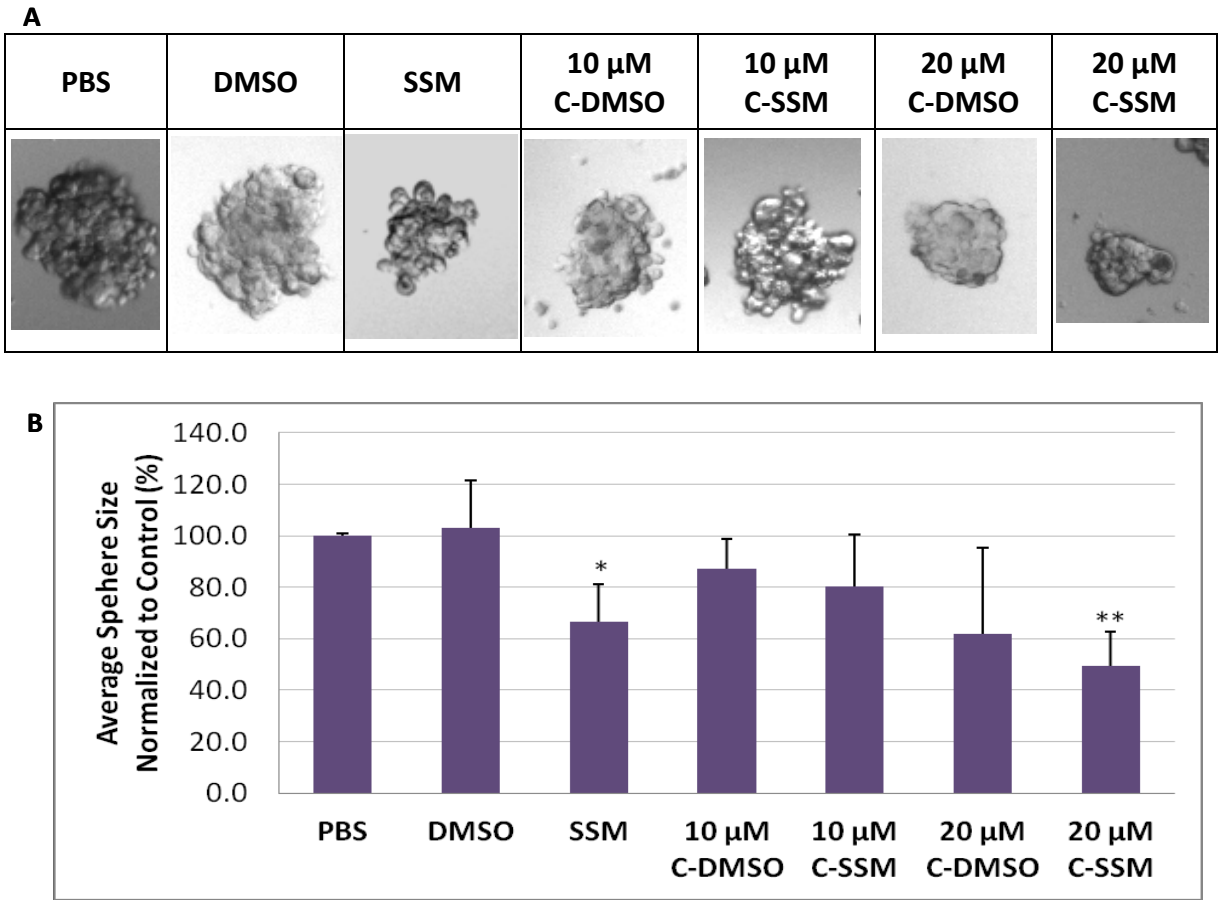

Figure 15. (A) Representative images of primary tumorspheres illustrating the change in sphere size with different treatments. (B) Effect of curcumin pre-treatments on the average sphere size of primary MCF-7 tumorspheres (n=3). *P <0.05 and ** P < 0.01 compared to the PBS control. Data are mean ± SD.

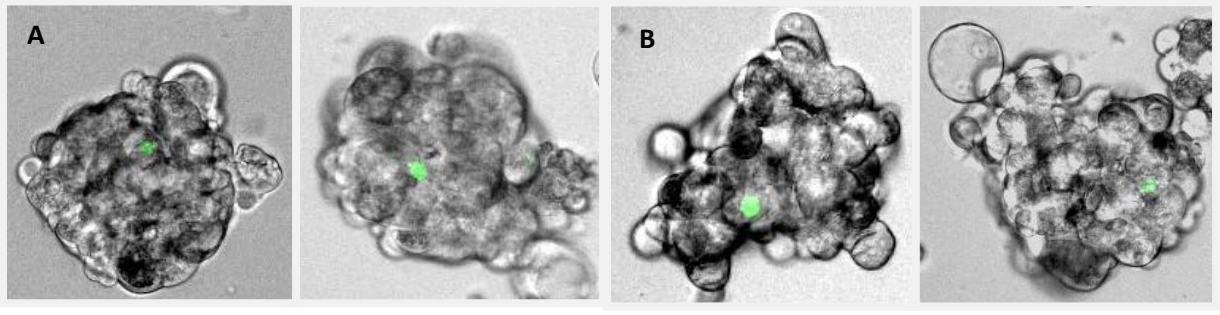

Figure 16. Curcumin-fluorescent cells of primary tumorspheres from MCF-7 cells treated with (A) 20 µM C-SSM or (B) 20 µM free curcumin.

2.2. Inhibition of Secondary Tumorsphere Formation

When primary tumorspheres were passaged in the absence of treatment, 20 µM C-SSM pre-treatment of MCF-7 cells was found to significantly inhibit the formation of secondary tumorspheres (22% reduction compared to PBS; $P < 0.05$), indicating impaired self-renewal capacity of these tumorsphere-initiating CSCs (Figure 17). However, this inhibition was less than the inhibition observed in primary tumorspheres, and found not to be significantly different compared to free curcumin. This observation may be related to the fact that curcumin treatment was applied in adherent conditions before cells were plated in the tumorsphere culture, but not directly on the tumorsphere culture. Therefore, the cancer stem-like cells surviving after the curcumin pre-treatment may have had enough time to repair their impaired self-renewal ability to give rise to secondary tumorspheres.

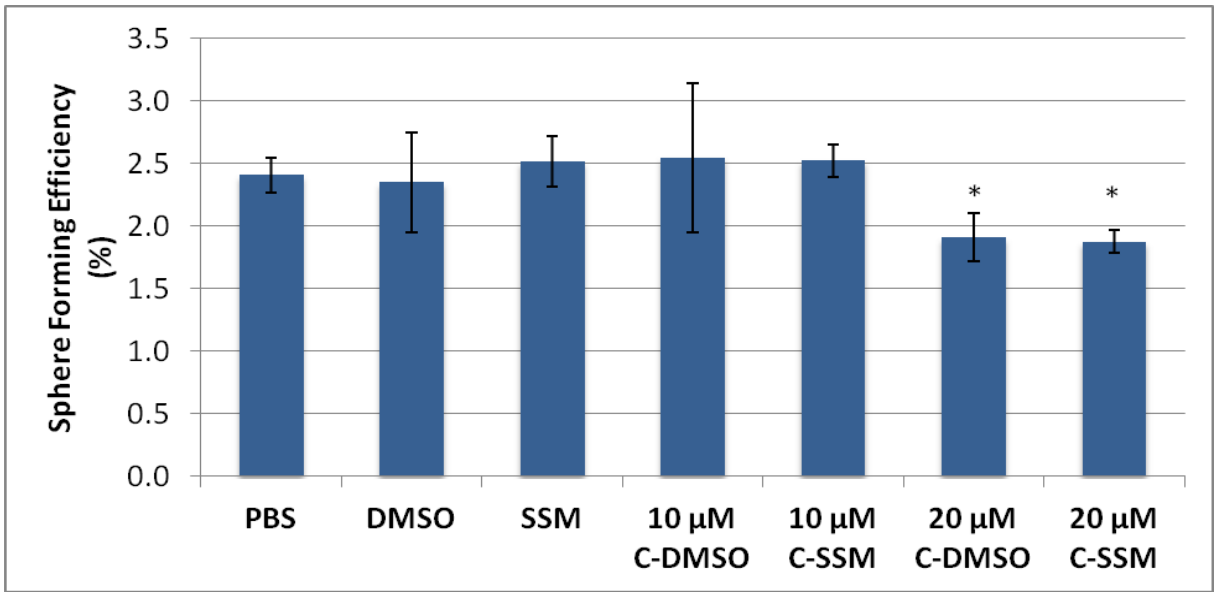

Figure 17. Inhibitory effect of curcumin pre-treatments on secondary sphere formation efficiency of MCF-7 cells (n=3). *P <0.05 compared to the PBS control. Data are mean ± SD.

Interestingly, as demonstrated in Figure 18, although SSM and 10 µM C-SSM did not show a significant effect on the SFE of secondary tumorspheres, these treatments and 20 µM C-SSM all resulted in a significant reduction of the average sphere size compared to the PBS control (around 25% decrease for all the three treatments; $P < 0.05$). This finding is in agreement with the results from primary tumorspheres and validates SSM's effect on the tumorsphere size as discussed in Section 2.1 above.

Taken together, these results suggest the dose-dependent anti-CSC activity of the C-SSM nanomedicine as demonstrated by its efficacy to eliminate tumorsphere-initiating breast cancer stem cells from MCF-7 cells. Moreover, this activity was found to be significantly higher compared to free curcumin, indicating the benefits offered by the SSM nanocarrier as it was previously shown to protect curcumin from degradation and to increase its internalization by MCF-7 cells, and thereby enhance its cytotoxicity (Thaqi, 2011; Gulcur et al., 2011).

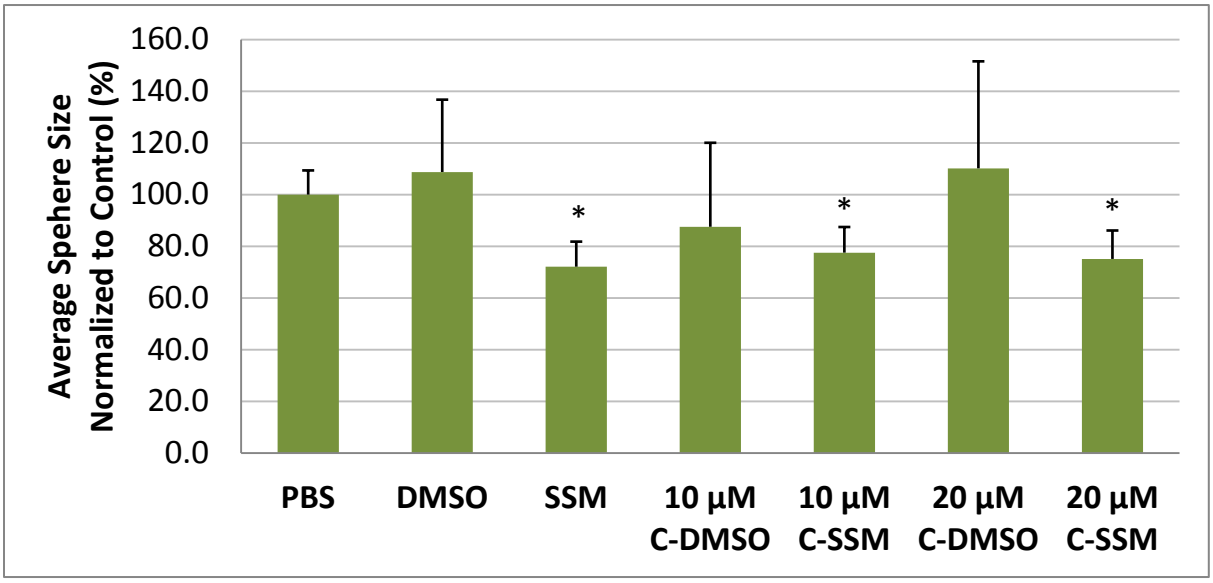

Figure 18. Effect of curcumin pre-treatments on the average sphere size of secondary MCF-7 tumorspheres (n=3). *P <0.05 compared to the PBS control. Data are mean ± SD.

3. C-SSM Enhance the Cytotoxicity of Curcumin to $CD44^{+}/CD24^{-/low}$ MCF-7 Cancer Stem Cells

Putative cancer stem cells were first isolated from the breast carcinoma based on a $CD44^{+}/CD24^{-/low}$ immunophenotype (Al-Hajj et al., 2003). These cells were highly tumorigenic when injected to mice and generated tumors resembling the parent tumors with respect to the phenotypic heterogeneity. For evaluating C-SSM's cytotoxicity against the $CD44^{+}/CD24^{-/low}$ breast CSCs, MCF-7 cells were treated with 10 µM and 20 µM C-SSM and C-DMSO, as well as the controls in adherent conditions. After 72 hours of treatment, cells were detached and stained with fluorescent antibodies against CD44 and CD24. Subsequently, CD44 and CD24 surface marker expressions of these cells were analyzed using flow cytometry, with the aims of evaluating the effect of the treatments on the $CD44^{+}/CD24^{-/low}$ CSC population and also determining the internalization of curcumin by the CSC and normal cancer cell populations.

3.1. C-SSM Increase Curcumin Internalization by the Cancer Stem Cell and Normal Cancer Cell Populations of MCF-7 Cells

The uptake of curcumin by $CD44^{+}/CD24^{-/low}$ CSCs and $CD44^{+}/CD24^{high}$ normal cancer cells was analyzed from the mean fluorescence intensity (MFI) of the curcumin-treated MCF-7 cells (Figure 19). The MFI of curcumin-treated cells was calculated after subtracting the background MFI obtained from PBS-treated samples and taking the average of the four trials. As shown in Figure 19, 10 µM C-SSM increased the curcumin internalization into normal cancer cell and cancer stem cell populations of MCF-7 cells by 6.4-fold (P=0.01) and by 3.5-fold (P<0.05),

respectively, compared to 10 µM C-DMSO. Likewise, 20 µM C-SSM also increased the curcumin uptake by 2.8-fold in normal cancer cells, and by 1.8-fold in cancer stem cells compared to 20 µM C-DMSO. Although the effect of 20 µM C-SSM was not found to be significant due to high variability in the measurements among different trials, 20 µM C-SSM constantly gave higher MFIs compared to its C-DMSO equivalent in all the trials (minimum 30% higher). This finding is in agreement with the previous data from our laboratory demonstrating increased internalization of C-SSM by MCF-7 cells compared to free curcumin, and validates the data from the tumorsphere formation assay discussed in Section 2 above (Gulcur et al., 2011).

Another interesting observation was that, in all the trials, curcumin uptake was found to be higher in normal cancer cells compared to cancer stem cells for all the treatment groups except 10 µM C-DMSO. This may be related to the higher activity of efflux pumps and other resistance mechanisms in CSCs resulting in lower accumulation of curcumin inside these cells.

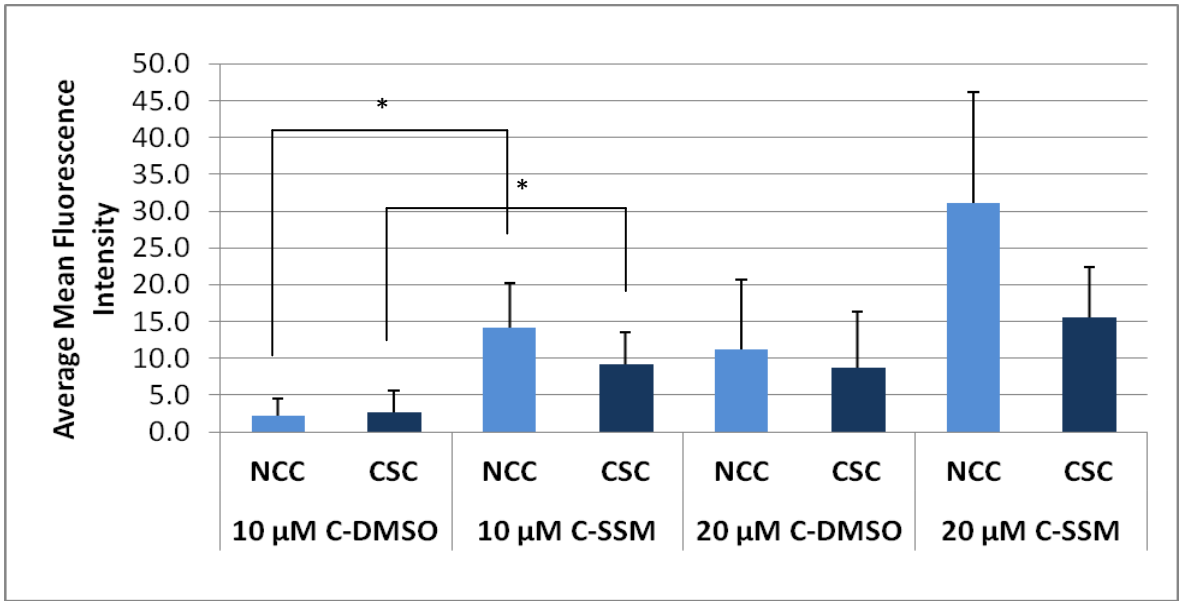

Figure 19. Flow cytometry results for the uptake of curcumin by $CD44^{+}/CD24^{-/low}$ cancer stem cells and $CD44^{+}/CD24^{high}$ normal cancer cells of the C-SSM- or C-DMSO-treated MCF-7 cells (n=4). NCC: normal cancer cells, CSC: cancer stem cells. * $P < 0.05$. Data are mean ± SD.

3.2. C-SSM Improve the Elimination of $CD44^{+}/CD24^{-/low}$ MCF-7 Cancer Stem Cells

Figure 20 summarizes the data from the flow cytometric analysis illustrating the effect of curcumin treatments on the $CD44^{+}/CD24^{-/low}$ CSCs from MCF-7 cells. According to these data, 20 μM C-SSM resulted in a significant reduction in the percentage of $CD44^{+}CD24^{-/low}$ CSC population compared to the PBS control (56% decrease, $P < 0.05$), while none of the other treatment groups showed a significant change in the percentage of the CSCs (Figure 20 A and B). The reduction in the $CD44^{+}CD24^{-/low}$ breast CSC population observed with 20 μM C-SSM is in agreement with the results from the tumorsphere formation assay discussed in Section 2 above, where the same formulation was found to inhibit the primary tumorsphere formation by 64%. However, the inhibitory effects of 10 μM C-SSM and 20 μM C-DMSO demonstrated in the tumorsphere assay were not observed in the flow cytometric analysis of the CSC population. One possible explanation for this finding is the discrepancies between the two methods. While the flow cytometric analysis of the $CD44^{+}/CD24^{-/low}$ CSCs is only a measure of the percentage of the surviving CSCs after treatments, the tumorsphere formation assay is a measure of both the number of surviving CSCs and their proliferative capacity, and therefore the additive effect in the latter could be expected to be higher.

As shown in Figure 20 C, the empty SSM-treated MCF-7 cells resulted in a high standard deviation for the percentage of the $CD44^{+}CD24^{-/low}$ CSC population. One explanation for this observation could be that the free DSPE-PEG_{2000} molecules from SSM is altering the surface properties of MCF-7 cells, and thereby interfering with the antibody binding. However, 20 μM C-SSM, despite having the same lipid concentration as the empty SSM control, did not lead to such a high deviation. We propose that when curcumin is associated with SSM, the CMC of

these micelles is reduced due to hydrogen bonding and hydrophobic interactions of the drug with SSM. This, in return, would lead to a reduction in the availability of free DSPE-PEG_{2000} molecules that will interfere with the antibody binding, and hence to the lower variability in the results.

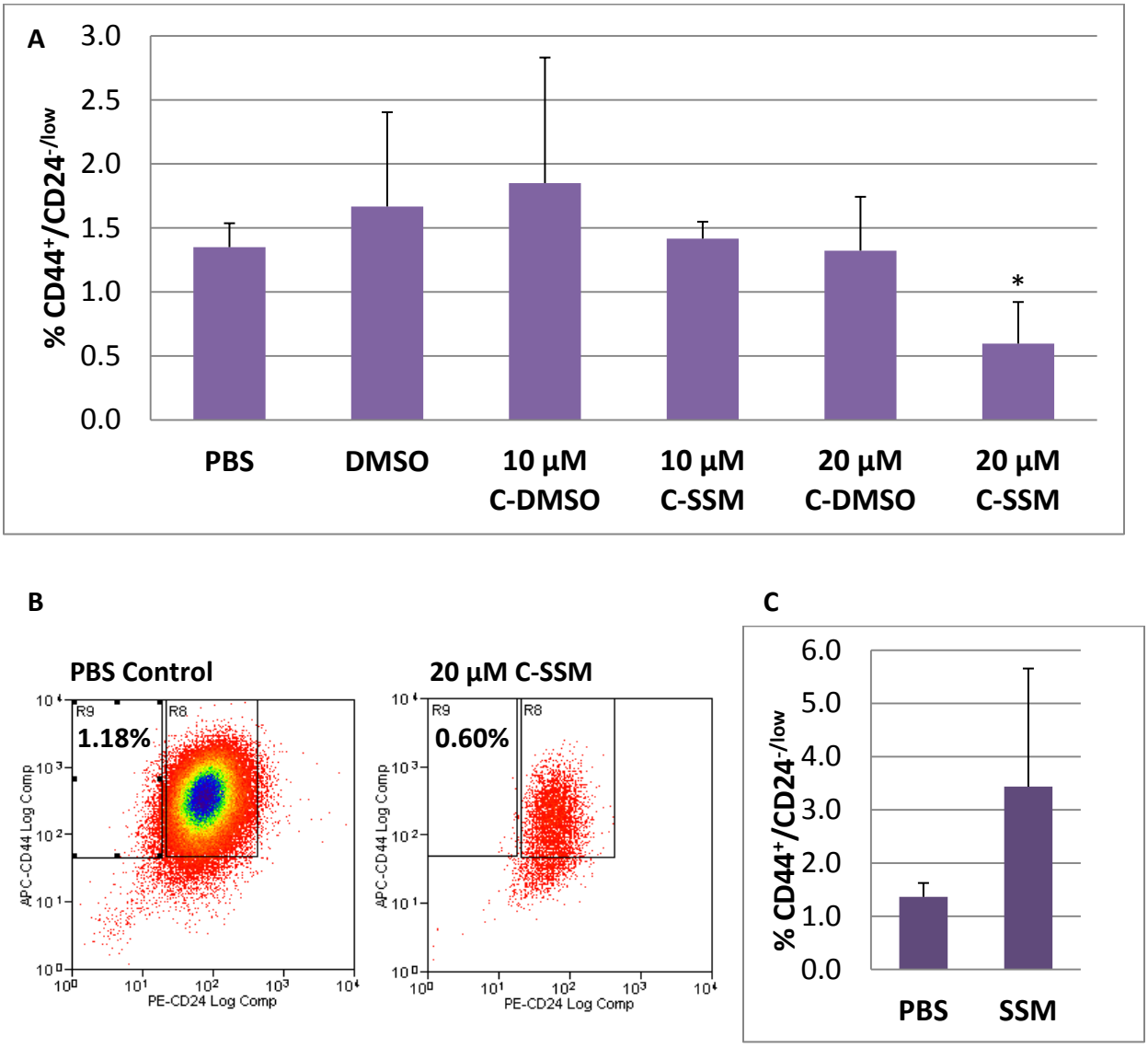

Figure 20. Effect of curcumin treatments on the $CD44^{+}/CD24^{-/low}$ CSCs from MCF-7 cells (n=3). Flow cytometry results showing (A) a significant reduction in the percentage of $CD44^{+}/CD24^{-/low}$ CSCs for the 20 µM C-SSM-treated MCF-7 cells (n=3), and (B) a high standard deviation for empty SSM. (C) Representative flow cytometry plots displaying APC fluorescence versus PE fluorescence for MCF-7 cells treated with the PBS control or 20 µM C-SSM. **P* <0.05 compared to the PBS control. Data are mean ± SD.

Taken together, these data suggest that the delivery of curcumin in SSM significantly improves the anti-CSC activity of the drug as demonstrated by the reduction in the $CD44^{+}CD24^{-/low}$ CSC population of MCF-7 cells after treatment and also by the increase in the cellular uptake of curcumin. These results support the findings from the previous study showing the enhanced efficacy of curcumin to inhibit tumorsphere formation with C-SSM treatment compared to free drug (Section 2).

B. $CD44^{+}/CD24^{-/low}$ MCF-7 BREAST CANCER STEM CELLS OVEREXPRESS VIP RECEPTORS

Identification of cellular targets overexpressed on the surface of CSCs holds great significance for developing nanomedicines actively targeted to these resistant cells. Yet there are currently only a few potential CSC markers exploited for targeting purposes (Schatzlein, 2006). In this respect, VIP receptors stand out as promising targets, as they have been previously shown to be overexpressed in many types of cancers including breast cancer and also to regulate stem cell-like properties (Reubi et al., 2000; Callihan et al., 2011). Therefore, we evaluated the expression of VIP receptors on CSCs isolated from MCF-7 cells, with the aim of identifying a novel molecular target to be employed in developing active-targeting strategies to these resistant cells. For this purpose, MCF-7 cells were first sorted into $CD44^{+}/CD24^{-/low}$ cancer stem cell and $CD44^{+}/CD24^{high}$ normal cancer cell populations using flow cytometry, which were then cytospun to glass slides and stained with fluorescence-labeled VIP (FAM-labeled VIP).

The average mean fluorescence intensities (MFIs) from the confocal microscope images of normal cancer cells and CSCs stained with FAM-labeled VIP were quantified after subtracting the MFIs measured from the autofluorescence and nonspecific binding controls. The specificity of the ligand-binding assay was confirmed by the low average MFI of the nonspecific binding control (6.4 MFI; data not shown). Figure 21 reveals an approximately 3 times higher expression of the VIP receptors in the $CD44^{+}/CD24^{-/low}$ cancer stem cell population compared to the $CD44^{+}/CD24^{high}$ normal cancer cells from the MCF-7 breast cancer line ($P < 0.05$). While the normal cancer cells showed a faint signal for the VIP receptors, the CSCs were bright when observed under the confocal microscope (Figure 22).

These results demonstrate that VIP receptors are overexpressed on the CSC population of MCF-7 cells compared to the normal cancer cell population, thus revealing the potential of active targeting through these receptors as a means to increase cell selectivity while improving drug internalization by the CSCs. The differential expression of the VIP receptors also render them a good candidate as surface markers for discriminating between the CSC and normal cancer cell populations of breast cancer cells. However, further studies are necessary to determine whether the VIP receptors are also differentially expressed on the surface of the CSCs derived from primary breast carcinoma tissues.

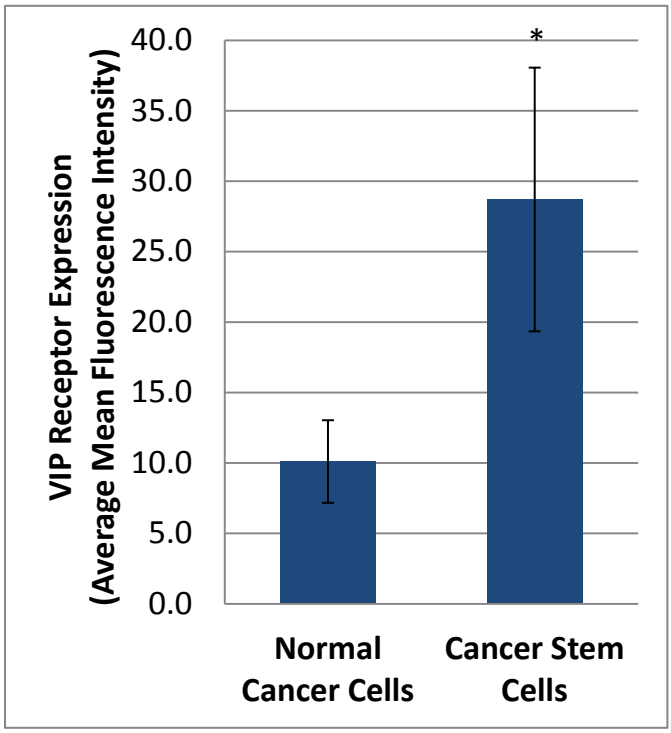

Figure 21. The average mean fluorescence intensities of $CD44^{+}/CD24^{high}$ normal cancer cells and $CD44^{+}/CD24^{-/low}$ cancer stem cells from MCF-7 breast cancer cell line stained with FAM-labeled VIP (n=3). Note that the level of VIP receptor expression on cancer stem cells is approximately 3 times the level in the normal cancer cell population. * $P<0.05$. Data are mean ± SD.

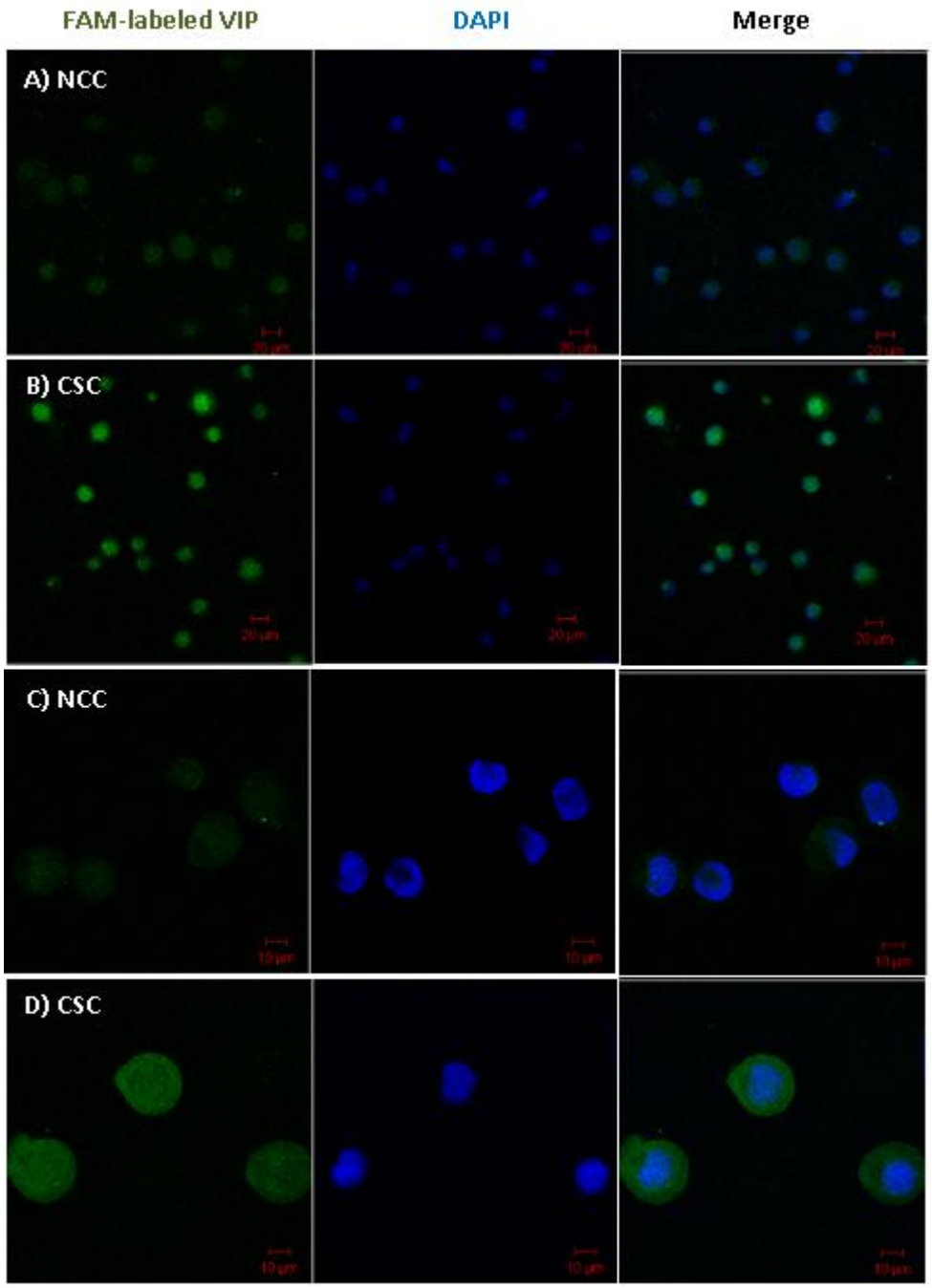

Figure 22. Representative confocal microscopy images showing VIP receptor expression of MCF-7 cells. 25x (A and B) and 63x (C and D) images of normal cancer cells and cancer stem cells, respectively, stained with FAM-labeled VIP (green) and DAPI (blue nuclear stain). NCC: normal cancer cells, CSC: cancer stem cells.

C. *IN VITRO* INHIBITORY EFFECT OF C-SSM-VIP ON MCF-7 BREAST CANCER STEM CELLS

Previous *in vitro* and *in vivo* work from our laboratory has demonstrated that active targeting through VIP receptors with VIP-surface grafted SSM significantly improves the cytotoxicity of anti-cancer agents (Onyuksel et al., 2009a; Krishnadas, 2004). Therefore, in this study, we aimed to improve the efficacy of C-SSM against CSCs by developing a novel VIP-surface grafted formulation of C-SSM to actively target the VIP receptors found to be overexpressed on the CSC population. For this purpose, a curcumin formulation in SSM-VIP was first developed and characterized for particle size distribution and curcumin concentration, and thereby tested for its inhibitory effect against CSCs using a tumorsphere formation assay.

1. Characterization of the C-SSM-VIP Formulation

VIP was successfully conjugated to DSPE-PEG_{3400}-NHS which was confirmed by SDS-PAGE electrophoresis (data not shown). The prepared DSPE-PEG_{3400}-VIP reaction mixture was added to the C-SSM stock dispersion to obtain C-SSM-VIP. The formulations were then tested for particle size using DLS. The DLS data showed unimodal particle size distributions with mean hydrodynamic diameters of ~15 nm for C-SSM and ~17 nm for C-SSM-VIP, indicating self-association of curcumin with SSM and SSM-VIP (Figure 23). We propose that the incorporation of DSPE-PEG_{3400} molecules to SSM could lead to a higher surface concentration of PEG molecules. This, in return, would lead to a more extended configuration of the PEG layer, which would explain the observed slight increase in the mean diameter of C-SSM-VIP compared to C-SSM.

A B

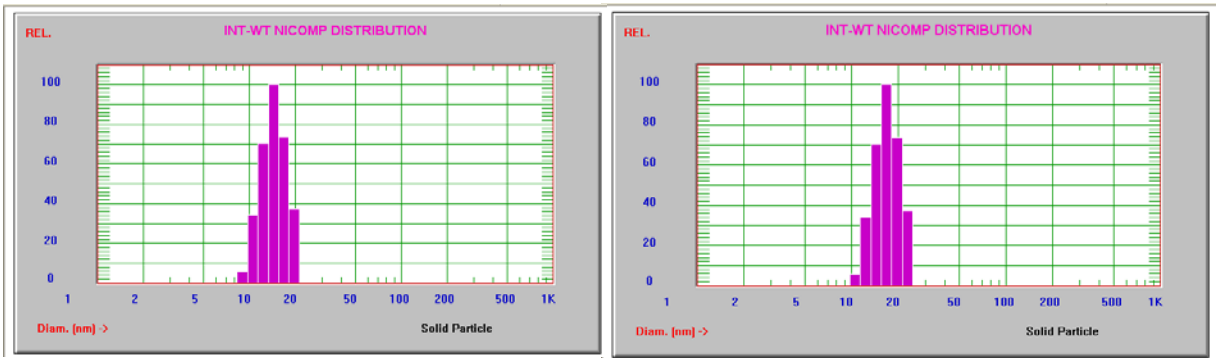

Mean diameter = 14.7 nm Mean diameter = 17.2 nm

Figure 23. Representative DLS data from C-SSM and C-SSM-VIP formulations. Intensity-weighted NICOMP particle size distributions of (A) C-SSM (mean particle diameter = 14.7 nm) and (B) C-SSM-VIP (mean particle diameter = 17.2 nm) showed single homogenous particle species.

The prepared C-SSM and C-SSM-VIP formulations were also characterized for curcumin content using HPLC. The curcumin concentration of the C-SSM-VIP formulation was found to be approximately 176.8 ± 4.2 µg/mL, which was similar to the loading efficiency of C-SSM. Necessary dilutions were made according to the HPLC data in order to obtain 5 µM and 10 µM curcumin concentrations.

2. C-SSM-VIP Further Improve the Inhibition of MCF-7 Tumorsphere Formation

For the tumorsphere formation assay, MCF-7 cells were seeded in ultra-low attachment plates in suspension, and treated with 5 µM or 10 µM curcumin concentrations of C-SSM-VIP, C-SSM or curcumin dissolved in DMSO, as well as with vehicle controls (PBS, empty SSM and DMSO) on the following day. Sphere forming efficiencies were evaluated under microscope after 7 days of culture.

As shown in Figure 24, MCF-7 cells treated with empty SSM formed aggregates of tumorspheres after 7 days of culture, and therefore tumorspheres could not be enumerated. However, aggregation of spheres was minimal in the C-SSM and C-SSM-VIP treatment groups, indicating that curcumin is reversing this unexpected effect of empty SSM. This observation is in agreement with the results discussed in Section 3.2 above (for the inhibitory effects of C-SSM and empty SSM on the percentage of $CD44^{+}/CD24^{-/low}$ CSC population of MCF-7 cells) and supports our proposition that the association of curcumin with SSM leads to a reduction in the availability of free DSPE-PEG_{2000} molecules.

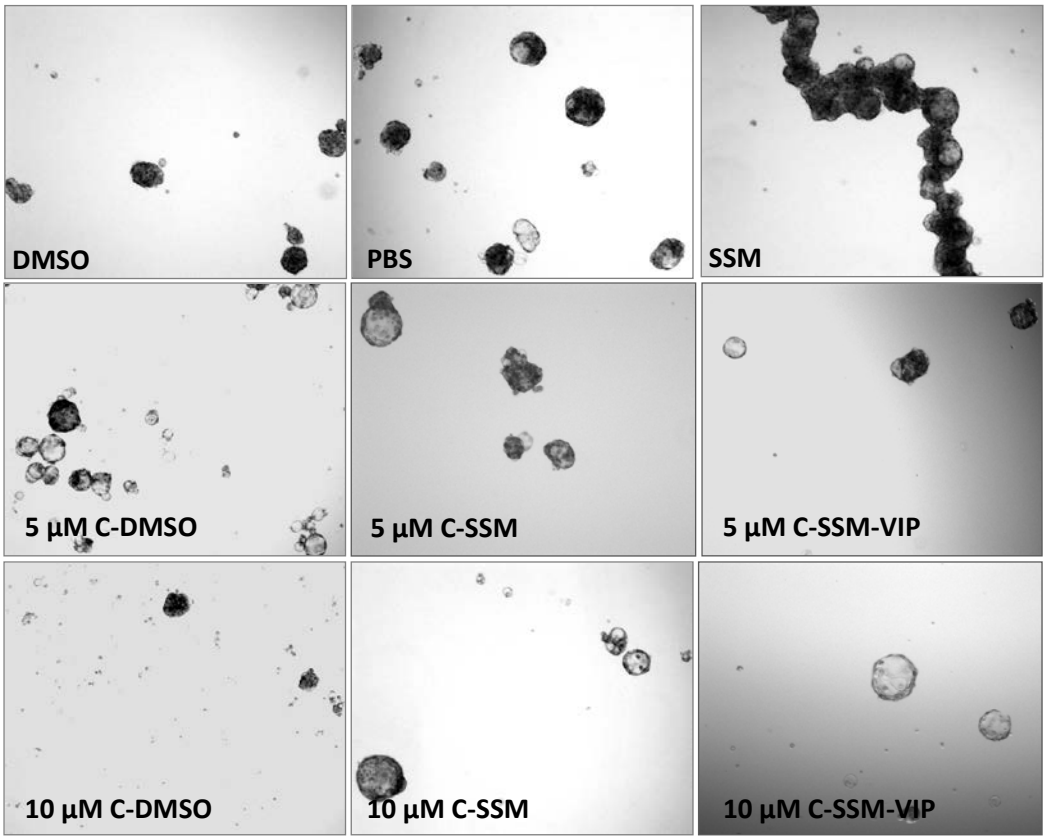

Figure 24. Representative bright field images of MCF-7 tumorspheres from different treatment groups captured after 7 days of culture. The tumorspheres from cells treated with empty SSM formed aggregates, but this aggregation was reversed by curcumin in C-SSM and C-SSM-VIP samples.

As determined from the tumorsphere formation assay, 0.5% DMSO control, when added directly onto the MCF-7 cell suspension in the tumorsphere culture, reduced the SFE by ~30% compared to the PBS control ($P < 0.05$; data not shown). Therefore, in Figure 25, the SFE data from MCF-7 cells treated with C-DMSO groups were normalized to the average SFE of the DMSO control, whereas the C-SSM and C-SSM-VIP groups were normalized to the PBS control. We found that C-SSM-VIP, at a 5 μM curcumin dose, significantly improved the inhibitory effects of both C-SSM and free curcumin on the tumorsphere formation (22% and 20% higher inhibition, respectively; $P < 0.05$). These results indicate the contribution of receptor-mediated particle internalization on increasing the overall cellular uptake of curcumin, leading to an amplified activity to inhibit tumorsphere formation. On the contrary, when the curcumin concentration was increased to 10 μM, C-DMSO almost completely suppressed the tumorsphere growth (9% SFE), whereas the sphere forming efficiencies of the C-SSM- or C-SSM-VIP- treated cells remained at approximately 35%.

The sphere forming efficiencies of C-SSM and C-SSM-VIP were found to be similar, due, most probably, to VIP receptor saturation at this concentration, which limits the contribution of receptor-mediated internalization to the overall uptake of nanomicellar curcumin by the cells. We have previously observed this phenomenon in our laboratory with paclitaxel-loaded micelles (Onyuksel et al., 2009a). Although the cytotoxicity of the VIP-grafted formulation was found to be significantly higher than the untargeted formulation at doses < 100 ng/mL, the two formulations were found to show similar effects at higher doses.

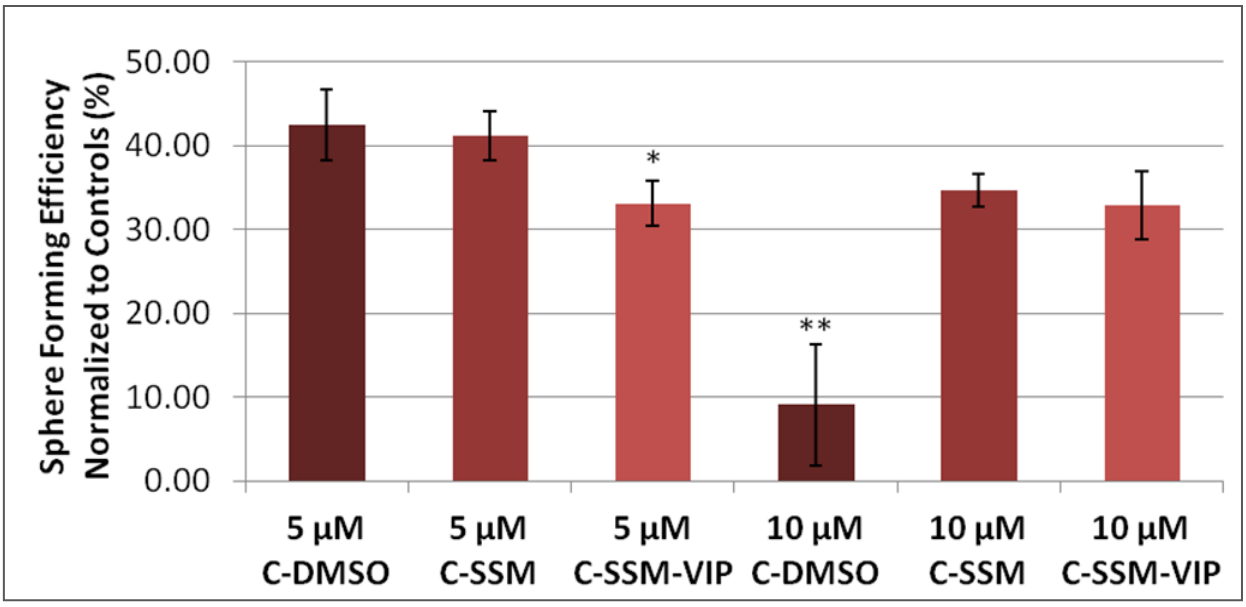

Figure 25. Sphere forming efficiencies of MCF-7 cells after 7 days of tumorsphere culture in the presence of the curcumin treatments. Data are normalized to relevant controls (DMSO control for C-DMSO treatments and PBS control for C-SSM and C-SSM-VIP treatments; n=3). *$P < 0.05$ compared to 5 µM C-SSM and 5 µM C-DMSO. **$P < 0.001$ compared to 10 µM C-SSM and 10 µM C-SSM-VIP. Data are mean ± SD.

Unlike the results of this study for the 10 µM curcumin dose, C-SSM were previously shown to have a greater inhibitory effect on tumorsphere formation compared to free curcumin as described in Section 2 above. The discrepancy between the results of the two studies is also reflected in the extent of suppression of tumorsphere growth, as the effect of even the 5 µM free curcumin dose in the current study was found to be higher compared with 20 µM free curcumin in the previous study. This could be attributed to the differences in the experimental design of the two studies. Whereas in the previous study, the MCF-7 cells were pre-treated in adherent conditions, the treatments were added directly on the single cell suspension in the tumorsphere culture in the present study. Therefore, kinetics of the tumorsphere formation plays a role in the results of the latter. Exposing single cells in

suspension on the first day of the tumorsphere culture to a high dose of (10 μM) free curcumin is possibly leading to immediate killing of cancer stem-like cells (more so than in adherent conditions) before they start growing as tumorspheres. On the other hand, this immediate effect of curcumin in the C-SSM and C-SSM-VIP formulations is most likely lessened due to controlled release of the drug over a longer period of time, during which the spheres start forming. The time-dependent release of curcumin, in turn, leads to attenuated anti-CSC activities for the nanomicellar formulations compared to free drug. Nevertheless, this time-dependency is not representative of the *in vivo* situation, where continuous exposure of the drug to the cancer cells is generally considered as an advantage.

Overall, these results indicate that VIP receptor-targeted delivery of curcumin-loaded nanomicelles further improves the anti-CSC activity of curcumin at lower concentrations, thus demonstrating the feasibility of employing an active-targeting strategy through the overexpressed VIP receptors for delivering CSC therapies.

IV. CONCLUSION

In summary, C-SSM were found to significantly suppress the primary tumorsphere formation in a dose-dependent manner, indicating its ability to eliminate the tumorsphere-initiating breast CSCs. Moreover, this inhibitory effect of 20 μM C-SSM on the sphere formation was found to be higher in comparison with free curcumin. C-SSM also impaired the self-renewal and proliferative capacities of cancer stem-like cells, as demonstrated by its efficacy to inhibit the secondary tumorsphere formation and to reduce the size of both primary and secondary spheres, respectively. These results were supported by the data from the flow cytometric analysis. The C-SSM nanomedicine showed a markedly increased cellular uptake of curcumin compared to free drug in both the normal cancer cell and cancer stem cell populations from the MCF-7 cell line. In addition, this amplified internalization of C-SSM resulted in a significant reduction in the percentage of the $CD44^{+}/CD24^{-/low}$ CSCs at a 20 μM curcumin concentration, while no significant change was observed with free curcumin. These data demonstrated the enhanced anti-CSC activity of the C-SSM nanomedicine on MCF-7 cells compared to free curcumin, indicating the benefits offered by the SSM nanocarrier.

In order to improve the anti-CSC activity of C-SSM even further, we aimed to integrate an active targeting strategy to this formulation. We demonstrated that the VIP receptors were overexpressed in the $CD44^{+}/CD24^{-/low}$ cancer stem cell population compared to the normal cancer cells. These data were indicative of the potential of VIP receptor-targeting for developing cancer therapies actively-targeted to breast CSCs. Next, a curcumin-loaded nanomicellar formulation surface-grafted with VIP was successfully developed and characterized. We found that C-SSM-VIP, at a lower 5 μM dose, significantly enhanced the

inhibitory effects of both C-SSM and free curcumin on the tumorsphere formation. These data suggested the augmentation of the overall cellular uptake of curcumin, and hence its anti-CSC activity, by the receptor-mediated particle internalization.

Overall, these studies provide a novel strategy for targeting and eliminating breast cancer stem cells in a safe and efficacious way. The C-SSM-VIP formulation combines the advantages of i) curcumin, as a natural compound with a potential anti-CSC activity and no observed toxicity, ii) sterically stabilized, biocompatible and biodegradable phospholipid nanomicelles as a safe delivery system that protects and hence increases the potency of curcumin, and iii) targeting of VIP receptors overexpressed on the CSCs, as a means to increase cell selectivity and cellular uptake by these cells. The data presented here suggest that the C-SSM-VIP nanomedicine, with its advantages listed above, has a potential to provide a relapse-free cure of breast cancer.

V. FUTURE DIRECTIONS

Preliminary data for C-SSM and C-SSM-VIP from this study have indicated the improved efficacy of the nanomicellar formulations of curcumin to eliminate the cancer stem cells from the MCF-7 human breast cancer cell line. However, there is a need to design more experiments before a clinical success can be achieved. Some of these studies include, but not limited to:

1. *Further evaluation of the in vitro performance of C-SSM and C-SSM-VIP on eliminating the cancer stem cells.* Anti-CSC activity of these formulation should be further evaluated on different breast cancer cell lines, or even cell lines of other types of cancers (e.g., pancreatic cancer) using the tumorsphere formation assay and the flow cytometric analysis of the CSC population. Other functional assays related to cancer stem cells such as the tumor cell invasion and the clonogenicity assays could also be used.

2. *Long-term stability studies for the C-SSM and C-SSM-VIP formulations*. A lyophilized formulation of the C-SSM-VIP nanomedicine should be successfully developed and characterized for its potential clinical application. Long-term stability studies of the lyophilized C-SSM and C-SSM-VIP products should be conducted for determining whether they can be stored long enough to be developed as commercial products.

3. *In vivo evaluation of C-SSM and C-SSM-VIP*. Effects of the C-SSM and C-SSM-VIP treatments on the *in vivo* tumorigenicity of breast carcinoma cells should be evaluated in an orthotopical xenograft model on NOD/SCID mice (Ginestier et al., 2010). Other models could be used for different types of cancers.

4. *Large scale production of C-SSM and/or C-SSM-VIP.* A feasible large scale manufacturing process should be developed for the successful translation of the products to the clinical arena.

VI. CITED LITERATURE

Aggarwal, B. B., Bhat, I. D., Ichikawa, H., Ahn, K. S., Sethi, G., Sandur, S. K., Sundaram, C., Seeram, N., & Shishodia, S. (2007a). Curcumin - biological and medicinal properties. In P. N. Ravindran, K. N. Babu & K. Sivaraman (Eds.), *Turmeric the genus Curcuma* (pp. 297-368). NY: CRC Press.

Aggarwal, B. B., Kumar, A., & Bharti, A. C. (2003). Anticancer potential of curcumin: preclinical and clinical studies. *Anticancer Res, 23*(1A), 363-398.

Aggarwal, B. B., Shishodia, S., Takada, Y., Banerjee, S., Newman, R. A., Bueso-Ramos, C. E., & Price, J. E. (2005). Curcumin suppresses the paclitaxel-induced nuclear factor-kappaB pathway in breast cancer cells and inhibits lung metastasis of human breast cancer in nude mice. *Clin Cancer Res, 11*(20), 7490-7498.

Aggarwal, B. B., Sundaram, C., Malani, N., & Ichikawa, H. (2007b). Curcumin: the Indian solid gold. In B. B. Aggarwal, Y.-J. Surh & S. Shishodia (Eds.), *The molecular targets and therapeutic uses of curcumin in health and disease*. New York, NY: Springer.

Aguilar, M.-I. (2004). Reversed-phase high-performance liquid chromatography. In M.-I. Aguilar (Ed.), *HPLC of peptides and proteins : methods and protocols*. Totowa, N.J.: Humana Press.

Al-Ejeh, F., Smart, C. E., Morrison, B. J., Chenevix-Trench, G., Lopez, J. A., Lakhani, S. R., Brown, M. P., & Khanna, K. K. (2011). Breast cancer stem cells: treatment resistance and therapeutic opportunities. *Carcinogenesis, 32*(5), 650-658.

Al-Hajj, M., Wicha, M. S., Benito-Hernandez, A., Morrison, S. J., & Clarke, M. F. (2003). Prospective identification of tumorigenic breast cancer cells. *Proc Natl Acad Sci U S A, 100*(7), 3983-3988.

Allen, T. M. (2002). Ligand-targeted therapeutics in anticancer therapy. *Nat Rev Cancer, 2*(10), 750-763.

Anand, P., Kunnumakkara, A. B., Newman, R. A., & Aggarwal, B. B. (2007). Bioavailability of curcumin: problems and promises. *Mol Pharm, 4*(6), 807-818.

Anand, P., Sundaram, C., Jhurani, S., Kunnumakkara, A. B., & Aggarwal, B. B. (2008). Curcumin and cancer: an "old-age" disease with an "age-old" solution. *Cancer Lett, 267*(1), 133-164.

Ashok, B., Arleth, L., Hjelm, R. P., Rubinstein, I., & Onyuksel, H. (2004). In vitro characterization of PEGylated phospholipid micelles for improved drug solubilization: effects of PEG chain length and PC incorporation. *J Pharm Sci, 93*(10), 2476-2487.

Bachmeier, B., Nerlich, A. G., Iancu, C. M., Cilli, M., Schleicher, E., Vene, R., Dell'Eva, R., Jochum, M., Albini, A., & Pfeffer, U. (2007). The chemopreventive polyphenol Curcumin prevents hematogenous breast cancer metastases in immunodeficient mice. *Cell Physiol Biochem, 19*(1-4), 137-152.

Bansal, S. S., Goel, M., Aqil, F., Vadhanam, M. V., & Gupta, R. C. (2011). Advanced drug delivery systems of curcumin for cancer chemoprevention. *Cancer Prev Res (Phila), 4*(8), 1158-1171.

Barry, J., Fritz, M., Brender, J. R., Smith, P. E., Lee, D. K., & Ramamoorthy, A. (2009). Determining the effects of lipophilic drugs on membrane structure by solid-state NMR spectroscopy: the case of the antioxidant curcumin. *J Am Chem Soc, 131*(12), 4490-4498.

Bisht, S., Mizuma, M., Feldmann, G., Ottenhof, N. A., Hong, S. M., Pramanik, D., Chenna, V., Karikari, C., Sharma, R., Goggins, M. G., Rudek, M. A., Ravi, R., & Maitra, A. (2010). Systemic administration of polymeric nanoparticle-encapsulated curcumin (NanoCurc) blocks tumor growth and metastases in preclinical models of pancreatic cancer. *Mol Cancer Ther, 9*(8), 2255-2264.

Block, G., Patterson, B., & Subar, A. (1992). Fruit, vegetables, and cancer prevention: a review of the epidemiological evidence. *Nutr Cancer, 18*(1), 1-29.

Bonnet, D., & Dick, J. E. (1997). Human acute myeloid leukemia is organized as a hierarchy that originates from a primitive hematopoietic cell. *Nat Med, 3*(7), 730-737.

Callihan, P., Mumaw, J., Machacek, D. W., Stice, S. L., & Hooks, S. B. (2011). Regulation of stem cell pluripotency and differentiation by G protein coupled receptors. *Pharmacol Ther, 129*(3), 290-306.

Carlson, R. W., Allred, D. C., Anderson, B. O., Burstein, H. J., Carter, W. B., Edge, S. B., Erban, J. K., Farrar, W. B., Goldstein, L. J., Gradishar, W. J., Hayes, D. F., Hudis, C. A., Jahanzeb, M., Kiel, K., Ljung, B. M., Marcom, P. K., Mayer, I. A., McCormick, B., Nabell, L. M., Pierce, L. J., Reed, E. C., Smith, M. L., Somlo, G., Theriault, R. L., Topham, N. S., Ward, J. H., Winer, E. P., & Wolff, A. C. (2009). Breast cancer. Clinical practice guidelines in oncology. *J Natl Compr Canc Netw, 7*(2), 122-192.

Chan, M. M., & Fong, D. (2009). Overcoming Drug Resistance by Phytochemicals. In K. Mehta & Z. H. Siddik (Eds.), *Drug resistance in cancer cells*. New York: Springer.

Charafe-Jauffret, E., Ginestier, C., Iovino, F., Wicinski, J., Cervera, N., Finetti, P., Hur, M. H., Diebel, M. E., Monville, F., Dutcher, J., Brown, M., Viens, P., Xerri, L., Bertucci, F., Stassi, G., Dontu, G., Birnbaum, D., & Wicha, M. S. (2009). Breast cancer cell lines contain functional cancer stem cells with metastatic capacity and a distinct molecular signature. *Cancer Res, 69*(4), 1302-1313.

Cheng, A. L., Hsu, C. H., Lin, J. K., Hsu, M. M., Ho, Y. F., Shen, T. S., Ko, J. Y., Lin, J. T., Lin, B. R., Ming-Shiang, W., Yu, H. S., Jee, S. H., Chen, G. S., Chen, T. M., Chen, C. A., Lai, M. K., Pu, Y. S., Pan, M. H., Wang, Y. J., Tsai, C. C., & Hsieh, C. Y. (2001). Phase I clinical trial of curcumin, a chemopreventive agent, in patients with high-risk or pre-malignant lesions. *Anticancer Res, 21*(4B), 2895-2900.

Choi, B. H., Kim, C. G., Lim, Y., Shin, S. Y., & Lee, Y. H. (2008). Curcumin down-regulates the multidrug-resistance mdr1b gene by inhibiting the PI3K/Akt/NF kappa B pathway. *Cancer Lett, 259*(1), 111-118.

Christgen, M., Ballmaier, M., Bruchhardt, H., von Wasielewski, R., Kreipe, H., & Lehmann, U. (2007). Identification of a distinct side population of cancer cells in the Cal-51 human breast carcinoma cell line. *Mol Cell Biochem, 306*(1-2), 201-212.

Connors, R. D., & E.J., E. (2004). Using a Portfolio of Particle Growth Technologies to Enable Delivery of Drugs with Poor Water Solubility. *Drug Delivery Technology, 4*(8), 78-83.

Dagar, S., Krishnadas, A., Rubinstein, I., Blend, M. J., & Onyuksel, H. (2003). VIP grafted sterically stabilized liposomes for targeted imaging of breast cancer: in vivo studies. *J Control Release, 91*(1-2), 123-133.

Dagar, S., Sekosan, M., Lee, B. S., Rubinstein, I., & Onyuksel, H. (2001a). VIP receptors as molecular targets of breast cancer: implications for targeted imaging and drug delivery. *J Control Release, 74*(1-3), 129-134.

Dagar, S., Sekosan, M., Rubinstein, I., & Onyuksel, H. (2001b). Detection of VIP receptors in MNU-induced breast cancer in rats: implications for breast cancer targeting. *Breast Cancer Res Treat, 65*(1), 49-54.

Danhier, F., Feron, O., & Preat, V. (2010). To exploit the tumor microenvironment: Passive and active tumor targeting of nanocarriers for anti-cancer drug delivery. *J Control Release, 148*(2), 135-146.

Dean, M., Fojo, T., & Bates, S. (2005). Tumour stem cells and drug resistance. *Nat Rev Cancer, 5*(4), 275-284.

Deng, T., Liu, J. C., Pritchard, K. I., Eisen, A., & Zacksenhaus, E. (2009). Preferential killing of breast tumor initiating cells by N,N-diethyl-2-[4-(phenylmethyl)phenoxy]ethanamine/tesmilifene. *Clin Cancer Res, 15*(1), 119-130.

Deonarain, M. P., Kousparou, C. A., & Epenetos, A. A. (2009). Antibodies targeting cancer stem cells: a new paradigm in immunotherapy? *MAbs, 1*(1), 12-25.

Dhillon, N., Aggarwal, B. B., Newman, R. A., Wolff, R. A., Kunnumakkara, A. B., Abbruzzese, J. L., Ng, C. S., Badmaev, V., & Kurzrock, R. (2008). Phase II trial of curcumin in patients with advanced pancreatic cancer. *Clin Cancer Res, 14*(14), 4491-4499.

Dickson, L., & Finlayson, K. (2009). VPAC and PAC receptors: From ligands to function. *Pharmacol Ther, 121*(3), 294-316.

Dontu, G., Abdallah, W. M., Foley, J. M., Jackson, K. W., Clarke, M. F., Kawamura, M. J., & Wicha, M. S. (2003). In vitro propagation and transcriptional profiling of human mammary stem/progenitor cells. *Genes Dev, 17*(10), 1253-1270.

Erie, J. C., McLaren, J. W., & Patel, S. V. (2009). Confocal microscopy in ophthalmology. *Am J Ophthalmol, 148*(5), 639-646.

Fillmore, C. M., & Kuperwasser, C. (2008). Human breast cancer cell lines contain stem-like cells that self-renew, give rise to phenotypically diverse progeny and survive chemotherapy. *Breast Cancer Res, 10*(2), R25.

Fong, D., Yeh, A., Naftalovich, R., Choi, T. H., & Chan, M. M. (2010). Curcumin inhibits the side population (SP) phenotype of the rat C6 glioma cell line: towards targeting of cancer stem cells with phytochemicals. *Cancer Lett, 293*(1), 65-72.

Gabizon, A. A. (2001). Pegylated liposomal doxorubicin: metamorphosis of an old drug into a new form of chemotherapy. *Cancer Invest, 19*(4), 424-436.

Garcia-Fernandez, M. O., Collado, B., Bodega, G., Cortes, J., Ruiz-Villaespesa, A., Carmena, M. J., & Prieto, J. C. (2005). Pituitary adenylate cyclase-activating peptide/vasoactive intestinal peptide receptors in human normal mammary gland and breast cancer tissue. *Gynecol Endocrinol, 20*(6), 327-333.

Gerber, B., Freund, M., & Reimer, T. (2010). Recurrent breast cancer: treatment strategies for maintaining and prolonging good quality of life. *Dtsch Arztebl Int, 107*(6), 85-91.

Gespach, C., Bawab, W., de Cremoux, P., & Calvo, F. (1988). Pharmacology, molecular identification and functional characteristics of vasoactive intestinal peptide receptors in human breast cancer cells. *Cancer Res, 48*(18), 5079-5083.

Ginestier, C., Hur, M. H., Charafe-Jauffret, E., Monville, F., Dutcher, J., Brown, M., Jacquemier, J., Viens, P., Kleer, C. G., Liu, S., Schott, A., Hayes, D., Birnbaum, D., Wicha, M. S., & Dontu, G. (2007). ALDH1 is a marker of normal and malignant human mammary stem cells and a predictor of poor clinical outcome. *Cell Stem Cell, 1*(5), 555-567.

Ginestier, C., Liu, S., Diebel, M. E., Korkaya, H., Luo, M., Brown, M., Wicinski, J., Cabaud, O., Charafe-Jauffret, E., Birnbaum, D., Guan, J. L., Dontu, G., & Wicha, M. S. (2010). CXCR1 blockade selectively targets human breast cancer stem cells in vitro and in xenografts. *J Clin Invest, 120*(2), 485-497.

Goel, A., & Aggarwal, B. B. (2010). Curcumin, the golden spice from Indian saffron, is a chemosensitizer and radiosensitizer for tumors and chemoprotector and radioprotector for normal organs. *Nutr Cancer, 62*(7), 919-930.

Gottesman, M. M., Fojo, T., & Bates, S. E. (2002). Multidrug resistance in cancer: role of ATP-dependent transporters. *Nat Rev Cancer, 2*(1), 48-58.

Gulcur, E., Thaqi, M., & Onyuksel, H. (2011). Curcumin nanomedicine enhances drug internalization into breast cancer cells and elimination of cancer stem cells. *The AAPS Journal, 13*(S2).

Gupta, P. B., Onder, T. T., Jiang, G., Tao, K., Kuperwasser, C., Weinberg, R. A., & Lander, E. S. (2009). Identification of selective inhibitors of cancer stem cells by high-throughput screening. *Cell, 138*(4), 645-659.

Harmar, A. J., Arimura, A., Gozes, I., Journot, L., Laburthe, M., Pisegna, J. R., Rawlings, S. R., Robberecht, P., Said, S. I., Sreedharan, S. P., Wank, S. A., & Waschek, J. A. (1998). International Union of Pharmacology. XVIII. Nomenclature of receptors for vasoactive intestinal peptide and pituitary adenylate cyclase-activating polypeptide. *Pharmacol Rev, 50*(2), 265-270.

Harrison, H., Farnie, G., Howell, S. J., Rock, R. E., Stylianou, S., Brennan, K. R., Bundred, N. J., & Clarke, R. B. (2010). Regulation of breast cancer stem cell activity by signaling through the Notch4 receptor. *Cancer Res, 70*(2), 709-718.

Hirsch, H. A., Iliopoulos, D., Tsichlis, P. N., & Struhl, K. (2009). Metformin selectively targets cancer stem cells, and acts together with chemotherapy to block tumor growth and prolong remission. *Cancer Res, 69*(19), 7507-7511.

Hirschmann-Jax, C., Foster, A. E., Wulf, G. G., Nuchtern, J. G., Jax, T. W., Gobel, U., Goodell, M. A., & Brenner, M. K. (2004). A distinct "side population" of cells with high drug efflux capacity in human tumor cells. *Proc Natl Acad Sci U S A, 101*(39), 14228-14233.

Jain, R. K., & Stylianopoulos, T. (2010). Delivering nanomedicine to solid tumors. *Nat Rev Clin Oncol, 7*(11), 653-664.

Jemal, A., Bray, F., Center, M. M., Ferlay, J., Ward, E., & Forman, D. (2011). Global cancer statistics. *CA Cancer J Clin, 61*(2), 69-90.

Kakarala, M., Brenner, D. E., Korkaya, H., Cheng, C., Tazi, K., Ginestier, C., Liu, S., Dontu, G., & Wicha, M. S. (2010). Targeting breast stem cells with the cancer preventive compounds curcumin and piperine. *Breast Cancer Res Treat, 122*(3), 777-785.

Kardinal, C. G., & Cole, J. T. (2008). Breast cancer. In M. C. Perry (Ed.), *The chemotherapy source book* (pp. 363-407). Philadelphia: Wolters Kluwer Health/Lippincott Williams & Wilkins.

Kim, H. I., Huang, H., Cheepala, S., Huang, S., & Chung, J. (2008). Curcumin inhibition of integrin (alpha6beta4)-dependent breast cancer cell motility and invasion. *Cancer Prev Res (Phila), 1*(5), 385-391.

Kirpotin, D. B., Drummond, D. C., Shao, Y., Shalaby, M. R., Hong, K., Nielsen, U. B., Marks, J. D., Benz, C. C., & Park, J. W. (2006). Antibody targeting of long-circulating lipidic nanoparticles does not increase tumor localization but does increase internalization in animal models. *Cancer Res, 66*(13), 6732-6740.

Kola, I., & Landis, J. (2004). Can the pharmaceutical industry reduce attrition rates? *Nat Rev Drug Discov, 3*(8), 711-715.

Koo, O. M., Rubinstein, I., & Onyuksel, H. (2005a). Camptothecin in sterically stabilized phospholipid micelles: a novel nanomedicine. *Nanomedicine, 1*(1), 77-84.

Koo, O. M., Rubinstein, I., & Onyuksel, H. (2005b). Role of nanotechnology in targeted drug delivery and imaging: a concise review. *Nanomedicine, 1*(3), 193-212.

Koo, O. M., Rubinstein, I., & Onyuksel, H. (2011). Actively targeted low-dose camptothecin as a safe, long-acting, disease-modifying nanomedicine for rheumatoid arthritis. *Pharm Res, 28*(4), 776-787.

Korkaya, H., Paulson, A., Charafe-Jauffret, E., Ginestier, C., Brown, M., Dutcher, J., Clouthier, S. G., & Wicha, M. S. (2009). Regulation of mammary stem/progenitor cells by PTEN/Akt/beta-catenin signaling. *PLoS Biol, 7*(6), e1000121.

Korkaya, H., Paulson, A., Iovino, F., & Wicha, M. S. (2008). HER2 regulates the mammary stem/progenitor cell population driving tumorigenesis and invasion. *Oncogene, 27*(47), 6120-6130.

Krishnadas, A. (2004). *Targeted delivery of paclitaxel in phospholipid micelles for improved chemotherapy of breast cancer.* University of Illinois at Chicago, Chicago.

Krishnadas, A., Rubinstein, I., & Onyüksel, H. (2003). Sterically stabilized phospholipid mixed micelles: in vitro evaluation as a novel carrier for water-insoluble drugs. *Pharmaceutical research, 20*(2), 297-302.

Kunnumakkara, A. B., Anand, P., & Aggarwal, B. B. (2008). Curcumin inhibits proliferation, invasion, angiogenesis and metastasis of different cancers through interaction with multiple cell signaling proteins. *Cancer Lett, 269*(2), 199-225.

Laburthe, M., & Couvineau, A. (2002). Molecular pharmacology and structure of VPAC Receptors for VIP and PACAP. *Regul Pept, 108*(2-3), 165-173.

Laburthe, M., Couvineau, A., & Tan, V. (2007). Class II G protein-coupled receptors for VIP and PACAP: structure, models of activation and pharmacology. *Peptides, 28*(9), 1631-1639.

Lammers, T., Hennink, W. E., & Storm, G. (2008). Tumour-targeted nanomedicines: principles and practice. *Br J Cancer, 99*(3), 392-397.

Leamon, C. P., Cooper, S. R., & Hardee, G. E. (2003). Folate-liposome-mediated antisense oligodeoxynucleotide targeting to cancer cells: evaluation in vitro and in vivo. *Bioconjug Chem, 14*(4), 738-747.

Lee, R. J., & Low, P. S. (1994). Delivery of liposomes into cultured KB cells via folate receptor-mediated endocytosis. *J Biol Chem, 269*(5), 3198-3204.

Lentz, B. R. (2007). PEG as a tool to gain insight into membrane fusion. *Eur Biophys J, 36*(4-5), 315-326.

Li, L., Braiteh, F. S., & Kurzrock, R. (2005). Liposome-encapsulated curcumin: in vitro and in vivo effects on proliferation, apoptosis, signaling, and angiogenesis. *Cancer, 104*(6), 1322-1331.

Li, X., Lewis, M. T., Huang, J., Gutierrez, C., Osborne, C. K., Wu, M. F., Hilsenbeck, S. G., Pavlick, A., Zhang, X., Chamness, G. C., Wong, H., Rosen, J., & Chang, J. C. (2008). Intrinsic resistance of tumorigenic breast cancer cells to chemotherapy. *J Natl Cancer Inst, 100*(9), 672-679.

Li, Y., Welm, B., Podsypanina, K., Huang, S., Chamorro, M., Zhang, X., Rowlands, T., Egeblad, M., Cowin, P., Werb, Z., Tan, L. K., Rosen, J. M., & Varmus, H. E. (2003). Evidence that transgenes encoding components of the Wnt signaling pathway preferentially induce mammary cancers from progenitor cells. *Proc Natl Acad Sci U S A, 100*(26), 15853-15858.

Li, Y., Zhang, T., Korkaya, H., Liu, S., Lee, H. F., Newman, B., Yu, Y., Clouthier, S. G., Schwartz, S. J., Wicha, M. S., & Sun, D. (2010). Sulforaphane, a dietary component of broccoli/broccoli sprouts, inhibits breast cancer stem cells. *Clin Cancer Res, 16*(9), 2580-2590.

Lim, K. J., Bisht, S., Bar, E. E., Maitra, A., & Eberhart, C. G. (2011a). A polymeric nanoparticle formulation of curcumin inhibits growth, clonogenicity and stem-like fraction in malignant brain tumors. *Cancer Biol Ther, 11*(5), 464-473.

Lim, S. B., Rubinstein, I., Sadikot, R. T., Artwohl, J. E., & Onyuksel, H. (2011b). A novel peptide nanomedicine against acute lung injury: GLP-1 in phospholipid micelles. *Pharm Res, 28*(3), 662-672.

Lippman, M. E. (2005). Breast Cancer. In B. E. Fauci A.S., Kasper D.L., Hauser S.L., Longo D.L., Jameson L.I., Loscalzo J. (Ed.), *HARRISONS PRINCIPLES OF INTERNAL MEDICINE* (Vol. 1, pp. 516-522). New York, NY: McGraw-Hill.

Liu, S., Dontu, G., Mantle, I. D., Patel, S., Ahn, N. S., Jackson, K. W., Suri, P., & Wicha, M. S. (2006). Hedgehog signaling and Bmi-1 regulate self-renewal of normal and malignant human mammary stem cells. *Cancer Res, 66*(12), 6063-6071.

Lopez-Lazaro, M. (2008). Anticancer and carcinogenic properties of curcumin: considerations for its clinical development as a cancer chemopreventive and chemotherapeutic agent. *Mol Nutr Food Res, 52 Suppl 1*, S103-127.

Magnifico, A., Albano, L., Campaner, S., Delia, D., Castiglioni, F., Gasparini, P., Sozzi, G., Fontanella, E., Menard, S., & Tagliabue, E. (2009). Tumor-initiating cells of HER2-positive carcinoma cell lines express the highest oncoprotein levels and are sensitive to trastuzumab. *Clin Cancer Res, 15*(6), 2010-2021.

Malvern Instruments. Dynamic lights scattering: an introduction in 30 minutes. Retrieved 10.15.2009: http://www.malvern.co.uk/malvern/kbase.nsf

Marcucci, F., & Lefoulon, F. (2004). Active targeting with particulate drug carriers in tumor therapy: fundamentals and recent progress. *Drug Discov Today, 9*(5), 219-228.

Marsh, S., & Liu, G. (2009). Pharmacokinetics and pharmacogenomics in breast cancer chemotherapy. *Adv Drug Deliv Rev, 61*(5), 381-387.

Matsumura, Y., & Maeda, H. (1986). A new concept for macromolecular therapeutics in cancer chemotherapy: mechanism of tumoritropic accumulation of proteins and the antitumor agent smancs. *Cancer Res, 46*(12 Pt 1), 6387-6392.

Michaud, L. B., Espirito, J., & Esteva, F. J. (2008). Breast Cancer. In M. A. Chisolm-Burns (Ed.), *Pharmacotherapy principles & practice* (pp. 2121 - 2258). New York: McGraw-Hill Medical Pub. Division.

Mill, C. P., Chester, J. A., & Riese, D. J. (2009). EGFR may couple moderate alcohol consumption to increased breast cancer risk. *Breast Cancer (London), 2009*(1), 31-38.

Mittag, A., & Tárnok, A. (2011). Perspectives in Cytometry *Advanced Optical Flow Cytometry* (pp. 1-23): Wiley-VCH Verlag GmbH & Co. KGaA.

Mukerjee, A., & Vishwanatha, J. K. (2009). Formulation, characterization and evaluation of curcumin-loaded PLGA nanospheres for cancer therapy. *Anticancer Res, 29*(10), 3867-3875.

Nicholson, R. I., & Johnston, S. R. (2005). Endocrine therapy--current benefits and limitations. *Breast Cancer Res Treat, 93 Suppl 1*, S3-10.

Normanno, N., Di Maio, M., De Maio, E., De Luca, A., de Matteis, A., Giordano, A., & Perrone, F. (2005). Mechanisms of endocrine resistance and novel therapeutic strategies in breast cancer. *Endocr Relat Cancer, 12*(4), 721-747.

Onyuksel, H., & Banerjee, A. (2011). Phospholipid-based nanomicelles in cancer nanomedicine. In R. J. Hunter & V. R. Preedy (Eds.), *Nanomedicine in health and disease* (1st ed., pp. 314-335). London, U.K.: CRC Press ; Science Publishers.

Onyuksel, H., Ikezaki, H., Patel, M., Gao, X. P., & Rubinstein, I. (1999). A novel formulation of VIP in sterically stabilized micelles amplifies vasodilation in vivo. *Pharm Res, 16*(1), 155-160.

Onyuksel, H., Jeon, E., & Rubinstein, I. (2009a). Nanomicellar paclitaxel increases cytotoxicity of multidrug resistant breast cancer cells. *Cancer Lett, 274*(2), 327-330.

Onyuksel, H., Mohanty, P. S., & Rubinstein, I. (2009b). VIP-grafted sterically stabilized phospholipid nanomicellar 17-allylamino-17-demethoxy geldanamycin: a novel targeted nanomedicine for breast cancer. *Int J Pharm, 365*(1-2), 157-161.

Park, C. H., Hahm, E. R., Park, S., Kim, H. K., & Yang, C. H. (2005). The inhibitory mechanism of curcumin and its derivative against beta-catenin/Tcf signaling. *FEBS Lett, 579*(13), 2965-2971.

Park, J. W., Hong, K., Kirpotin, D. B., Colbern, G., Shalaby, R., Baselga, J., Shao, Y., Nielsen, U. B., Marks, J. D., Moore, D., Papahadjopoulos, D., & Benz, C. C. (2002). Anti-HER2 immunoliposomes: enhanced efficacy attributable to targeted delivery. *Clin Cancer Res, 8*(4), 1172-1181.

Peer, D., Karp, J. M., Hong, S., Farokhzad, O. C., Margalit, R., & Langer, R. (2007). Nanocarriers as an emerging platform for cancer therapy. *Nat Nanotechnol, 2*(12), 751-760.

Phillips, T. M., McBride, W. H., & Pajonk, F. (2006). The response of CD24(-/low)/CD44+ breast cancer-initiating cells to radiation. *J Natl Cancer Inst, 98*(24), 1777-1785.

Ponti, D., Costa, A., Zaffaroni, N., Pratesi, G., Petrangolini, G., Coradini, D., Pilotti, S., Pierotti, M. A., & Daidone, M. G. (2005). Isolation and in vitro propagation of tumorigenic breast cancer cells with stem/progenitor cell properties. *Cancer Res, 65*(13), 5506-5511.

Preffer, F., & Dombkowski, D. (2009). Advances in complex multiparameter flow cytometry technology: Applications in stem cell research. *Cytometry B Clin Cytom, 76*(5), 295-314.

Prendergast, G. C., & Jaffee, E. M. (2007). *Cancer immunotherapy : immune suppression and tumor growth*. Amsterdam; Boston: Academic Press/Elsevier.

Rafter, J. J. (2002). Scientific basis of biomarkers and benefits of functional foods for reduction of disease risk: cancer. *Br J Nutr, 88 Suppl 2*, S219-224.

Ramachandran, C., & You, W. (1999). Differential sensitivity of human mammary epithelial and breast carcinoma cell lines to curcumin. *Breast Cancer Res Treat, 54*(3), 269-278.

Ravindran, J., Prasad, S., & Aggarwal, B. B. (2009). Curcumin and cancer cells: how many ways can curry kill tumor cells selectively? *AAPS J, 11*(3), 495-510.

Reubi, J. C. (2003). Peptide receptors as molecular targets for cancer diagnosis and therapy. *Endocr Rev, 24*(4), 389-427.

Reubi, J. C., Laderach, U., Waser, B., Gebbers, J. O., Robberecht, P., & Laissue, J. A. (2000). Vasoactive intestinal peptide/pituitary adenylate cyclase-activating peptide receptor subtypes in human tumors and their tissues of origin. *Cancer Res, 60*(11), 3105-3112.

Reya, T., Morrison, S. J., Clarke, M. F., & Weissman, I. L. (2001). Stem cells, cancer, and cancer stem cells. *Nature, 414*(6859), 105-111.

Rothenberg, M., & Clarke, M. F. (2009). Chapter 53 - Cancer Stem Cells. In L. Robert, G. John, H. Brigid, M. Douglas, P. Roger, E. D. Thomas, T. James, J. G. B. H. D. M. R. P. E. D. T. J. T. Sir Ian WilmutA2 - Robert Lanza & W. Sir Ian (Eds.), *Essentials of Stem Cell Biology (Second Edition)* (pp. 467-483). San Diego: Academic Press.

Salmaso, S., Bersani, S., Semenzato, A., & Caliceti, P. (2007). New cyclodextrin bioconjugates for active tumour targeting. *J Drug Target, 15*(6), 379-390.

Schatzlein, A. G. (2006). Delivering cancer stem cell therapies - a role for nanomedicines? *Eur J Cancer, 42*(9), 1309-1315.

Schulz, S., Rocken, C., Mawrin, C., Weise, W., & Hollt, V. (2004). Immunocytochemical identification of VPAC1, VPAC2, and PAC1 receptors in normal and neoplastic human tissues with subtype-specific antibodies. *Clin Cancer Res, 10*(24), 8235-8242.

Semrock Inc. (2011). Filters for flow cytometry. Retrieved 11.02, 2011, from http://www.semrock.com/flow-cytometry.aspx

Serpe, L. (2006). Conventional Chemotherapeutic Drug Nanoparticles for Cancer Treatment. In C. S. S. R. Kumar (Ed.), *Nanomaterials for cancer therapy* (pp. 1-39). Weinheim: Wiley-VCH.

Sezgin, Z., Yuksel, N., & Baykara, T. (2006). Preparation and characterization of polymeric micelles for solubilization of poorly soluble anticancer drugs. *Eur J Pharm Biopharm, 64*(3), 261-268.

Shaikh, J., Ankola, D. D., Beniwal, V., Singh, D., & Kumar, M. N. (2009). Nanoparticle encapsulation improves oral bioavailability of curcumin by at least 9-fold when compared to curcumin administered with piperine as absorption enhancer. *Eur J Pharm Sci, 37*(3-4), 223-230.

Sharma, R. A., Euden, S. A., Platton, S. L., Cooke, D. N., Shafayat, A., Hewitt, H. R., Marczylo, T. H., Morgan, B., Hemingway, D., Plummer, S. M., Pirmohamed, M., Gescher, A. J., & Steward, W. P. (2004). Phase I clinical trial of oral curcumin: biomarkers of systemic activity and compliance. *Clin Cancer Res, 10*(20), 6847-6854.

Shoba, G., Joy, D., Joseph, T., Majeed, M., Rajendran, R., & Srinivas, P. S. (1998). Influence of piperine on the pharmacokinetics of curcumin in animals and human volunteers. *Planta Med, 64*(4), 353-356.

Sladek, N. E. (2003). Human aldehyde dehydrogenases: potential pathological, pharmacological, and toxicological impact. *J Biochem Mol Toxicol, 17*(1), 7-23.

Szakacs, G., Paterson, J. K., Ludwig, J. A., Booth-Genthe, C., & Gottesman, M. M. (2006). Targeting multidrug resistance in cancer. *Nat Rev Drug Discov, 5*(3), 219-234.

Thaqi, M. (2011). *Lipid-based nanomedicine of curcumin.* Unpublished Master's thesis, University of Illinois at Chicago, Chicago.

Torchilin, V. P. (2010). Passive and active drug targeting: drug delivery to tumors as an example. *Handb Exp Pharmacol*(197), 3-53.

Torchilin, V. P., Rammohan, R., Weissig, V., & Levchenko, T. S. (2001). TAT peptide on the surface of liposomes affords their efficient intracellular delivery even at low temperature and in the presence of metabolic inhibitors. *Proc Natl Acad Sci U S A, 98*(15), 8786-8791.

Torchilin, V. P., & Trubetskoy, V. S. (1995). Which polymers can make nanoparticulate drug carriers long-circulating? *Advanced drug delivery reviews., 16*(2-3), 141.

Usdin, T. B., Bonner, T. I., & Mezey, E. (1994). Two receptors for vasoactive intestinal polypeptide with similar specificity and complementary distributions. *Endocrinology, 135*(6), 2662-2680.

Vance, J. E. (2008). Phosphatidylserine and phosphatidylethanolamine in mammalian cells: two metabolically related aminophospholipids. *J Lipid Res, 49*(7), 1377-1387.

Velasco-Velazquez, M. A., Jiao, X., & Pestell, R. G. (2011a). Breast cancer stem cells. In S. Shostak (Ed.), *Cancer stem cells theories and practice* (pp. 63-75). Rijeka, Croatia: InTech.

Velasco-Velazquez, M. A., Jiao, X., & Pestell, R. G. (2011b). Cancer stem cells theories and practice. In S. Shostak (Ed.), *Cancer stem cells theories and practice* (pp. 63-75). Rijeka, Croatia: InTech.

Wang, Z., Zhang, Y., Banerjee, S., Li, Y., & Sarkar, F. H. (2006). Notch-1 down-regulation by curcumin is associated with the inhibition of cell growth and the induction of apoptosis in pancreatic cancer cells. *Cancer, 106*(11), 2503-2513.

Widakowich, C., de Azambuja, E., Gil, T., Cardoso, F., Dinh, P., Awada, A., & Piccart-Gebhart, M. (2007). Molecular targeted therapies in breast cancer: where are we now? *Int J Biochem Cell Biol, 39*(7-8), 1375-1387.

Winquist, R. J., Boucher, D. M., Wood, M., & Furey, B. F. (2009). Targeting cancer stem cells for more effective therapies: Taking out cancer's locomotive engine. *Biochem Pharmacol, 78*(4), 326-334.

Working, P. K., & Dayan, A. D. (1996). Pharmacological-toxicological expert report. CAELYX. (Stealth liposomal doxorubicin HCl). *Hum Exp Toxicol, 15*(9), 751-785.

Wu, C., & Alman, B. A. (2008). Side population cells in human cancers. *Cancer Lett, 268*(1), 1-9.

Yallapu, M. M., Maher, D. M., Sundram, V., Bell, M. C., Jaggi, M., & Chauhan, S. C. (2010). Curcumin induces chemo/radio-sensitization in ovarian cancer cells and curcumin nanoparticles inhibit ovarian cancer cell growth. *J Ovarian Res, 3*, 11.

Yu, Y., Kanwar, S. S., Patel, B. B., Nautiyal, J., Sarkar, F. H., & Majumdar, A. P. (2009). Elimination of Colon Cancer Stem-Like Cells by the Combination of Curcumin and FOLFOX. *Transl Oncol, 2*(4), 321-328.

VITA

NAME: Ece GULCUR

EDUCATION: B.S., Chemical Engineering, Istanbul Technical University, Istanbul, Turkey, 2007.

M.S., Biopharmaceutical Sciences, University of Illinois at Chicago, Chicago, Illinois, 2012.

PROFESSIONAL EXPERIENCE: Research Assistant, Department of Biopharmaceutical Sciences, University of Illinois at Chicago, 2011.

Formulation and Process Development Assistant Specialist, Research and Development Department, Biopharma Pharmaceutical Inc., Istanbul, Turkey, 2007-2009.

TEACHING EXPERIENCE: Principles of Drug Action and Therapeutics II and Drug Delivery Systems II Laboratory for Pharm.D. students, College of Pharmacy, University of Illinois at Chicago, 2009-2011.

ABSTRACTS: **Gulcur, E.** and Onyuksel, H. (2012). A novel vasoactive intestinal peptide-grafted curcumin nanomedicine for targeting breast cancer stem cells. AACR Annual Meeting, 03/31-04/04 2012, Chicago, IL.

Gulcur, E., Thaqi, M., and Onyuksel, H. (2011). Curcumin nanomedicine enhances drug internalization into breast cancer cells and elimination of cancer stem cells. *The AAPS Journal, 13*(S2). Available from: http://www.aapsj.org/.

PROFESSIONAL MEMBERSHIPS: American Association of Pharmaceutical Scientists (AAPS)
Controlled Release Society (CRS)
American Association for Cancer Research (AACR)